

Supporting Information

Flexible Amorphous Metal–Organic Frameworks with π Lewis Acidic Pore Surface for Selective Adsorptive Separations

*Javier Fonseca**, and *Sunho Choi**

Nanomaterial Laboratory for Catalysis and Advanced Separations, Department of Chemical Engineering, Northeastern University, 313 Snell Engineering Center, 360 Huntington Avenue, Boston, Massachusetts 02115-5000, United States

* Corresponding Author. E-mail: fonsecagarcia.j@northeastern.edu

* Corresponding Author. E-mail: s.choi@northeastern.edu

Table of Content

1. Supplementary Figures

Fig. S1. ^1H NMR (500 MHz, CD₃OD) spectra of H₂BPDI

Fig. S2. FTIR (KBr cm⁻¹) spectra of H₂BPDI

Fig. S3. DSC of H₂BPDI

Fig. S4. ^1H NMR (500 MHz, CD₃OD) spectra of H₂PMDA

Fig. S5. FTIR (KBr cm⁻¹) spectra of H₂PMDA

Fig. S6. DSC of H₂PMDA

Fig. S7. Coordinates of each atom in the local molecular structure of zinc within NEU-3

Fig. S8. X-ray absorption spectrum at the Zn K-edge of the NEU-3 before (a) and after normalization (b)

Fig. S9. Coordinates of each atom in the local molecular structure of iron within NEU-4

Fig. S10. X-ray absorption spectrum at the Fe K-edge of the NEU-4 before (a) and after normalization (b)

Fig. S11. EDX characterization of NEU-3

Fig. S12. EDX characterization of NEU-4

Fig. S13. TGA of NEU-3 from room temperature to 1000 °C

Fig. S14. TGA of NEU-4 from room temperature to 1000 °C

Fig. S15. Nitrogen adsorption/desorption isotherms of NEU-1c

Fig. S16. Nitrogen adsorption/desorption isotherms of NEU-2

Fig. S17. Nitrogen adsorption/desorption isotherms of NEU-3

Fig. S18. Nitrogen adsorption/desorption isotherms of NEU-4

Fig. S19. Nitrogen adsorption/desorption isotherms of NEU-4 after one cycle of aromatic hydrocarbon-cyclohexane separation

Fig. S20. DFT pore analysis of NEU-1c

Fig. S21. DFT pore analysis of NEU-2

Fig. S22. DFT pore analysis of NEU-3

Fig. S23. DFT pore analysis of NEU-4

Fig. S24. DFT pore analysis of NEU-4 after one cycle of aromatic hydrocarbon-cyclohexane separation

Fig. S25. FTIR spectra of NEU-1c before and after benzene sorption

Fig. S26. XRD of NEU-1c before and after benzene sorption

Fig. S27. SEM of NEU-1c before and after benzene sorption

Fig. S28. TEM of NEU-1c before and after benzene sorption

Fig. S29. FTIR spectra of NEU-2 before and after benzene sorption

Fig. S30. SEM of NEU-2 before and after benzene sorption

Fig. S31. TEM of NEU-2 before and after benzene sorption

Fig. S32. FTIR spectra of NEU-3 before and after benzene sorption

Fig. S33. SEM of NEU-3 before and after benzene sorption

Fig. S34. TEM of NEU-3 before and after benzene sorption

Fig. S35. FTIR spectra of NEU-4 before and after benzene sorption

Fig. S36. SEM of NEU-3 before and after benzene sorption

Fig. S37. TEM of NEU-3 before and after benzene sorption

Fig. S38. Regression test between intensity ratio – of benzene and cyclohexane ^1H NMR signals – and volume ratio of the solution

Fig. S39. ^1H NMR of benzene and cyclohexane mixtures: 1 %v/v, 2 %v/v, 3 %v/v, 5 %v/v, 8 %v/v, 10 %v/v, 12 %v/v, 15 %v/v, 20 %v/v, 25 %v/v, 30 %v/v, 35 %v/v, 40 %v/v, 45 %v/v, and 50 %v/v

Fig. S40. Regression test between intensity ratio – of toluene and cyclohexane ^1H NMR signals – and volume ratio of the solution

Fig. S41. ^1H NMR of toluene and cyclohexane mixtures: 1 %v/v, 2 %v/v, 3 %v/v, 5 %v/v, 8 %v/v, 10 %v/v, 12 %v/v, 15 %v/v, 20 %v/v, 25 %v/v, 30 %v/v, 35 %v/v, 40 %v/v, 45 %v/v, and 50 %v/v

Fig. S42. Regression test between intensity ratio – of 1,4-dioxane and cyclohexane ^1H NMR signals – and volume ratio of the solution

Fig. S43. ^1H NMR of 1,4-dioxane and cyclohexane mixtures: 1 %v/v, 2 %v/v, 3 %v/v, 5 %v/v, 8 %v/v, 10 %v/v, 12 %v/v, 15 %v/v, 20 %v/v, 25 %v/v, 30 %v/v, 35 %v/v, 40 %v/v, 45 %v/v, and 50 %v/v

Fig. S44. Regression test between intensity ratio – of p-xylene and cyclohexane ^1H NMR signals – and volume ratio of the solution

Fig. S45. ^1H NMR of p-xylene and cyclohexane mixtures: 1 %v/v, 2 %v/v, 3 %v/v, 5 %v/v, 8 %v/v, 10 %v/v, 12 %v/v, 15 %v/v, 20 %v/v, 25 %v/v, 30 %v/v, 35 %v/v, 40 %v/v, 45 %v/v, and 50 %v/v

Fig. S46. Regression test between intensity ratio – of nitrobenzene and cyclohexane ^1H NMR signals – and volume ratio of the solution

Fig. S47. ^1H NMR of nitrobenzene and cyclohexane mixtures: 1 %v/v, 2 %v/v, 3 %v/v, 5 %v/v, 8 %v/v, 10 %v/v, 12 %v/v, 15 %v/v, 20 %v/v, 25 %v/v, 30 %v/v, 35 %v/v, 40 %v/v, 45 %v/v, and 50 %v/v

Fig. S48. ^1H NMR of benzene/cyclohexane eluent after 1st cs, 2nd cs, 3rd cs, 4th cs, 5th cs, 6th cs, 7th cs, 8th cs, 9th cs, 10th cs, and after 1st cs and 1st regeneration in NEU-1c (initial mixture 5 %v/v)

Fig. S49. ^1H NMR of benzene/cyclohexane eluent after 1st cs, 2nd cs, 3rd cs, 4th cs, 5th cs, 6th cs, 7th cs, 8th cs, and after 1st cs and 1st regeneration in NEU-1c (initial mixture 10 %v/v)

Fig. S50. ^1H NMR of benzene/cyclohexane eluent after 1st cs, 2nd cs, 3rd cs, 4th cs, 5th cs, 6th cs, and after 1st cs and 1st regeneration in NEU-1c (initial mixture 25 %v/v)

Fig. S51. ^1H NMR of benzene/cyclohexane eluent after 1st cs, 2nd cs, 3rd cs, 4th cs, 5th cs, 6th cs, and after 1st cs and 1st regeneration in NEU-1c (initial mixture 50 %v/v)

Fig. S52. ^1H NMR of benzene/cyclohexane eluent after 1st cs, 2nd cs, 3rd cs, 4th cs, 5th cs, 6th cs, 7th cs, 8th cs, 9th cs, 10th cs, and after 1st cs and 1st regeneration in NEU-2 (initial mixture 5 %v/v)

Fig. S53. ^1H NMR of benzene/cyclohexane eluent after 1st cs, 2nd cs, 3rd cs, 4th cs, 5th cs, 6th cs, 7th cs, 8th cs, 9th cs, 10th cs, and after 1st cs and 1st regeneration in NEU-2 (initial mixture 10 %v/v)

Fig. S54. ^1H NMR of benzene/cyclohexane eluent after 1st cs, 2nd cs, 3rd cs, 4th cs, 5th cs, 6th cs, 7th cs, 8th cs, 9th cs, 10th cs, and after 1st cs and 1st regeneration in NEU-2 (initial mixture 25 %v/v)

Fig. S55. ^1H NMR of benzene/cyclohexane eluent after 1st cs, 2nd cs, 3rd cs, 4th cs, 5th cs, 6th cs, 7th cs, 8th cs, and after 1st cs and 1st regeneration in NEU-2 (initial mixture 50 %v/v)

Fig. S56. ^1H NMR of benzene/cyclohexane eluent after 1st cs, 2nd cs, 3rd cs, 4th cs, 5th cs, 6th cs, 7th cs, 8th cs, 9th cs, 10th cs, and after 1st cs and 1st regeneration in NEU-3 (initial mixture 5 %v/v)

Fig. S57. ^1H NMR of benzene/cyclohexane eluent after 1st cs, 2nd cs, 3rd cs, 4th cs, 5th cs, 6th cs, 7th cs, 8th cs, 9th cs, 10th cs, and after 1st cs and 1st regeneration in NEU-3 (initial mixture 10 %v/v)

Fig. S58. ^1H NMR of benzene/cyclohexane eluent after 1st cs, 2nd cs, 3rd cs, 4th cs, 5th cs, 6th cs, 7th cs, 8th cs, 9th cs, 10th cs, and after 1st cs and 1st regeneration in NEU-3 (initial mixture 25 %v/v)

Fig. S59. ^1H NMR of benzene/cyclohexane eluent after 1st cs, 2nd cs, 3rd cs, 4th cs, 5th cs, 6th cs, 7th cs, and after 1st cs and 1st regeneration in NEU-3 (initial mixture 50 %v/v)

Fig. S60. ^1H NMR of benzene/cyclohexane eluent after 1st cs, 2nd cs, 3rd cs, 4th cs, 5th cs, 6th cs, 7th cs, 8th cs, 9th cs, 10th cs, and after 1st cs and 1st regeneration in NEU-4 (initial mixture 5 %v/v)

Fig. S61. ^1H NMR of benzene/cyclohexane eluent after 1st cs, 2nd cs, 3rd cs, 4th cs, 5th cs, 6th cs, 7th cs, 8th cs, 9th cs, 10th cs, and after 1st cs and 1st regeneration in NEU-4 (initial mixture 10 %v/v)

Fig. S62. ^1H NMR of benzene/cyclohexane eluent after 1th cs, 2nd cs, 3rd cs, 4th cs, 5th cs, 6th cs, 7th cs, 8th cs, 9th cs, 10th cs, after 1st cs and 1st regeneration, after 2nd cs and 1st regeneration, after 3rd cs and 1st regeneration, after 4th cs and 1st regeneration, after 5th cs and 1st regeneration, after

6th cs and 1st regeneration, after 7th cs and 1st regeneration, after 8th cs and 1st regeneration, after 9th cs and 1st regeneration, after 10th cs and 1st regeneration, after 1st cs and 2nd regeneration, after 2nd cs and 2nd regeneration, after 3rd cs and 2nd regeneration, after 4th cs and 2nd regeneration, after 5th cs and 2nd regeneration, after 6th cs and 2nd regeneration, after 7th cs and 2nd regeneration, after 8th cs and 2nd regeneration, after 9th cs and 2nd regeneration, after 10th cs and 2nd regeneration, after 1st cs and 3rd regeneration, after 2nd cs and 3rd regeneration, after 3rd cs and 3rd regeneration, after 4th cs and 3rd regeneration, after 5th cs and 3rd regeneration, after 6th cs and 3rd regeneration, after 7th cs and 3rd regeneration, after 8th cs and 3rd regeneration, after 9th cs and 3rd regeneration, after 10th cs and 3rd regeneration, after 1st cs and 4th regeneration, after 2nd cs and 4th regeneration, after 3rd cs and 4th regeneration, after 4th cs and 4th regeneration, after 5th cs and 4th regeneration, after 6th cs and 4th regeneration, after 7th cs and 4th regeneration, after 8th cs and 4th regeneration, after 9th cs and 4th regeneration, after 10th cs and 4th regeneration in NEU-4 (initial mixture 25 % v/v)

Fig. S63. ¹H NMR of benzene/cyclohexane eluent after 1st cs, 2nd cs, 3rd cs, 4th cs, 5th cs, 6th cs, 7th cs, 8th cs, 9th cs, 10th cs, and after 1st cs and 1st regeneration in NEU-4 (initial mixture 50 % v/v)

Fig. S64. ¹H NMR of toluene/cyclohexane eluent after 1st cs, 2nd cs, 3rd cs, 4th cs, 5th cs, 6th cs, 7th cs, 8th cs, 9th cs, 10th cs, and after 1st cs and 1st regeneration in NEU-4 (initial mixture 25 % v/v)

Fig. S65. ¹H NMR of 1,4-dioxane/cyclohexane eluent after 1st cs, 2nd cs, 3rd cs, 4th cs, 5th cs, 6th cs, 7th cs, 8th cs, 9th cs, 10th cs, and after 1st cs and 1st regeneration in NEU-4 (initial mixture 25 % v/v)

Fig. S66. ¹H NMR of p-xylene/cyclohexane eluent after 1st cs, 2nd cs, 3rd cs, 4th cs, 5th cs, 6th cs and 7th cs in NEU-4 (initial mixture 25 % v/v)

Fig. S67. ¹H NMR of nitrobenzene/cyclohexane eluent after 1st cs, 2nd cs, and after 1st cs and 1st regeneration in NEU-4 (initial mixture 25 % v/v)

Fig. S68. Schematic procedure of the selective adsorptive separations

Fig. S69. FTIR spectra of NEU-1c before and after 10 cycles of benzene/cyclohexane (50 % v/v, 25 % v/v, 10 % v/v and 5 % v/v) separation and one regeneration. NEU-1c did not suffer structural alterations upon selective separations

Fig. S70. XRD of NEU-1c before and after 10 cycles of benzene/cyclohexane (50 % v/v, 25 % v/v, 10 % v/v and 5 % v/v) separation and one regeneration. NEU-1c did not suffer structural alterations upon selective separations

Fig. S71. FTIR spectra of NEU-2 before and after 10 cycles of benzene/cyclohexane (50 % v/v, 25 % v/v, 10 % v/v and 5 % v/v) separation and one regeneration. NEU-2 did not suffer structural alterations upon selective separations

Fig. S72. FTIR spectra of NEU-3 before and after 10 cycles of benzene/cyclohexane (50 %v/v, 25 %v/v, 10 %v/v and 5 %v/v) separation and one regeneration. NEU-3 did not suffer structural alterations upon selective separations

Fig. S73. FTIR spectra of NEU-4 before and after 10 cycles of benzene/cyclohexane (50 %v/v, 10 %v/v and 5 %v/v) separation and one regeneration (50 cycles of benzene/cyclohexane 25 %v/v separation and 4 regenerations). NEU-4 did not suffer structural alterations upon selective separations

Fig. S74. SEM of NEU-1c (a) before and (b) after 10 cycles of benzene/cyclohexane 50 %v/v separation and one regeneration. The overall morphology of the frameworks was maintained

Fig. S75. TEM of NEU-1c (a) before and (b) after 10 cycles of benzene/cyclohexane 50 %v/v separation and one regeneration. The overall morphology of the frameworks was maintained

Fig. S76. SEM of NEU-1c (a) before and (b) after 10 cycles of benzene/cyclohexane 25 %v/v separation and one regeneration. The overall morphology of the frameworks was maintained

Fig. S77. TEM of NEU-1c (a) before and (b) after 10 cycles of benzene/cyclohexane 25 %v/v separation and one regeneration. The overall morphology of the frameworks was maintained

Fig. S78. SEM of NEU-1c (a) before and (b) after 10 cycles of benzene/cyclohexane 10 %v/v separation and one regeneration. The overall morphology of the frameworks was maintained

Fig. S79. TEM of NEU-1c (a) before and (b) after 10 cycles of benzene/cyclohexane 10 %v/v separation and one regeneration. The overall morphology of the frameworks was maintained

Fig. S80. SEM of NEU-1c (a) before and (b) after 10 cycles of benzene/cyclohexane 5 %v/v separation and one regeneration. The overall morphology of the frameworks was maintained

Fig. S81. TEM of NEU-1c (a) before and (b) after 10 cycles of benzene/cyclohexane 5 %v/v separation and one regeneration. The overall morphology of the frameworks was maintained

Fig. S82. SEM of NEU-2 (a) before and (b) after 10 cycles of benzene/cyclohexane 50 %v/v separation and one regeneration. The overall morphology of the frameworks was maintained

Fig. S83. TEM of NEU-2 (a) before and (b) after 10 cycles of benzene/cyclohexane 50 %v/v separation and one regeneration. The overall morphology of the frameworks was maintained

Fig. S84. SEM of NEU-2 (a) before and (b) after 10 cycles of benzene/cyclohexane 25 %v/v separation and one regeneration. The overall morphology of the frameworks was maintained

Fig. S85. TEM of NEU-2 (a) before and (b) after 10 cycles of benzene/cyclohexane 25 %v/v separation and one regeneration. The overall morphology of the frameworks was maintained

Fig. S86. SEM of NEU-2 (a) before and (b) after 10 cycles of benzene/cyclohexane 10 %v/v separation and one regeneration. The overall morphology of the frameworks was maintained

Fig. S87. TEM of NEU-2 (a) before and (b) after 10 cycles of benzene/cyclohexane 10 %v/v separation and one regeneration. The overall morphology of the frameworks was maintained

Fig. S88. SEM of NEU-2 (a) before and (b) after 10 cycles of benzene/cyclohexane 5 %v/v separation and one regeneration. The overall morphology of the frameworks was maintained

Fig. S89. TEM of NEU-2 (a) before and (b) after 10 cycles of benzene/cyclohexane 5 %v/v separation and one regeneration. The overall morphology of the frameworks was maintained

Fig. S90. SEM of NEU-3 (a) before and (b) after 10 cycles of benzene/cyclohexane 50 %v/v separation and one regeneration. The overall morphology of the frameworks was maintained

Fig. S91. TEM of NEU-3 (a) before and (b) after 10 cycles of benzene/cyclohexane 50 %v/v separation and one regeneration. The overall morphology of the frameworks was maintained

Fig. S92. SEM of NEU-3 (a) before and (b) after 10 cycles of benzene/cyclohexane 25 %v/v separation and one regeneration. The overall morphology of the frameworks was maintained

Fig. S93. TEM of NEU-3 (a) before and (b) after 10 cycles of benzene/cyclohexane 25 %v/v separation and one regeneration. The overall morphology of the frameworks was maintained

Fig. S94. SEM of NEU-3 (a) before and (b) after 10 cycles of benzene/cyclohexane 10 %v/v separation and one regeneration. The overall morphology of the frameworks was maintained

Fig. S95. TEM of NEU-3 (a) before and (b) after 10 cycles of benzene/cyclohexane 10 %v/v separation and one regeneration. The overall morphology of the frameworks was maintained

Fig. S96. SEM of NEU-3 (a) before and (b) after 10 cycles of benzene/cyclohexane 5 %v/v separation and one regeneration. The overall morphology of the frameworks was maintained

Fig. S97. TEM of NEU-3 (a) before and (b) after 10 cycles of benzene/cyclohexane 5 %v/v separation and one regeneration. The overall morphology of the frameworks was maintained

Fig. S98. SEM of NEU-4 (a) before and (b) after 10 cycles of benzene/cyclohexane 50 %v/v separation and one regeneration. The overall morphology of the frameworks was maintained

Fig. S99. TEM of NEU-4 (a) before and (b) after 10 cycles of benzene/cyclohexane 50 %v/v separation and one regeneration. The overall morphology of the frameworks was maintained

Fig. S100. SEM of NEU-4 (a) before and (b) after 50 cycles of benzene/cyclohexane 25 %v/v separation and four regenerations. The overall morphology of the frameworks was maintained

Fig. S101. TEM of NEU-4 (a) before and (b) after 50 cycles of benzene/cyclohexane 25 %v/v separation and four regenerations. The overall morphology of the frameworks was maintained

Fig. S102. SEM of NEU-4 (a) before and (b) after 10 cycles of benzene/cyclohexane 10 %v/v separation and one regeneration. The overall morphology of the frameworks was maintained

Fig. S103. TEM of NEU-4 (a) before and (b) after 10 cycles of benzene/cyclohexane 10 %v/v separation and one regeneration. The overall morphology of the frameworks was maintained

Fig. S104. SEM of NEU-4 (a) before and (b) after 10 cycles of benzene/cyclohexane 5 %v/v separation and one regeneration. The overall morphology of the frameworks was maintained

Fig. S105. TEM of NEU-4 (a) before and (b) after 10 cycles of benzene/cyclohexane 5 %v/v separation and one regeneration. The overall morphology of the frameworks was maintained

Fig. S106. FTIR spectra of NEU-4 after separation of aliphatic-aromatic hydrocarbons (25 %v/v). NEU-4 did not suffer structural alterations upon selective separations

Fig. S107. SEM of NEU-4 (a) before and (b) after separation of toluene/cyclohexane (25 %v/v). The overall morphology of NEU-4 was maintained

Fig. S108. TEM of NEU-4 (a) before and (b) after separation of toluene/cyclohexane (25 %v/v). The overall morphology of NEU-4 was maintained

Fig. S109. SEM of NEU-4 (a) before and (b) after separation of 1,4-dioxane/cyclohexane (25 %v/v). The overall morphology of NEU-4 was maintained

Fig. S110. TEM of NEU-4 (a) before and (b) after separation of 1,4-dioxane/cyclohexane (25 %v/v). The overall morphology of NEU-4 was maintained

Fig. S111. SEM of NEU-4 (a) before and (b) after separation of p-xylene/cyclohexane (25 %v/v). The overall morphology of NEU-4 was maintained

Fig. S112. TEM of NEU-4 (a) before and (b) after separation of p-xylene/cyclohexane (25 %v/v). The overall morphology of NEU-4 was maintained

Fig. S113. SEM of NEU-4 (a) before and (b) after separation of nitrobenzene/cyclohexane (25 %v/v). The overall morphology of NEU-4 was maintained

Fig. S114. TEM of NEU-4 (a) before and (b) after separation of nitrobenzene/cyclohexane (25 %v/v). The overall morphology of NEU-4 was maintained

Fig. S115. Condensed Fukui functions determined for Bader charges and isosurface of dual descriptor of BPDI²⁻ and benzene

Fig. S116. Condensed Fukui functions determined for Bader charges and isosurface of dual descriptor of PMDA²⁻ and benzene

2. Supplementary Tables

Table S1. Summaries of the EXAFS fitting results of the NEU-3

Table S2. Summaries of the EXAFS fitting results of the NEU-4

Table S3. BET surface area and total pore volume before and after separation

Table S4. Condensed and local Fukui functions of BPDI²⁻ gotten by using Hirshfeld, Mulliken, Voronoi and Bader charges

Table S5. Condensed and local Fukui functions of PMDA²⁻ gotten by using Hirshfeld, Mulliken, Voronoi and Bader charges

Table S6. Condensed and local Fukui functions of cyclohexane gotten by using Hirshfeld, Mulliken, Voronoi and Bader charges

Table S7. Condensed and local Fukui functions of benzene gotten by using Hirshfeld, Mulliken, Voronoi and Bader charges

Table S8. Condensed and local Fukui functions of 1,4-dioxane gotten by using Hirshfeld, Mulliken, Voronoi and Bader charges

Table S9. Condensed and local Fukui functions of toluene gotten by using Hirshfeld, Mulliken, Voronoi and Bader charges

Table S10. Condensed and local Fukui functions of p-xylene gotten by using Hirshfeld, Mulliken, Voronoi and Bader charges

Table S11. Condensed and local Fukui functions of nitrobenzene gotten by using Hirshfeld, Mulliken, Voronoi and Bader charge

Table S12. Benzene/cyclohexane separation performance of different materials

1. Supplementary Figures

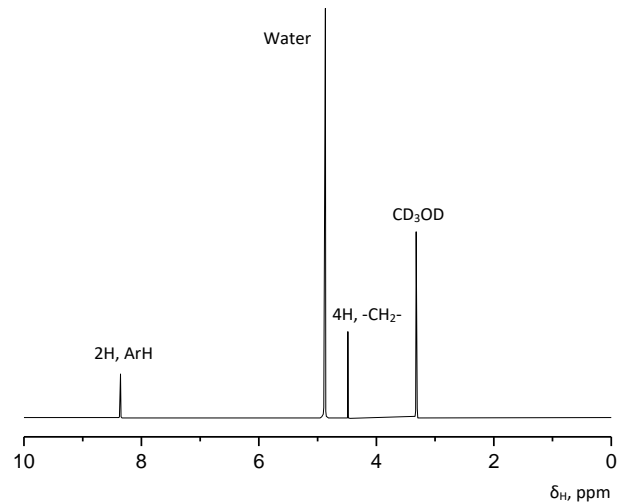


Fig. S1. ¹H NMR (500 MHz, CD₃OD) spectra of H₂BPDI: δ 8.39 (s, 2H, ArH), 4.52 (s, 4H, -CH₂-). H₂BPDI structure is confirmed by ¹H NMR.

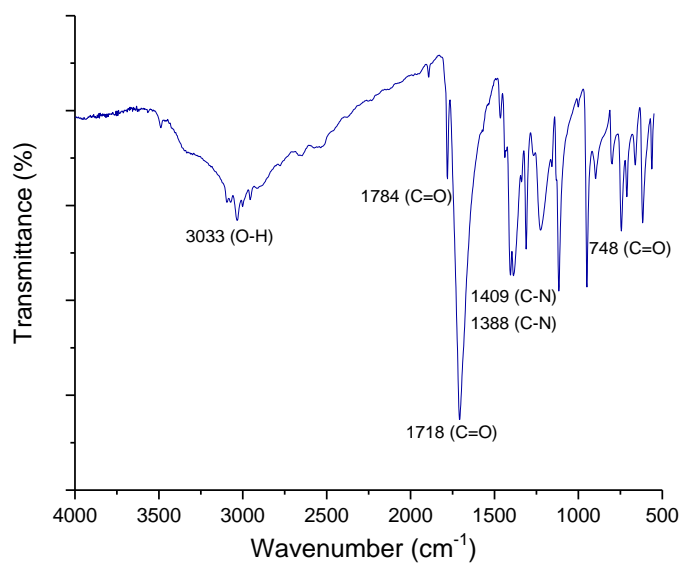


Fig. S2. FTIR (KBr cm^{-1}) spectra of H_2BPDI : 3033 (O-H), 1784 (C=O), 1718 (C=O), 1409 (C-N), 1388 (C-N), 748 (C=O). H_2BPDI structure is confirmed by FTIR.

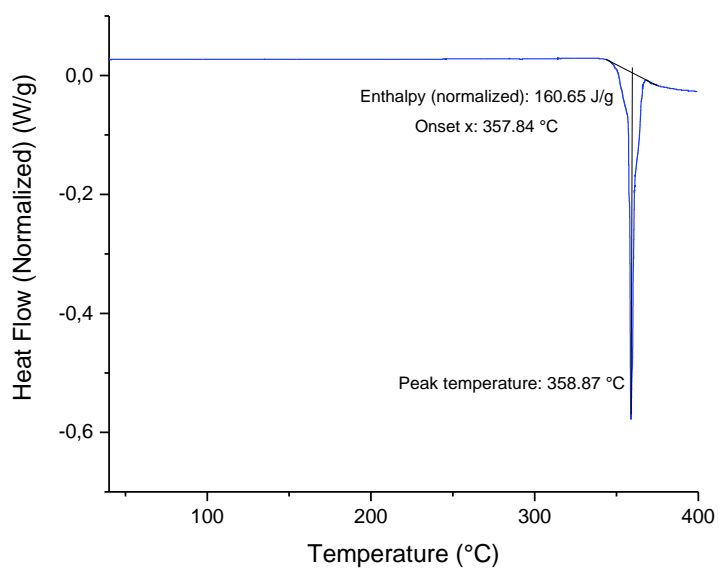


Fig. S3. DSC of H₂BPDI. The analysis shows the heat of boiling as well as the boiling temperature of H₂BPDI. The boiling point depression due to impurities in the sample is zero.

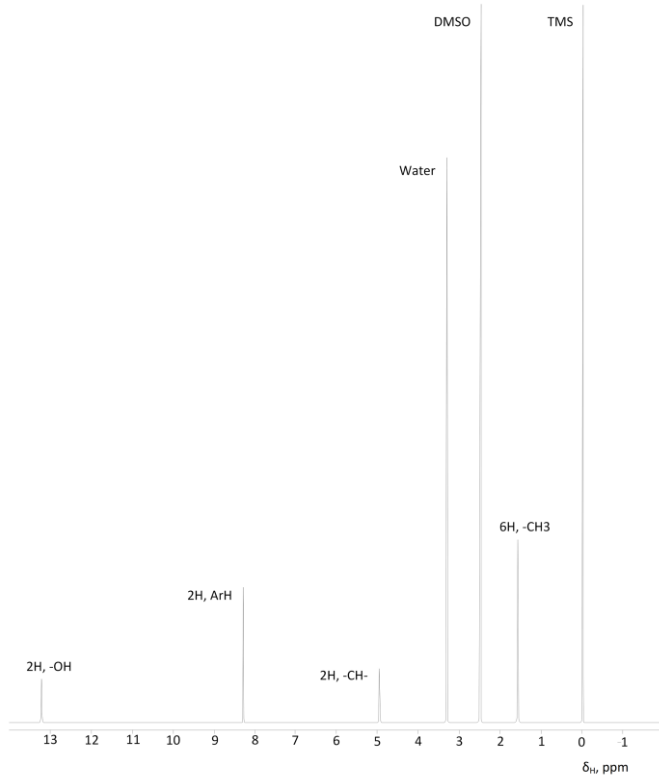


Fig. S4. ^1H NMR (500 MHz, DMSO-d_6) spectra of H_2PMDA : δ 13.26 (s, 2H, -OH), 8.29 (s, 2H, ArH), 4.95 (q, 2H, -CH-), 1.57 (d, 6H, $-\text{CH}_3$). H_2PMDA structure is confirmed by ^1H NMR.

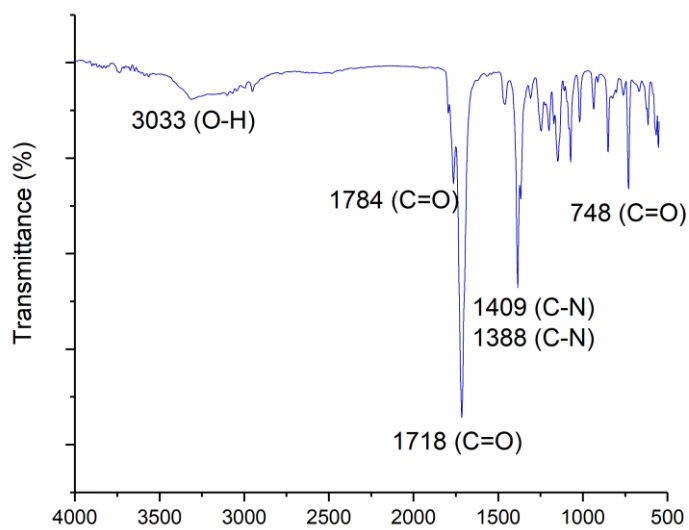


Fig. S5. FTIR (KBr cm^{-1}) spectra of H_2PMDA : 3033 (O-H), 1784 (C=O), 1718 (C=O), 1409 (C-N), 1388 (C-N), 748 (C=O). H_2PMDA structure is confirmed by FTIR.

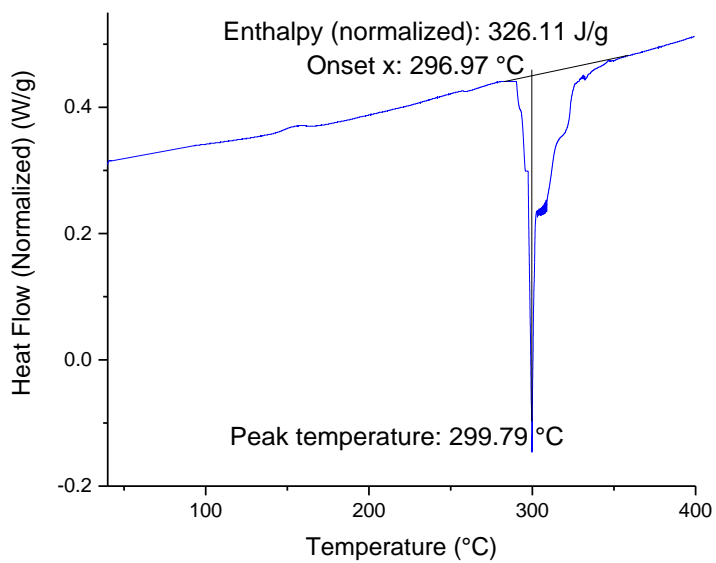
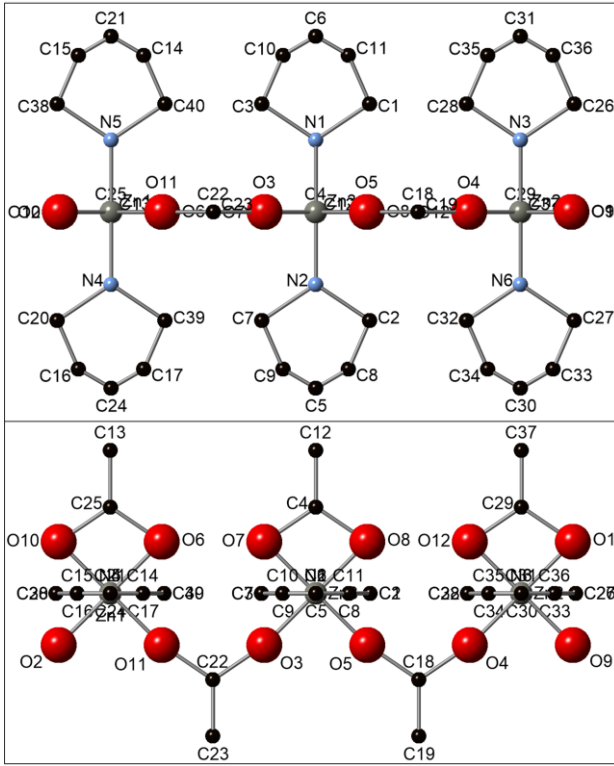


Fig. S6. DSC of H₂PMDA. The analysis shows the heat of boiling as well as the boiling temperature of H₂PMDA. The boiling point depression due to impurities in the sample is zero.



Spacegroup: P1

Lattice Parameters: $a[\text{\AA}] = 21.3078$; $b[\text{\AA}] = 8.6933$; $c[\text{\AA}] = 6.4049$;
 $\alpha[^\circ] = 90.0$; $\beta[^\circ] = 90.0$; $\gamma[^\circ] = 90.0$

Label	Elmt	Fractional Coordinates			Orthogonal Coordinates		
		x	y	z	xor[Å]	yor[Å]	zor[Å]
1. C1	C	0.5695	0.2948	0.4912	11.986	-5.668	4.216
2. C2	C	0.5695	0.7052	0.4912	11.986	-5.668	10.084
3. C3	C	0.4305	0.2948	0.4912	9.060	-5.668	4.216
4. C4	C	0.5000	0.5000	0.6929	10.523	-7.995	7.150
5. C5	C	0.5000	0.8333	0.4912	10.523	-5.668	11.916
6. C6	C	0.5000	0.1667	0.4912	10.523	-5.668	2.384
7. C7	C	0.4305	0.7052	0.4912	9.060	-5.668	10.084
8. C8	C	0.5422	0.7972	0.4912	11.411	-5.668	11.400
9. C9	C	0.4578	0.7972	0.4912	9.635	-5.668	11.400
10. C10	C	0.4578	0.2028	0.4912	9.635	-5.668	2.900
11. C11	C	0.5422	0.2028	0.4912	11.411	-5.668	2.900
12. C12	C	0.5000	0.5000	0.8246	10.523	-9.515	7.150

13.	C13	C	0.2361	0.5000	0.8246	4.969	-9.515	7.150
14.	C14	C	0.2784	0.2028	0.4912	5.859	-5.668	2.900
15.	C15	C	0.1939	0.2028	0.4912	4.081	-5.668	2.900
16.	C16	C	0.1939	0.7972	0.4912	4.081	-5.668	11.400
17.	C17	C	0.2784	0.7972	0.4912	5.859	-5.668	11.400
18.	C18	C	0.6319	0.5000	0.2896	13.299	-3.342	7.150
19.	C19	C	0.6319	0.5000	0.1579	13.299	-1.822	7.150
20.	C20	C	0.1667	0.7052	0.4912	3.508	-5.668	10.084
21.	C21	C	0.2361	0.1667	0.4912	4.969	-5.668	2.384
22.	C22	C	0.3680	0.5000	0.2896	7.745	-3.342	7.150
23.	C23	C	0.3680	0.5000	0.1579	7.745	-1.822	7.150
24.	C24	C	0.2361	0.8333	0.4912	4.969	-5.668	11.916
25.	C25	C	0.2361	0.5000	0.6929	4.969	-7.995	7.150
26.	C26	C	0.8333	0.2948	0.4912	17.537	-5.668	4.216
27.	C27	C	0.8333	0.7052	0.4912	17.537	-5.668	10.084
28.	C28	C	0.6944	0.2948	0.4912	14.614	-5.668	4.216
29.	C29	C	0.7639	0.5000	0.6929	16.077	-7.995	7.150
30.	C30	C	0.7639	0.8333	0.4912	16.077	-5.668	11.916
31.	C31	C	0.7639	0.1667	0.4912	16.077	-5.668	2.384
32.	C32	C	0.6944	0.7052	0.4912	14.614	-5.668	10.084
33.	C33	C	0.8061	0.7972	0.4912	16.965	-5.668	11.400
34.	C34	C	0.7217	0.7972	0.4912	15.189	-5.668	11.400
35.	C35	C	0.7217	0.2028	0.4912	15.189	-5.668	2.900
36.	C36	C	0.8061	0.2028	0.4912	16.965	-5.668	2.900
37.	C37	C	0.7639	0.5000	0.8246	16.077	-9.515	7.150
38.	C38	C	0.1667	0.2948	0.4912	3.508	-5.668	4.216
39.	C39	C	0.3056	0.7052	0.4912	6.432	-5.668	10.084
40.	C40	C	0.3056	0.2948	0.4912	6.432	-5.668	4.216
41.	N1	N	0.5000	0.3632	0.4912	10.523	-5.668	5.194
42.	N2	N	0.5000	0.6368	0.4912	10.523	-5.668	9.106
43.	N3	N	0.7639	0.3632	0.4912	16.077	-5.668	5.194
44.	N4	N	0.2361	0.6368	0.4912	4.969	-5.668	9.106
45.	N5	N	0.2361	0.3632	0.4912	4.969	-5.668	5.194
46.	N6	N	0.7639	0.6368	0.4912	16.077	-5.668	9.106

47.	O1	O	0.8298	0.5000	0.6115	17.464	-7.056	7.150
48.	O2	O	0.1701	0.5000	0.3710	3.580	-4.281	7.150
49.	O3	O	0.4340	0.5000	0.3710	9.134	-4.281	7.150
50.	O4	O	0.6978	0.5000	0.3710	14.686	-4.281	7.150
51.	O5	O	0.5659	0.5000	0.3710	11.910	-4.281	7.150
52.	O6	O	0.3021	0.5000	0.6115	6.358	-7.056	7.150
53.	O7	O	0.4341	0.5000	0.6115	9.136	-7.056	7.150
54.	O8	O	0.5660	0.5000	0.6115	11.912	-7.056	7.150
55.	O9	O	0.8298	0.5000	0.3710	17.464	-4.281	7.150
56.	O10	O	0.1702	0.5000	0.6115	3.582	-7.056	7.150
57.	O11	O	0.3021	0.5000	0.3710	6.358	-4.281	7.150
58.	O12	O	0.6979	0.5000	0.6115	14.688	-7.056	7.150
59.	Zn1	Zn	0.2361	0.5000	0.4912	4.969	-5.668	7.150
60.	Zn2	Zn	0.7639	0.5000	0.4912	16.077	-5.668	7.150
61.	Zn3	Zn	0.5000	0.5000	0.4912	10.523	-5.668	7.150

Fig. S7. Coordinates of each atom in the local molecular structure of zinc within NEU-3.

Atom labelling scheme: C = black; O = red; N = blue; Zn = grey. H atoms are omitted for clarity.

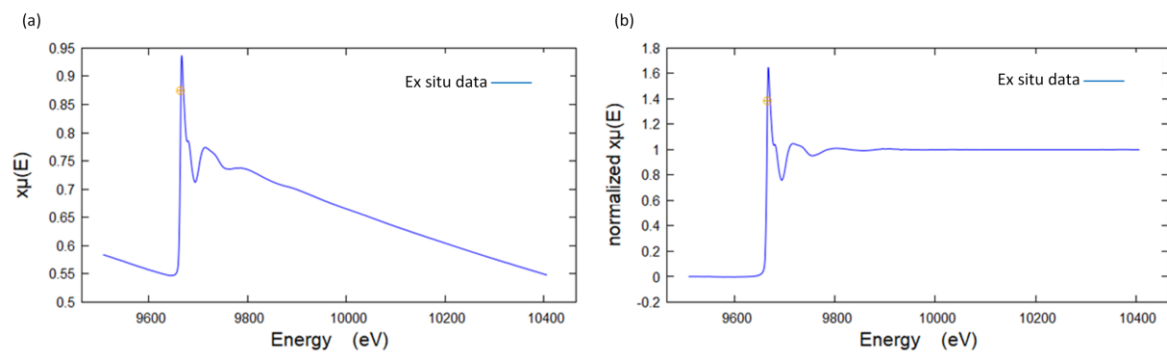
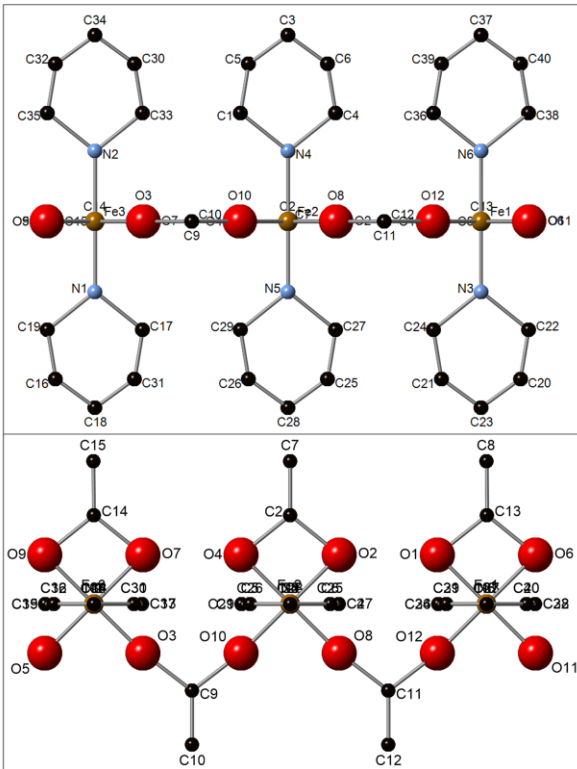


Fig. S8. X-ray absorption spectrum at the Zn K-edge of the NEU-3 before (a) and after normalization (b).



Spacegroup: P1

Lattice Parameters: $a[\text{\AA}] = 21.3078$; $b[\text{\AA}] = 8.6933$; $c[\text{\AA}] = 6.4049$;
 $\alpha[^\circ] = 90.0$; $\beta[^\circ] = 90.0$; $\gamma[^\circ] = 90.0$

Label	Elmt	Fractional Coordinates			Orthogonal Coordinates		
		x	y	z	xor[{\AA}]	yor[{\AA}]	zor[{\AA}]
1. C1	C	0.4507	0.6456	0.5069	12.515	13.836	8.107
2. C2	C	0.5000	0.5000	0.3502	13.884	10.716	5.601
3. C3	C	0.5000	0.7500	0.5069	13.884	16.074	8.107
4. C4	C	0.5493	0.6456	0.5069	15.253	13.836	8.107
5. C5	C	0.4590	0.7114	0.5069	12.746	15.247	8.107
6. C6	C	0.5410	0.7114	0.5069	15.022	15.247	8.107
7. C7	C	0.5000	0.5000	0.2552	13.884	10.716	4.082
8. C8	C	0.7000	0.5000	0.2552	19.438	10.716	4.082
9. C9	C	0.4000	0.5000	0.6602	11.107	10.716	10.559
10. C10	C	0.4000	0.5000	0.7552	11.107	10.716	12.079
11. C11	C	0.6000	0.5000	0.6601	16.661	10.716	10.558
12. C12	C	0.6000	0.5000	0.7552	16.661	10.716	12.079

13.	C13	C	0.7005	0.5000	0.3503	19.451	10.716	5.603
14.	C14	C	0.3000	0.5000	0.3503	8.330	10.716	5.603
15.	C15	C	0.2995	0.5000	0.2552	8.317	10.716	4.082
16.	C16	C	0.2591	0.2887	0.5069	7.195	6.187	8.107
17.	C17	C	0.3493	0.3544	0.5069	9.699	7.596	8.107
18.	C18	C	0.3000	0.2500	0.5069	8.330	5.358	8.107
19.	C19	C	0.2507	0.3544	0.5069	6.961	7.596	8.107
20.	C20	C	0.7409	0.2887	0.5069	20.573	6.187	8.107
21.	C21	C	0.6590	0.2887	0.5069	18.299	6.187	8.107
22.	C22	C	0.7493	0.3544	0.5069	20.807	7.595	8.107
23.	C23	C	0.6999	0.2500	0.5069	19.435	5.358	8.107
24.	C24	C	0.6506	0.3544	0.5069	18.066	7.595	8.107
25.	C25	C	0.5410	0.2887	0.5069	15.022	6.187	8.107
26.	C26	C	0.4590	0.2887	0.5069	12.746	6.187	8.107
27.	C27	C	0.5493	0.3544	0.5069	15.253	7.596	8.107
28.	C28	C	0.5000	0.2500	0.5069	13.884	5.358	8.107
29.	C29	C	0.4507	0.3544	0.5069	12.515	7.596	8.107
30.	C30	C	0.3410	0.7114	0.5069	9.469	15.247	8.107
31.	C31	C	0.3410	0.2887	0.5069	9.469	6.187	8.107
32.	C32	C	0.2591	0.7114	0.5069	7.195	15.247	8.107
33.	C33	C	0.3493	0.6456	0.5069	9.699	13.836	8.107
34.	C34	C	0.3000	0.7500	0.5069	8.330	16.074	8.107
35.	C35	C	0.2507	0.6456	0.5069	6.961	13.836	8.107
36.	C36	C	0.6506	0.6456	0.5069	18.066	13.836	8.107
37.	C37	C	0.6999	0.7500	0.5069	19.435	16.074	8.107
38.	C38	C	0.7493	0.6456	0.5069	20.807	13.836	8.107
39.	C39	C	0.6590	0.7114	0.5069	18.299	15.247	8.107
40.	C40	C	0.7409	0.7114	0.5069	20.573	15.247	8.107
41.	Fe1	Fe	0.7000	0.5000	0.5069	19.438	10.716	8.107
42.	Fe2	Fe	0.5000	0.5000	0.5069	13.884	10.716	8.107
43.	Fe3	Fe	0.3000	0.5000	0.5069	8.330	10.716	8.107
44.	N1	N	0.3000	0.4057	0.5069	8.330	8.695	8.107
45.	N2	N	0.3000	0.5943	0.5069	8.330	12.737	8.107
46.	N3	N	0.7000	0.4057	0.5069	19.438	8.695	8.107

47.	N4	N	0.5000	0.5943	0.5069	13.884	12.737	8.107
48.	N5	N	0.5000	0.4057	0.5069	13.884	8.695	8.107
49.	N6	N	0.6999	0.5943	0.5069	19.435	12.737	8.107
50.	O1	O	0.6500	0.5000	0.4201	18.049	10.716	6.719
51.	O2	O	0.5499	0.5000	0.4201	15.270	10.716	6.719
52.	O3	O	0.3501	0.5000	0.5936	9.722	10.716	9.494
53.	O4	O	0.4500	0.5000	0.4201	12.496	10.716	6.719
54.	O5	O	0.2500	0.5000	0.5936	6.942	10.716	9.494
55.	O6	O	0.7500	0.5000	0.4201	20.826	10.716	6.719
56.	O7	O	0.3500	0.5000	0.4201	9.719	10.716	6.719
57.	O8	O	0.5500	0.5000	0.5936	15.272	10.716	9.494
58.	O9	O	0.2500	0.5000	0.4201	6.942	10.716	6.719
59.	O10	O	0.4500	0.5000	0.5936	12.496	10.716	9.494
60.	O11	O	0.7500	0.5000	0.5936	20.826	10.716	9.494
61.	O12	O	0.6500	0.5000	0.5936	18.049	10.716	9.494

Fig. S9. Coordinates of each atom in the local molecular structure of iron within NEU-4.

Atom labelling scheme: C = black; O = red; N = blue; Fe = brown. H atoms are omitted for clarity.

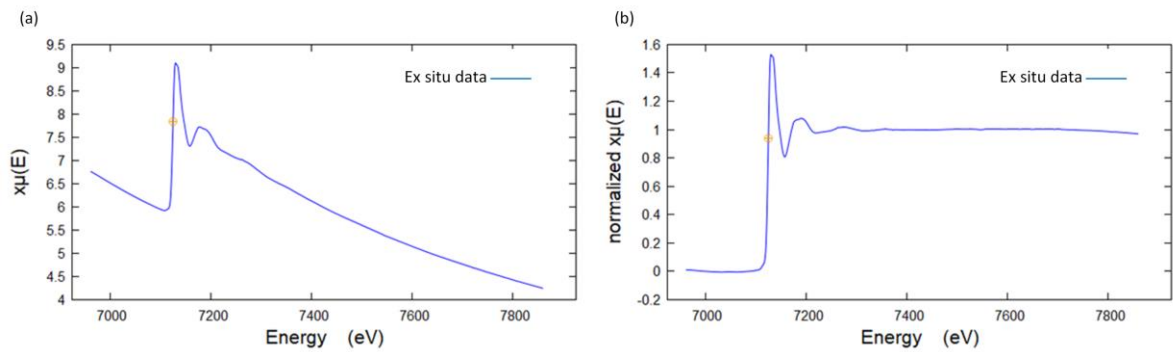


Fig. S10. X-ray absorption spectrum at the Fe K-edge of the NEU-4 before (a) and after normalization (b).

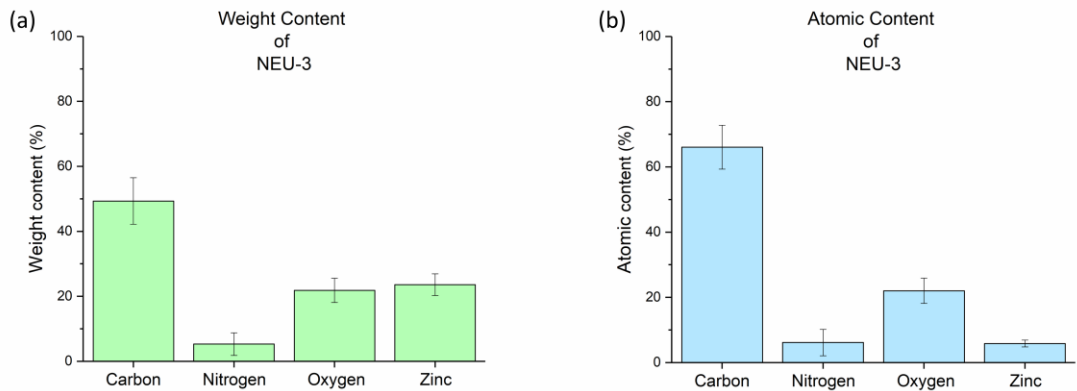


Fig. S11. EDX characterization of NEU-3. It shows the presence of zinc (23.57 %w, 5.83 %m) within the sample, as well as that of carbon (49.31 %w, 66.06 %m), nitrogen (5.29 %w, 6.12 %m), and oxygen (21.82 %w, 21.99 %m). Both weight and atomic content were determined in different zones and the average was calculated.

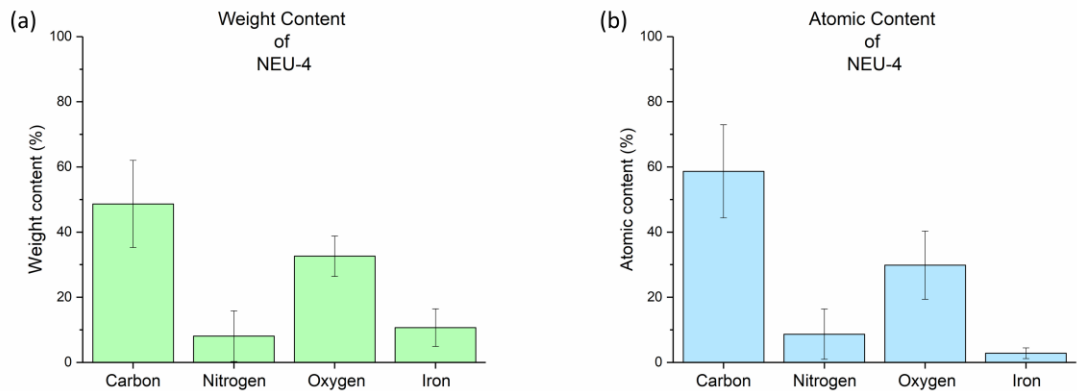


Fig. S12. EDX characterization of NEU-4. It shows the presence of iron (10.69 %w, 2.83 %m) within the sample, as well as that of carbon (48.65 %w, 58.66 %m), nitrogen (8.06 %w, 8.66 %m), and oxygen (32.60 %w, 29.86 %m). Both weight and atomic content were determined in different zones and the average was calculated.

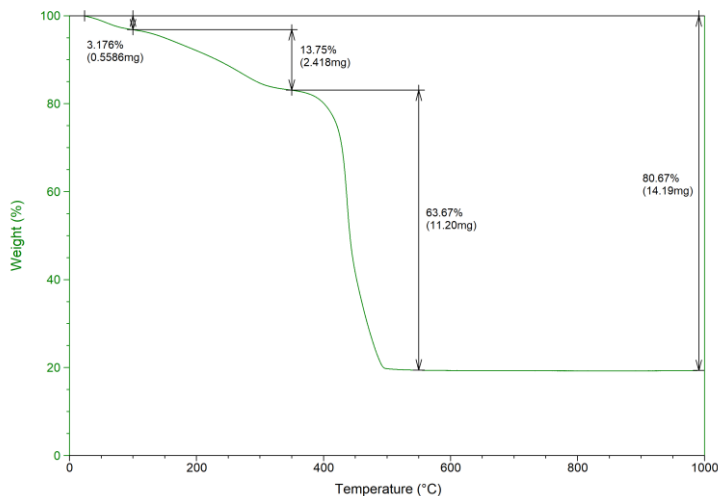


Fig. S13. TGA of NEU-3 from room temperature to 1000 °C at a rate of 5 °C min⁻¹ under a nitrogen flow. NEU-3 showed a total mass loss of ~80.7 wt% on heating up to 1000 °C. The mass loss occurred in three steps: (1) mass loss of ~3.2 wt% at ~100 °C due to the desorption of trapped moisture, which is common in porous materials with a high surface area, (2) mass loss of ~13.8 wt% on heating up to ~350 °C due to the decomposition of ligated pyridine in axial position, (3) mass loss of ~63.7 wt% on heating up to 550 °C due to the decomposition of the remaining PMDA²⁻ ligands.

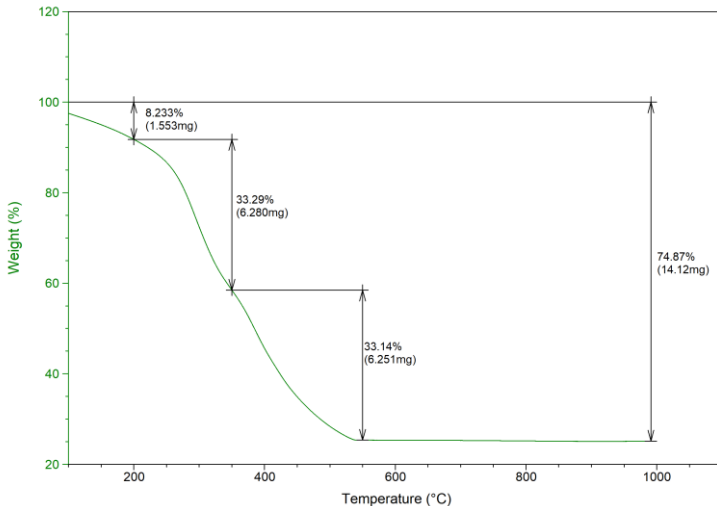


Fig. S14. TGA of NEU-4 from room temperature to 1000 °C at a rate of 5 °C min⁻¹ under a nitrogen flow. NEU-4 showed a total mass loss of ~74.9 wt% on heating up to 1000 °C. The mass loss occurred in three steps: (1) mass loss of ~8.2 wt% at ~200 °C due to the desorption of trapped moisture, which is common in porous materials with a high surface area, (2) mass loss of ~33.3 wt% on heating up to ~350 °C due to the decomposition of ligated pyridine in axial position, (3) mass loss of ~33.1 wt% on heating up to 550 °C due to the decomposition of the remaining PMDA²⁻ ligands.

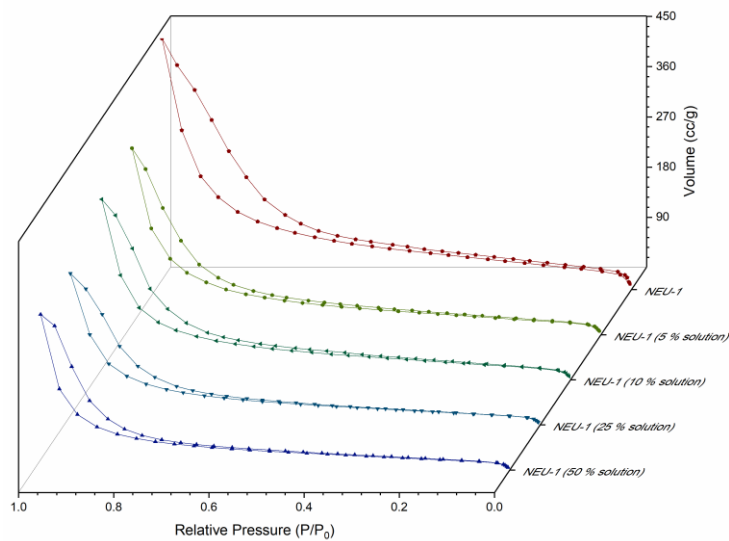


Fig. S15. Nitrogen adsorption/desorption isotherms of pristine NEU-1c as well as NEU-1c after one cycle of benzene-cyclohexane (50 % v/v, 25 % v/v, 10 % v/v and 5 % v/v) separation.

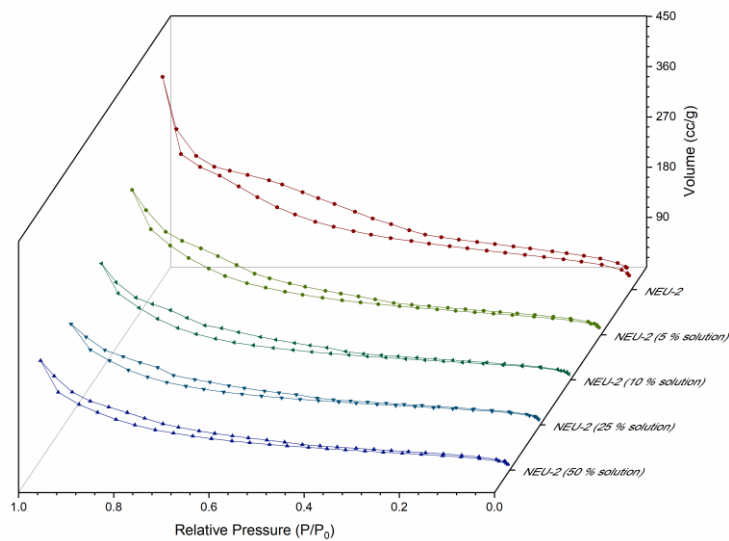


Fig. S16. Nitrogen adsorption/desorption isotherms of pristine NEU-2 as well as NEU-2 after one cycle of benzene-cyclohexane (50 % v/v, 25 % v/v, 10 % v/v and 5 % v/v) separation.

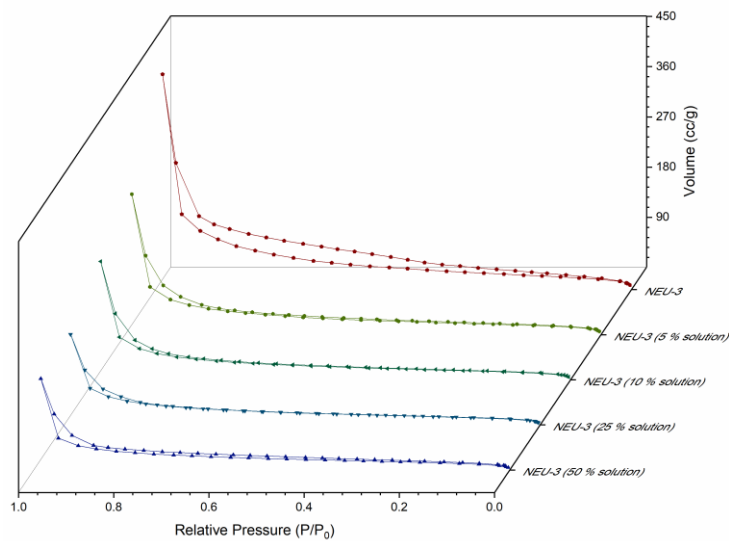


Fig. S17. Nitrogen adsorption/desorption isotherms of pristine NEU-3 as well as NEU-3 after one cycle of benzene-cyclohexane (50 % v/v, 25 % v/v, 10 % v/v and 5 % v/v) separation.

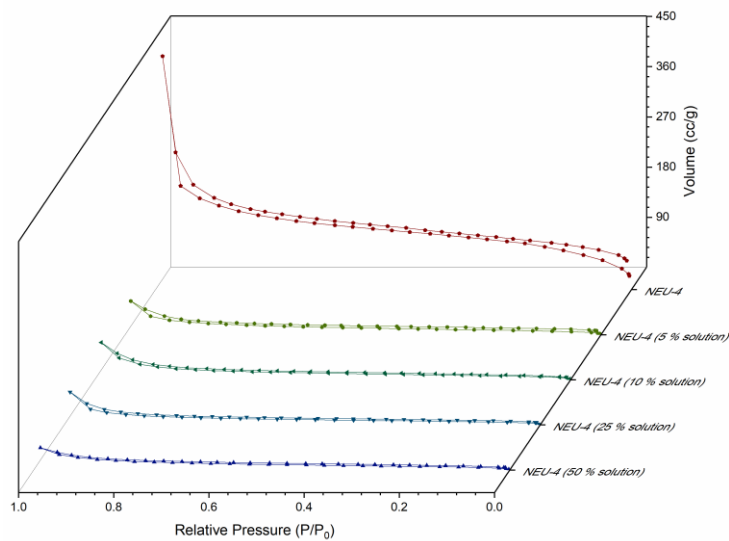


Fig. S18. Nitrogen adsorption/desorption isotherms of pristine NEU-4 as well as NEU-4 after one cycle of benzene-cyclohexane (50 % v/v, 25 % v/v, 10 % v/v and 5 % v/v) separation.

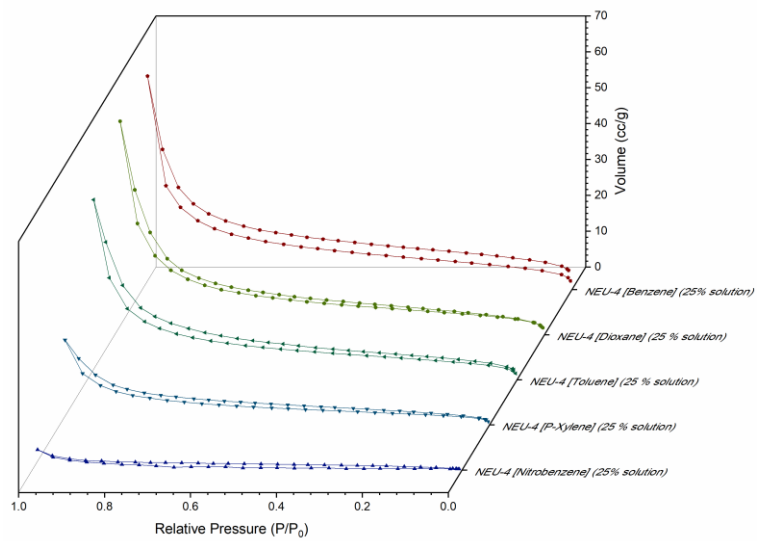


Fig. S19. Nitrogen adsorption/desorption isotherms of NEU-4 after one cycle of aromatic hydrocarbon-cyclohexane separation.

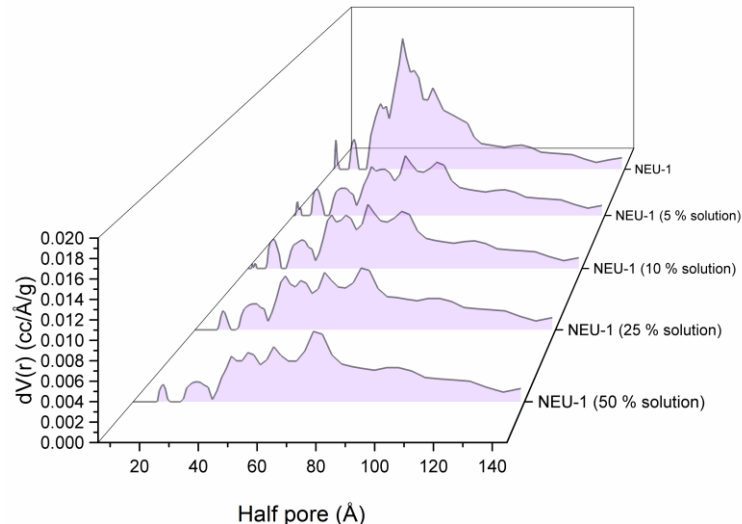


Fig. S20. DFT pore analysis of pristine NEU-1c as well as NEU-1c after one cycle of benzene-cyclohexane (50 % v/v, 25 % v/v, 10 % v/v and 5 % v/v) separation.

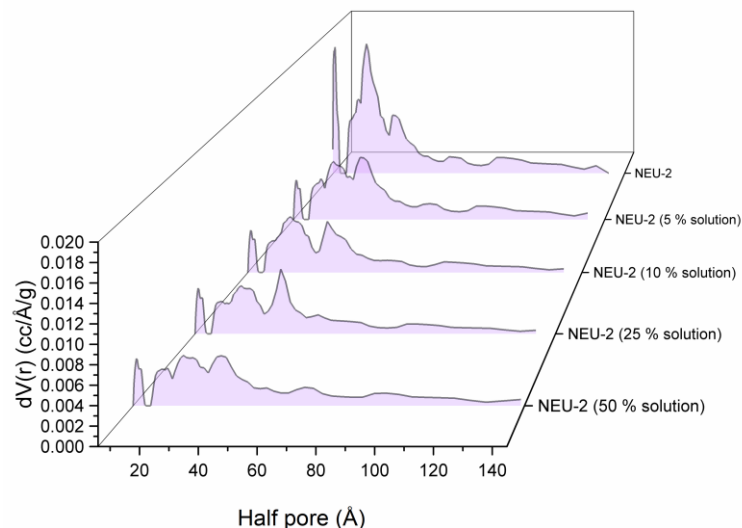


Fig. S21. DFT pore analysis of pristine NEU-2 as well as NEU-2 after one cycle of benzene-cyclohexane (50 % v/v, 25 % v/v, 10 % v/v and 5 % v/v) separation.

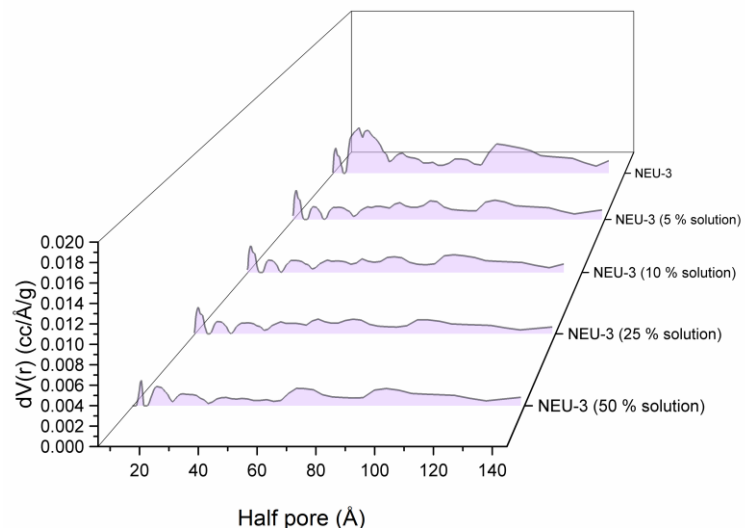


Fig. S22. DFT pore analysis of pristine NEU-3 as well as NEU-3 after one cycle of benzene-cyclohexane (50 % v/v, 25 % v/v, 10 % v/v and 5 % v/v) separation.

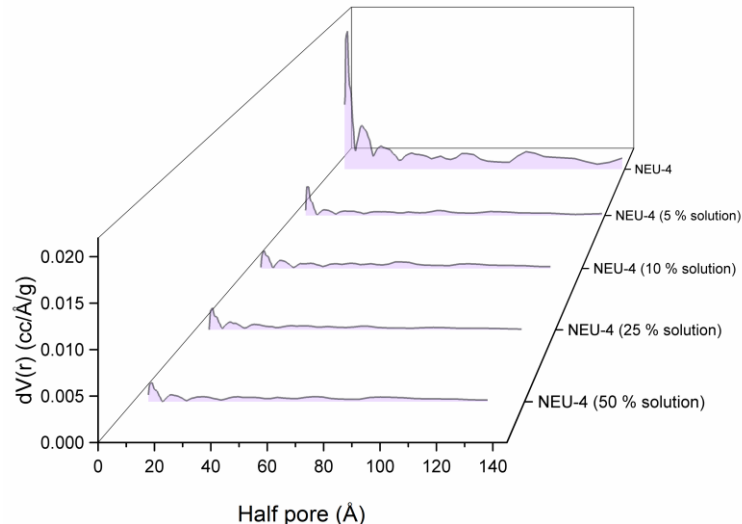


Fig. S23. DFT pore analysis of pristine NEU-4 as well as NEU-4 after one cycle of benzene-cyclohexane (50 %v/v, 25 %v/v, 10 %v/v and 5 %v/v) separation.

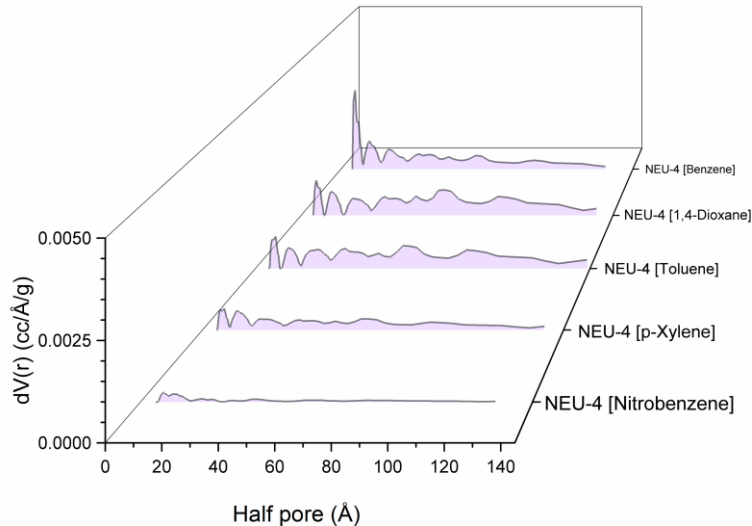


Fig. S24. DFT pore analysis of NEU-4 after one cycle of aromatic hydrocarbon-cyclohexane separation.

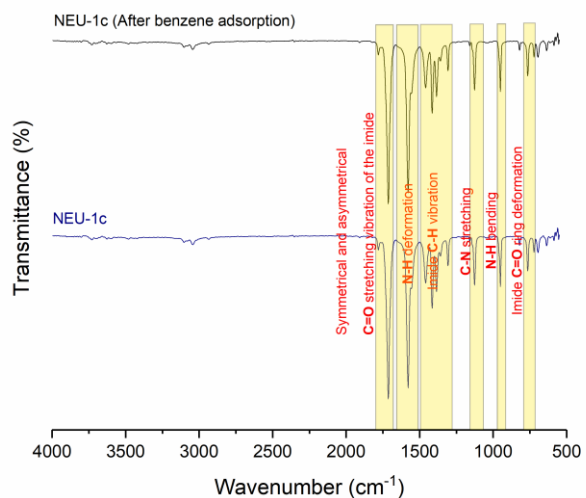


Fig. S25. FTIR spectra of NEU-1c before and after benzene sorption.

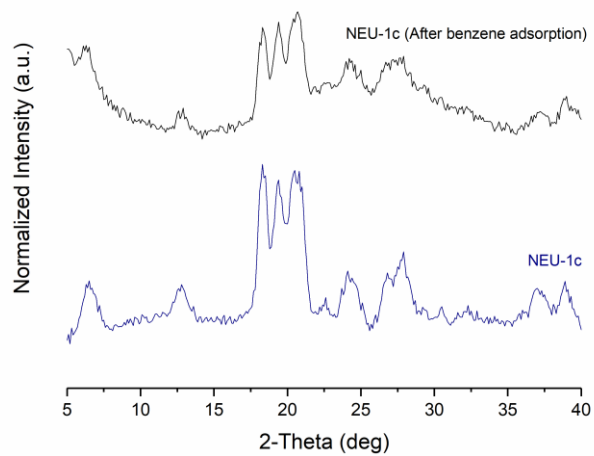


Fig. S26. XRD of NEU-1c before and after benzene sorption.

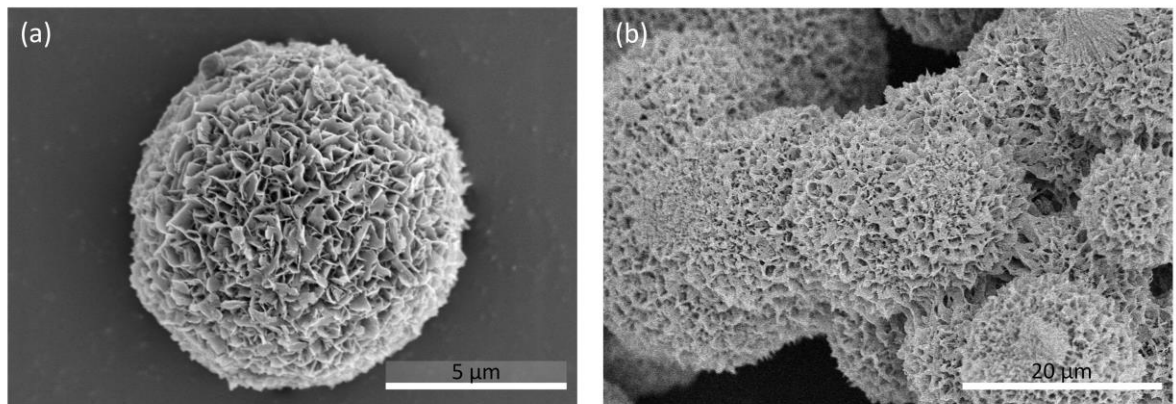


Fig. S27. SEM of NEU-1c before (a) and after (b) benzene sorption.

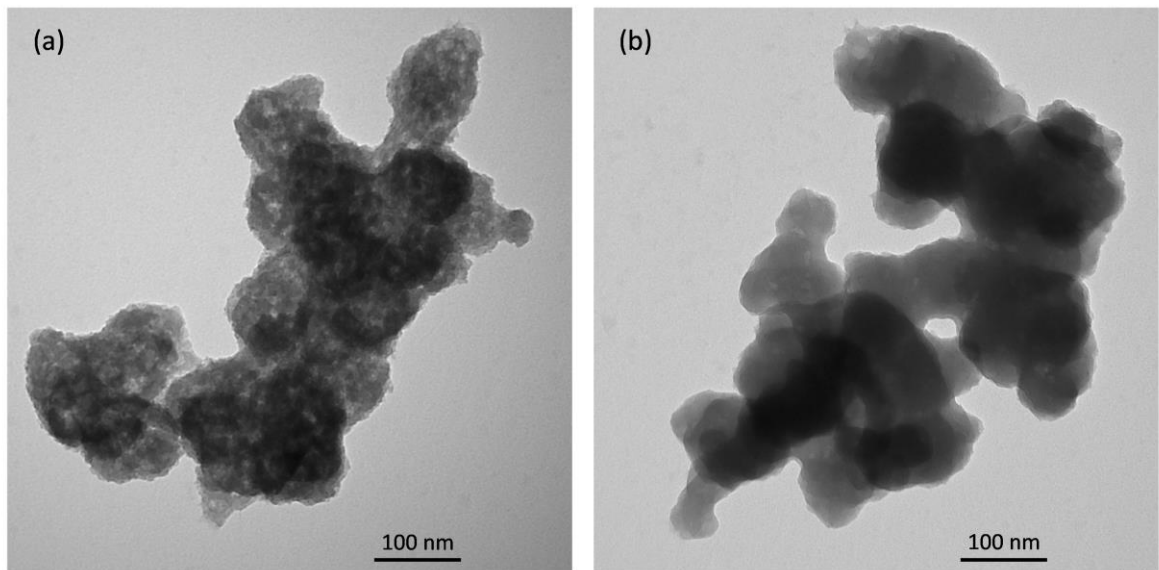


Fig. S28. TEM of NEU-1c before (a) and after (b) benzene sorption.

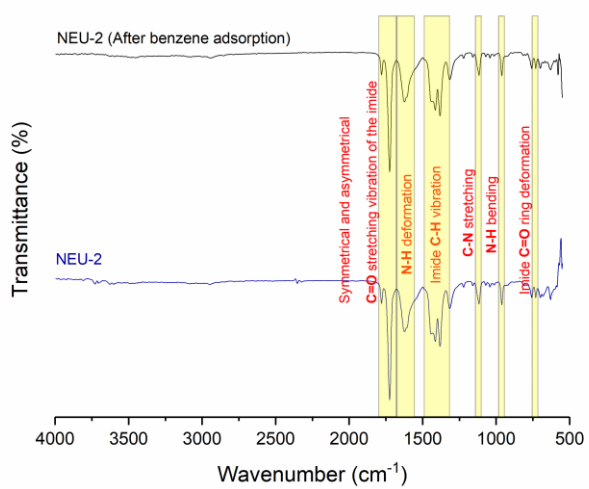


Fig. S29. FTIR spectra of NEU-2 before and after benzene sorption.

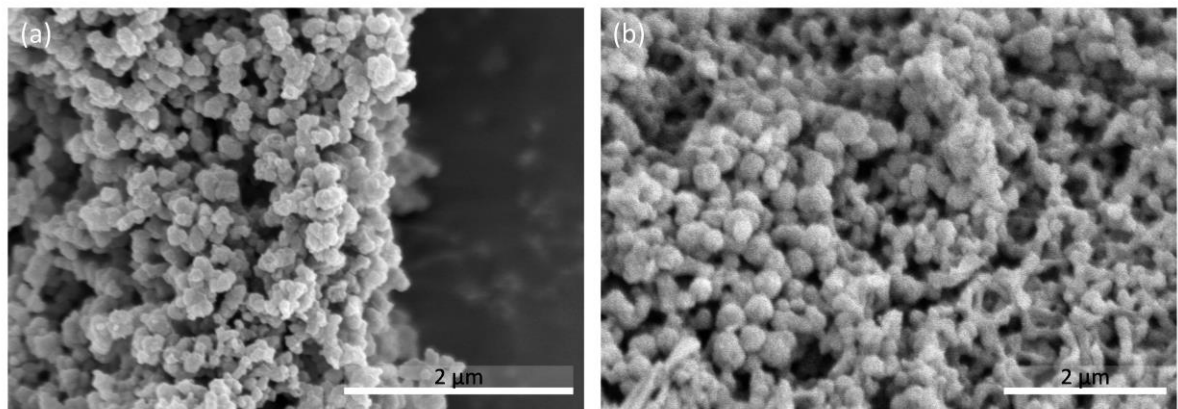


Fig. S30. SEM of NEU-2 before (a) and after (b) benzene sorption.

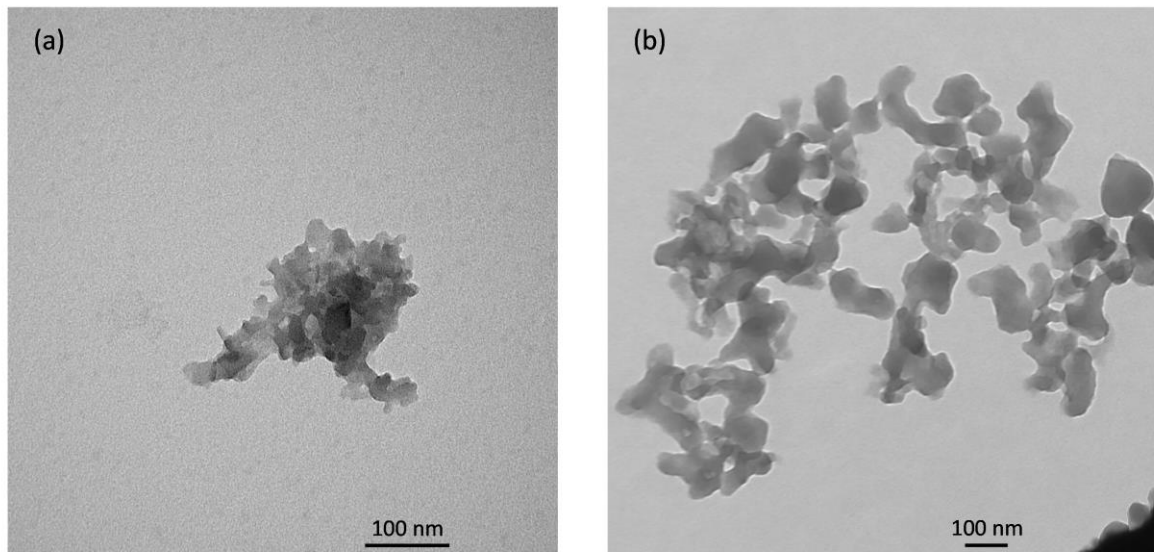


Fig. S31. TEM of NEU-2 before (a) and after (b) benzene sorption.

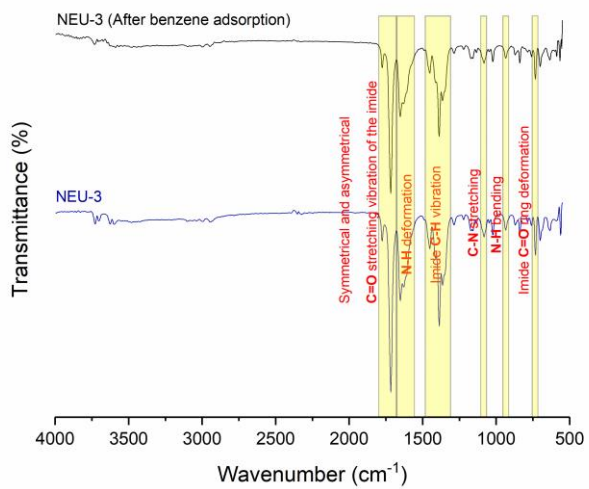


Fig. S32. FTIR spectra of NEU-3 before and after benzene sorption.

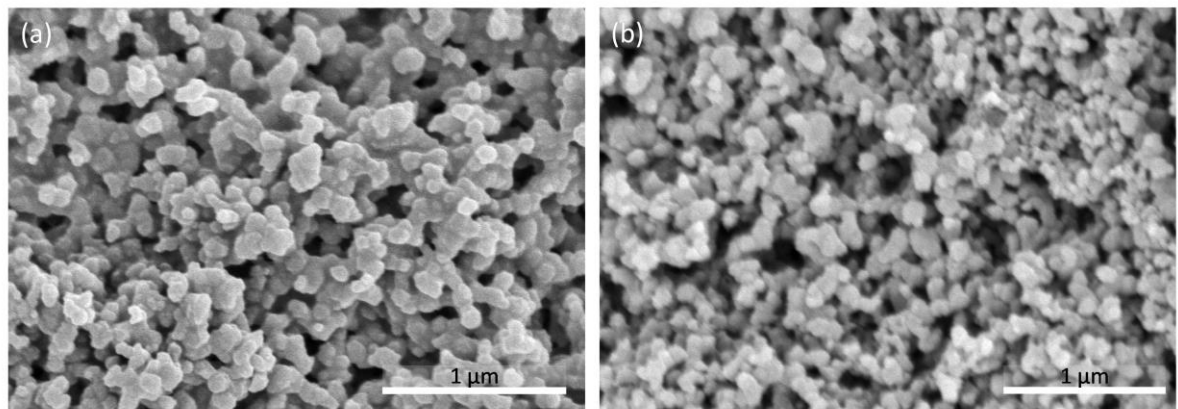


Fig. S33. SEM of NEU-3 before (a) and after (b) benzene sorption.

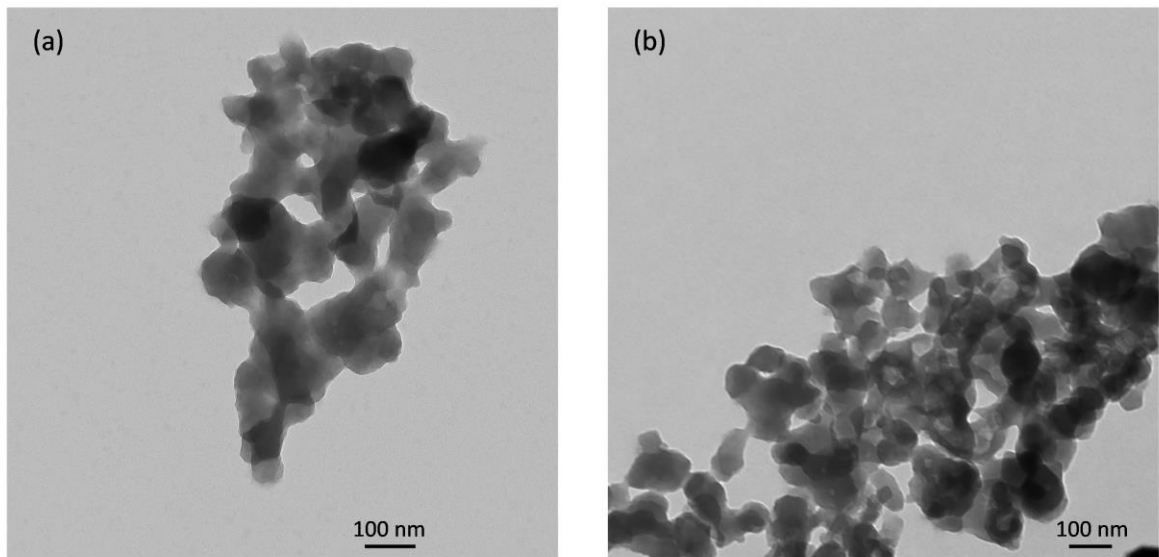


Fig. S34. TEM of NEU-3 before and after benzene sorption.

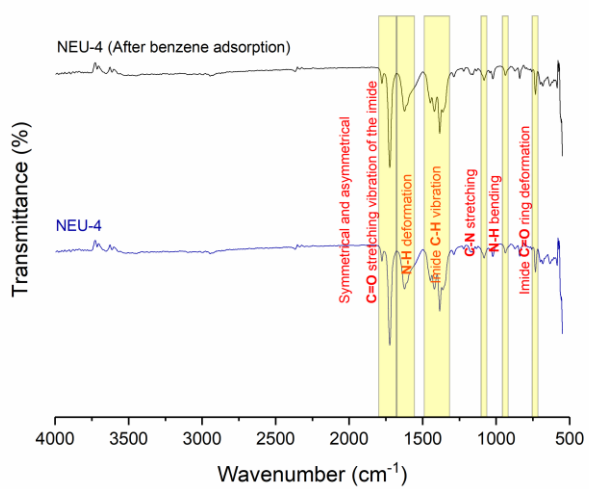


Fig. S35. FTIR spectra of NEU-4 before and after benzene sorption.

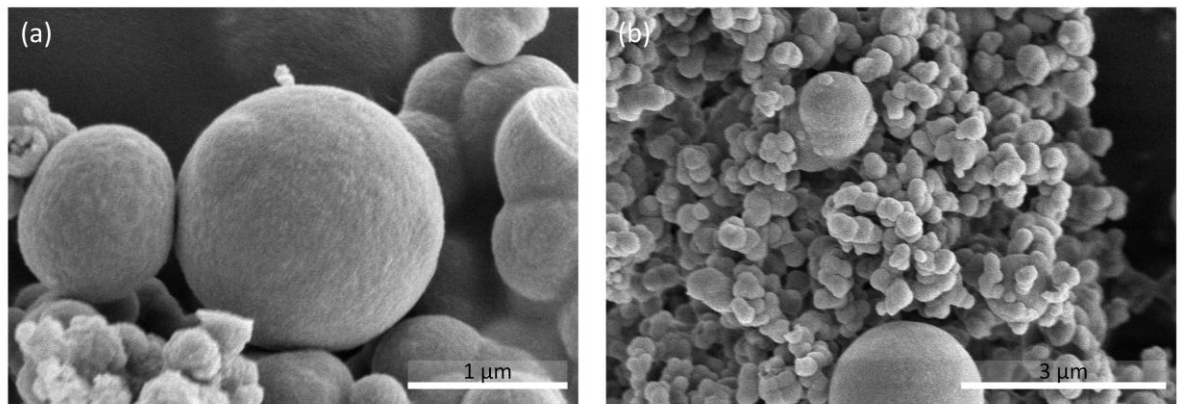


Fig. S36. SEM of NEU-4 before (a) and after (b) benzene sorption.

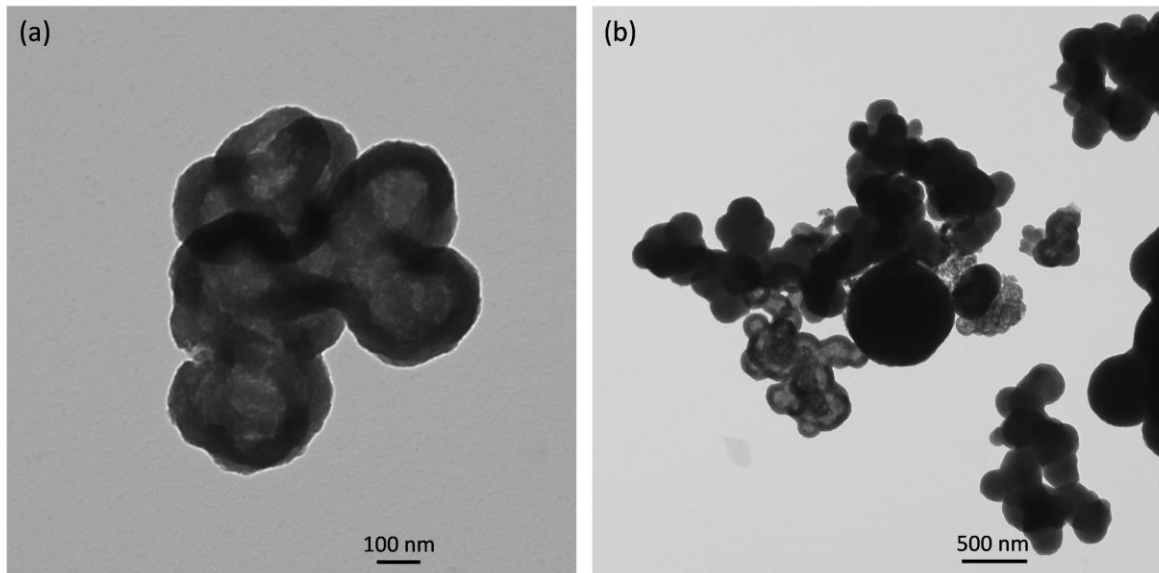


Fig. S37. TEM of NEU-4 before and after benzene sorption.

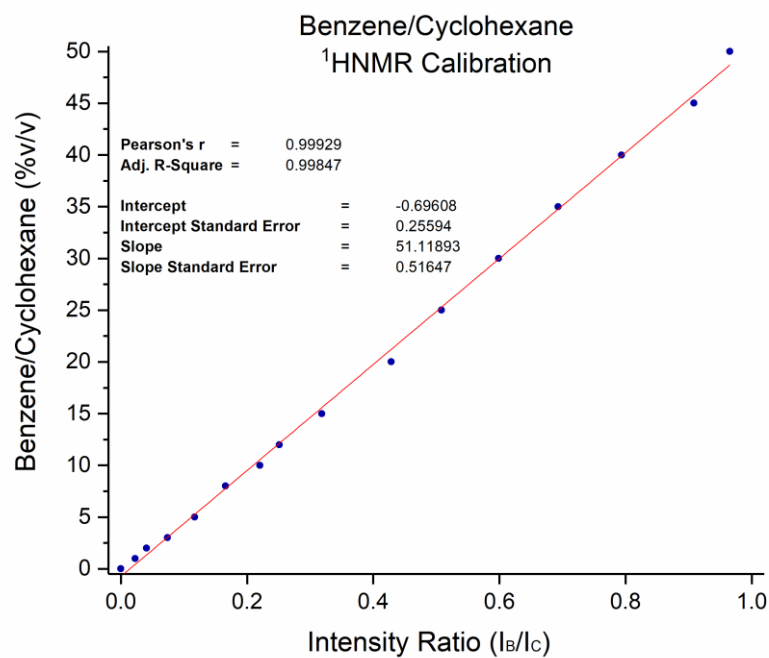


Fig. S38. Regression test between intensity ratio – of benzene and cyclohexane ^1H NMR signals – and volume ratio of the solution.

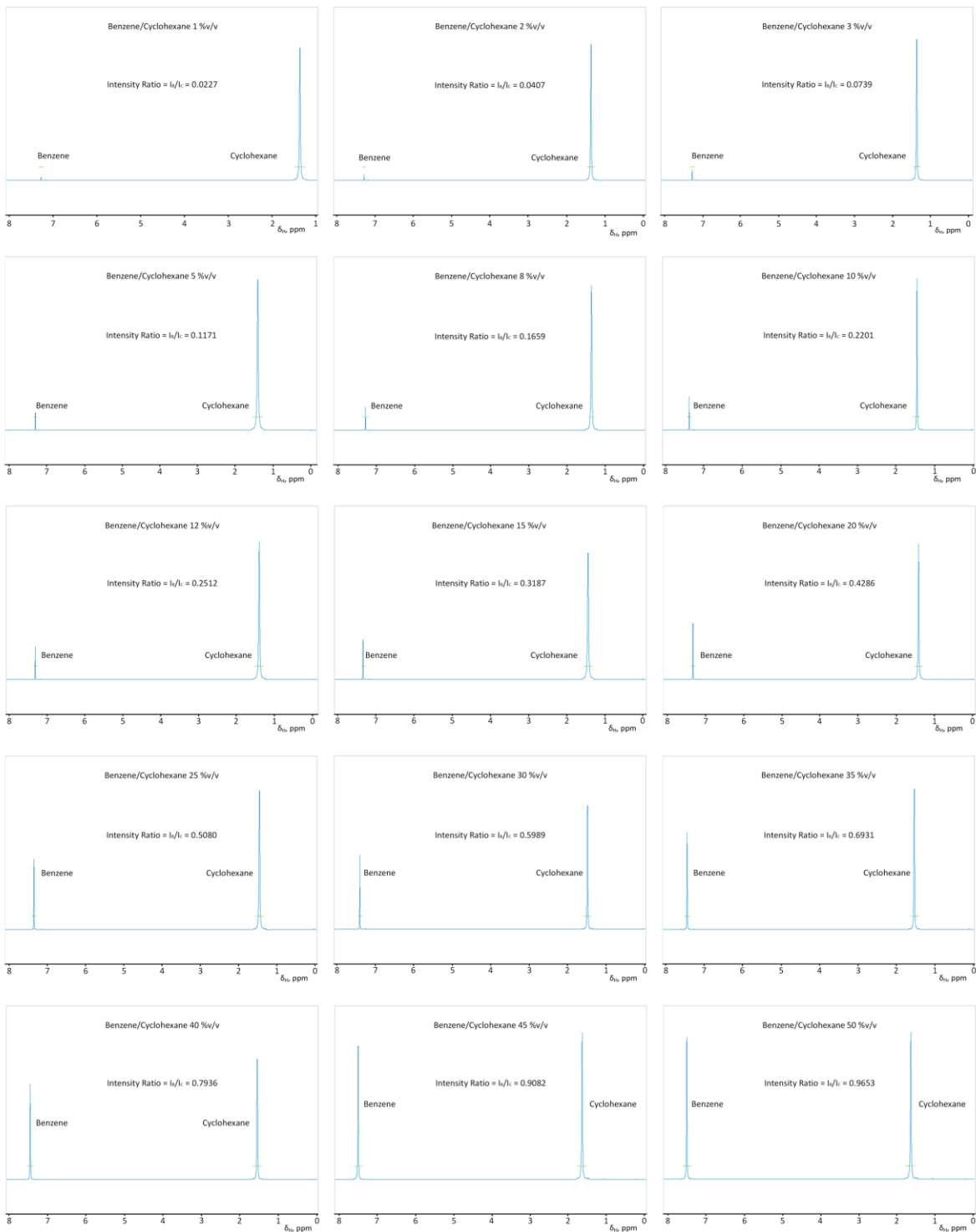


Fig. S39. ${}^1\text{H}$ NMR of benzene and cyclohexane mixtures: 1 %v/v, 2 %v/v, 3 %v/v, 5 %v/v, 8 %v/v, 10 %v/v, 12 %v/v, 15 %v/v, 20 %v/v, 25 %v/v, 30 %v/v, 35 %v/v, 40 %v/v, 45 %v/v, and 50 %v/v.

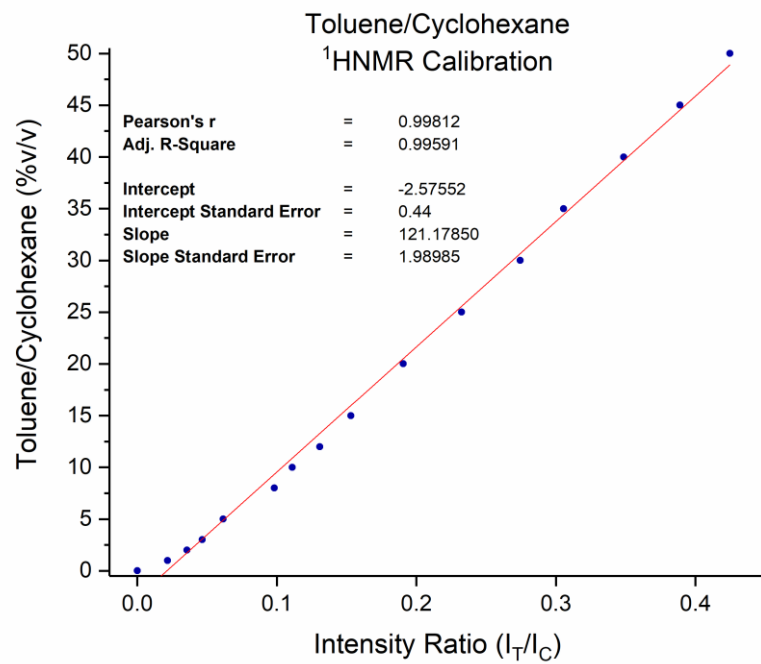


Fig. S40. Regression test between intensity ratio – of toluene and cyclohexane ^1H NMR signals – and volume ratio of the solution.

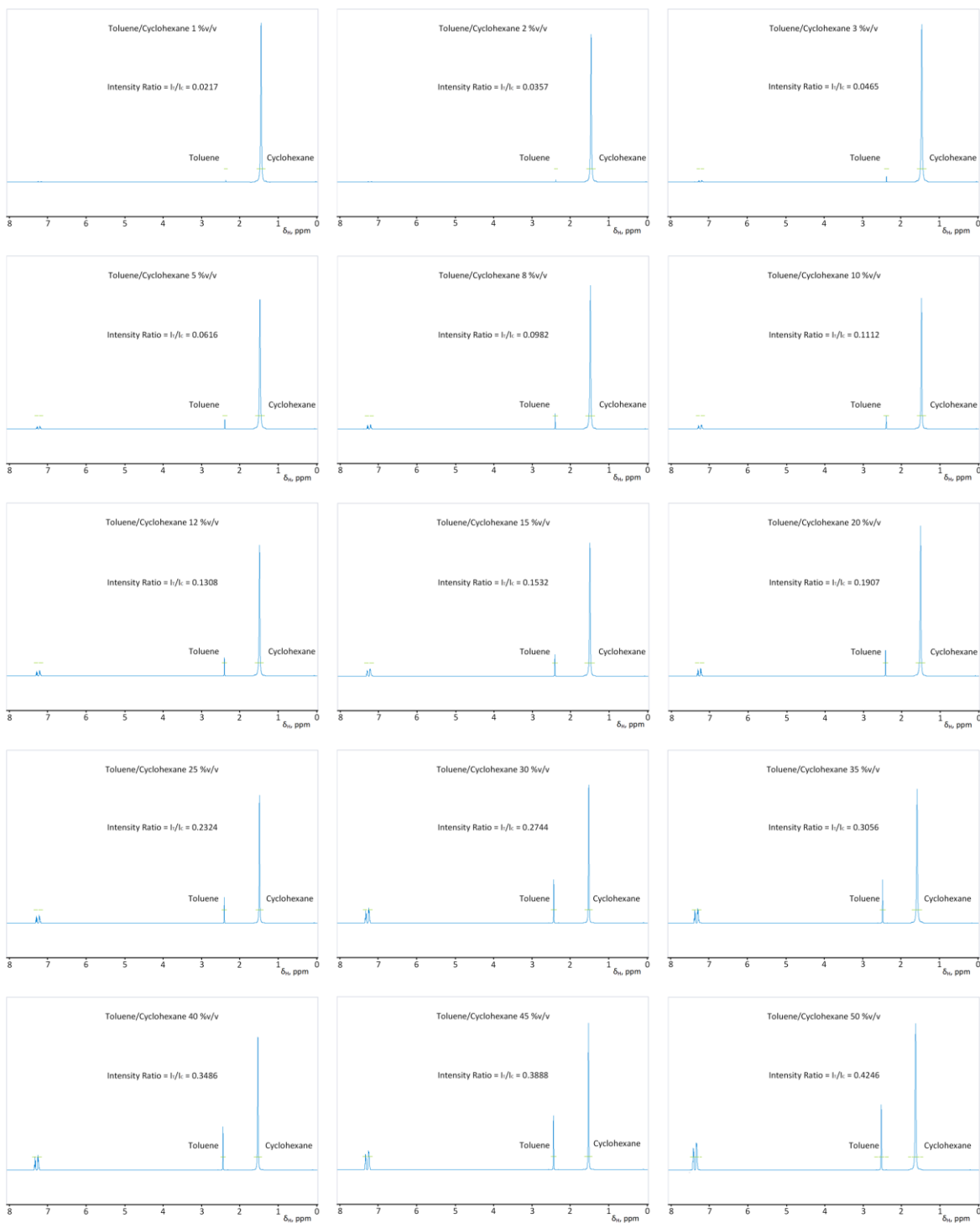


Fig. S41. ^1H NMR of toluene and cyclohexane mixtures: 1 %v/v, 2 %v/v, 3 %v/v, 5 %v/v, 8 %v/v, 10 %v/v, 12 %v/v, 15 %v/v, 20 %v/v, 25 %v/v, 30 %v/v, 35 %v/v, 40 %v/v, 45 %v/v, and 50 %v/v.

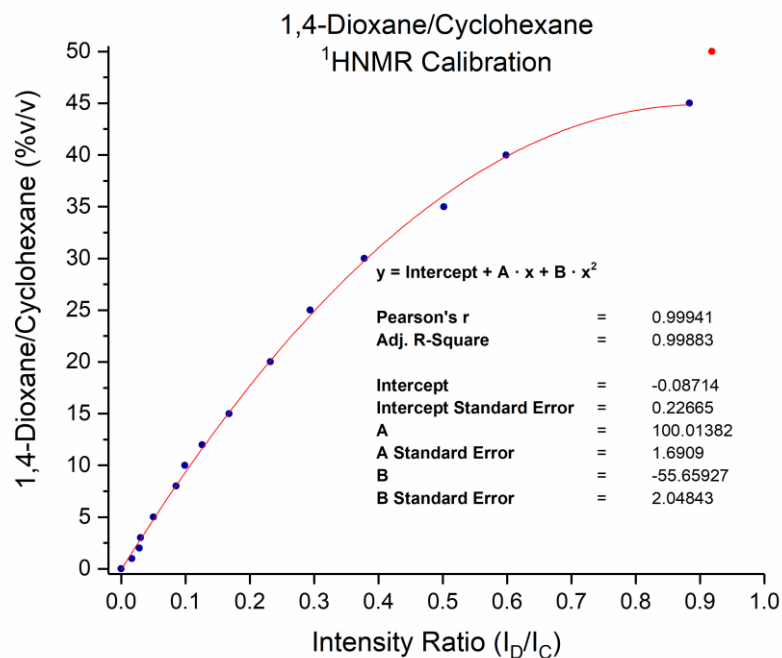


Fig. S42. Regression test between intensity ratio – of 1,4-dioxane and cyclohexane ^1H NMR signals – and volume ratio of the solution.

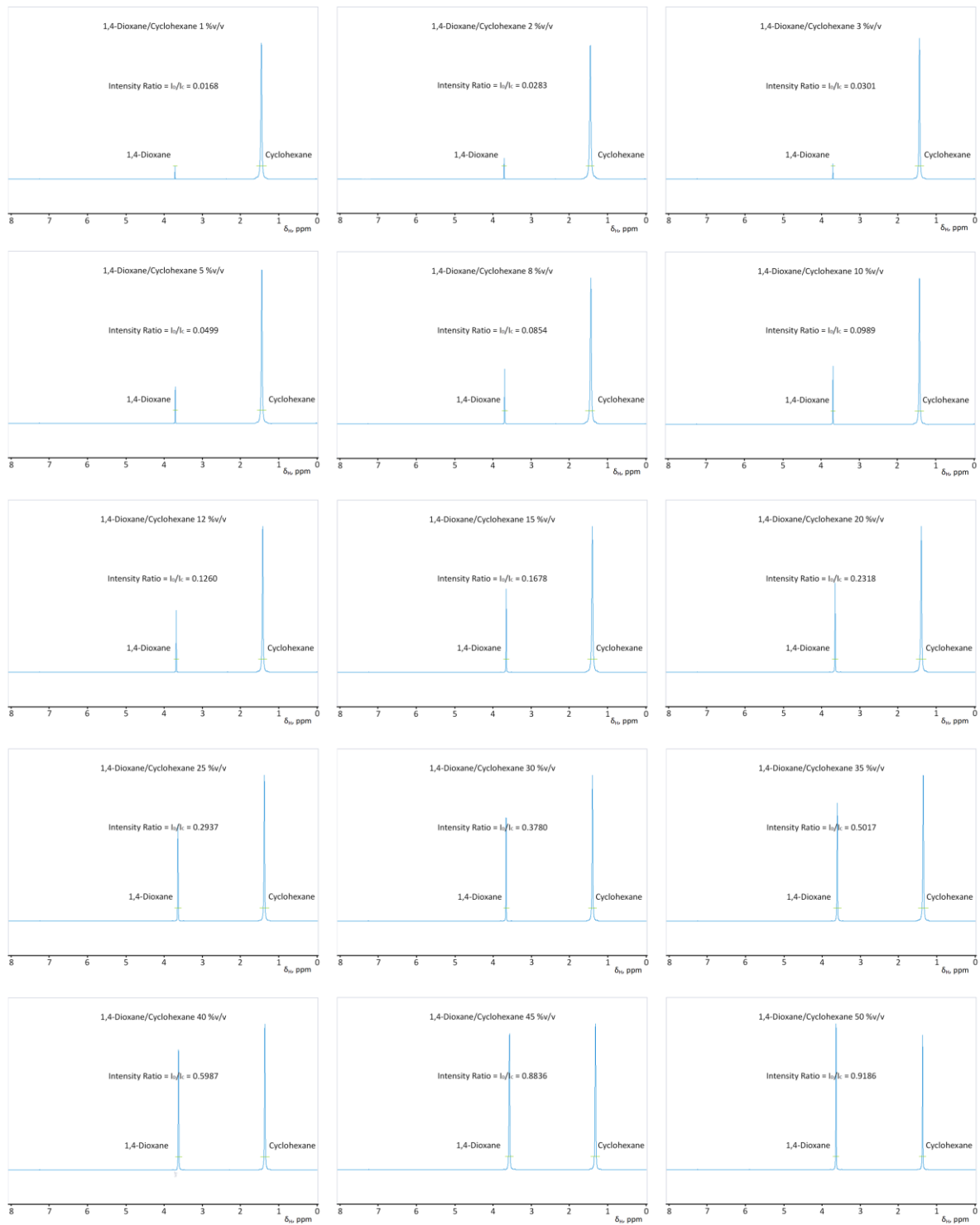


Fig. S43. ^1H NMR of 1,4-dioxane and cyclohexane mixtures: 1 %v/v, 2 %v/v, 3 %v/v, 5 %v/v, 8 %v/v, 10 %v/v, 12 %v/v, 15 %v/v, 20 %v/v, 25 %v/v, 30 %v/v, 35 %v/v, 40 %v/v, 45 %v/v, and 50 %v/v.

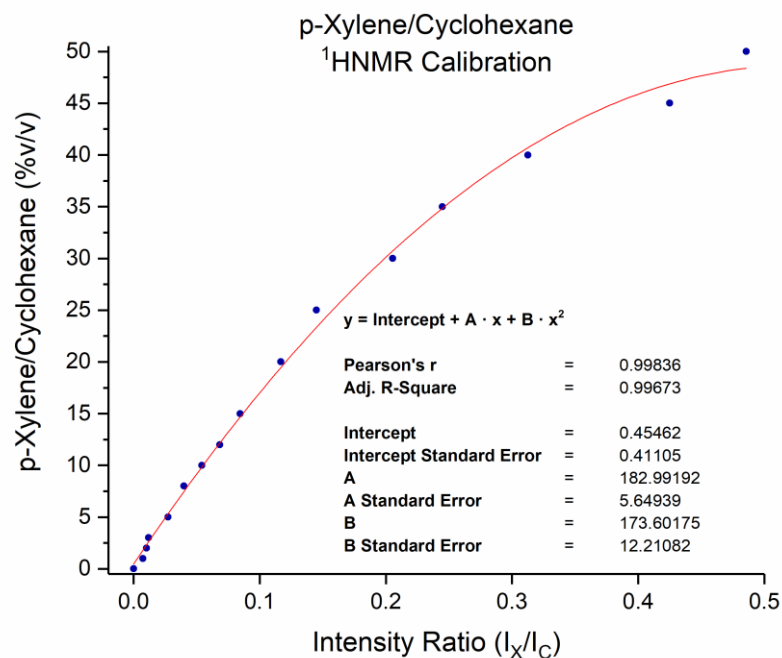


Fig. S44. Regression test between intensity ratio – of p-xylene and cyclohexane ^1H NMR signals – and volume ratio of the solution.

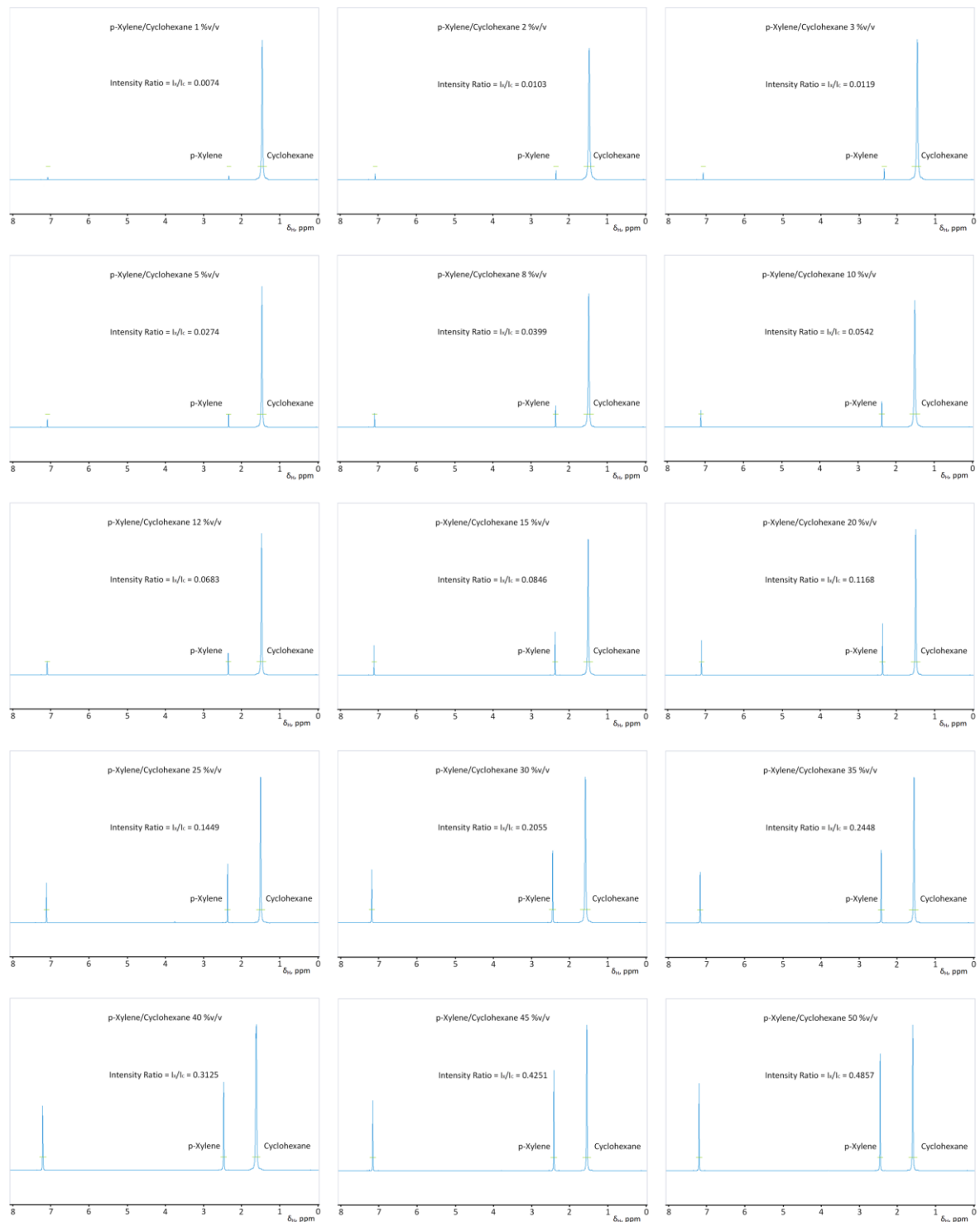


Fig. S45. ${}^1\text{H}$ NMR of p-xylene and cyclohexane mixtures: 1 %v/v, 2 %v/v, 3 %v/v, 5 %v/v, 8 %v/v, 10 %v/v, 12 %v/v, 15 %v/v, 20 %v/v, 25 %v/v, 30 %v/v, 35 %v/v, 40 %v/v, 45 %v/v, and 50 %v/v.

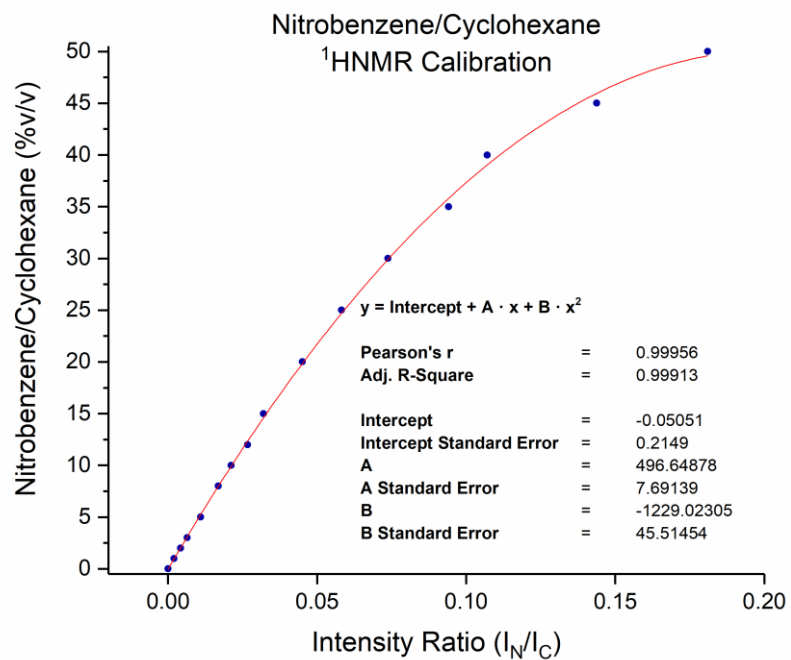


Fig. S46. Regression test between intensity ratio – of nitrobenzene and cyclohexane ^1H NMR signals – and volume ratio of the solution.



Fig. S47. ${}^1\text{H}$ NMR of nitrobenzene and cyclohexane mixtures: 1 % v/v, 2 % v/v, 3 % v/v, 5 % v/v, 8 % v/v, 10 % v/v, 12 % v/v, 15 % v/v, 20 % v/v, 25 % v/v, 30 % v/v, 35 % v/v, 40 % v/v, 45 % v/v, and 50 % v/v.

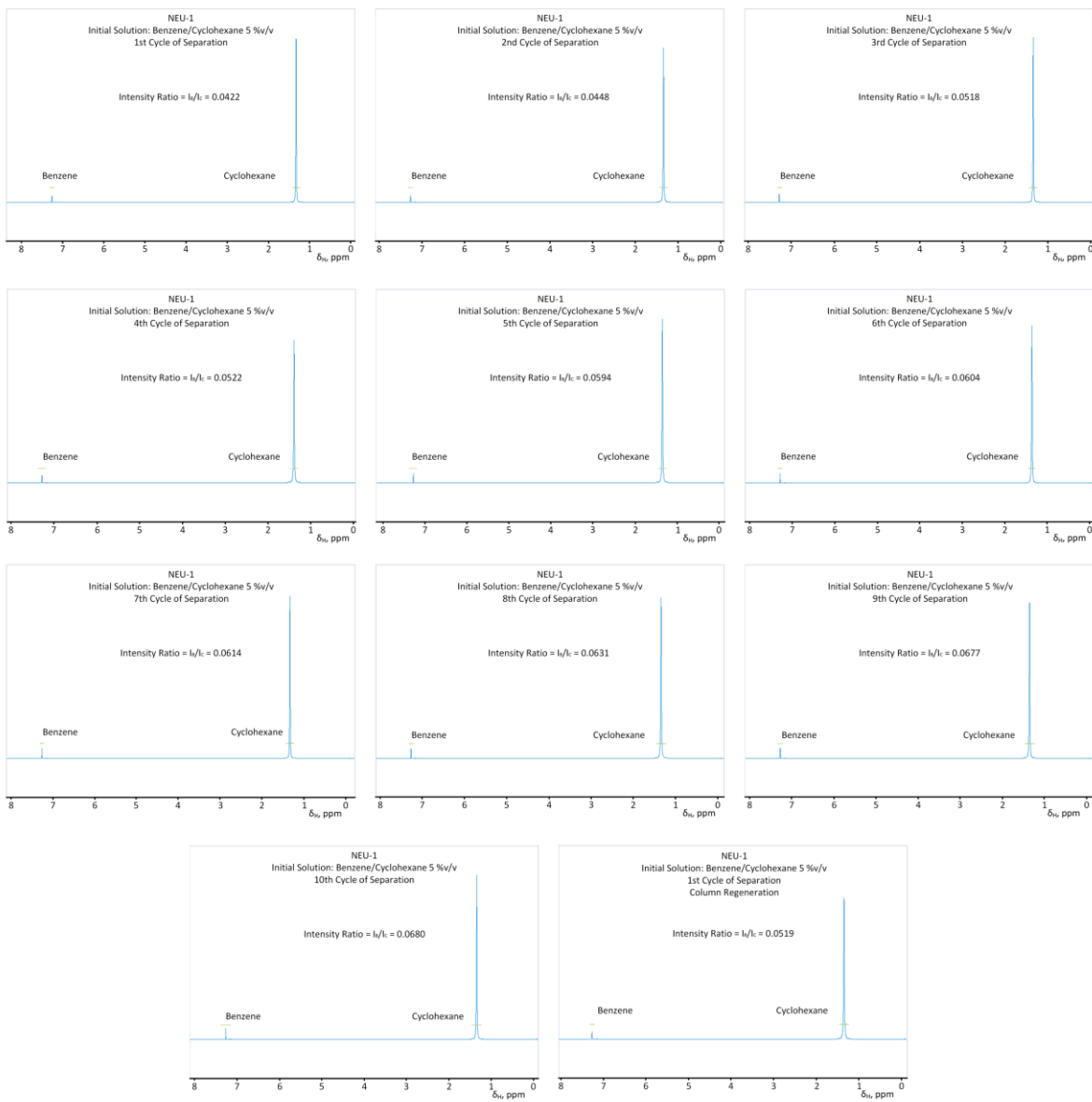


Fig. S48. ^1H NMR of benzene/cyclohexane eluent after 1st cs, 2nd cs, 3rd cs, 4th cs, 5th cs, 6th cs, 7th cs, 8th cs, 9th cs, 10th cs, and after 1st cs and 1st regeneration in NEU-1c (initial mixture 5 %v/v).

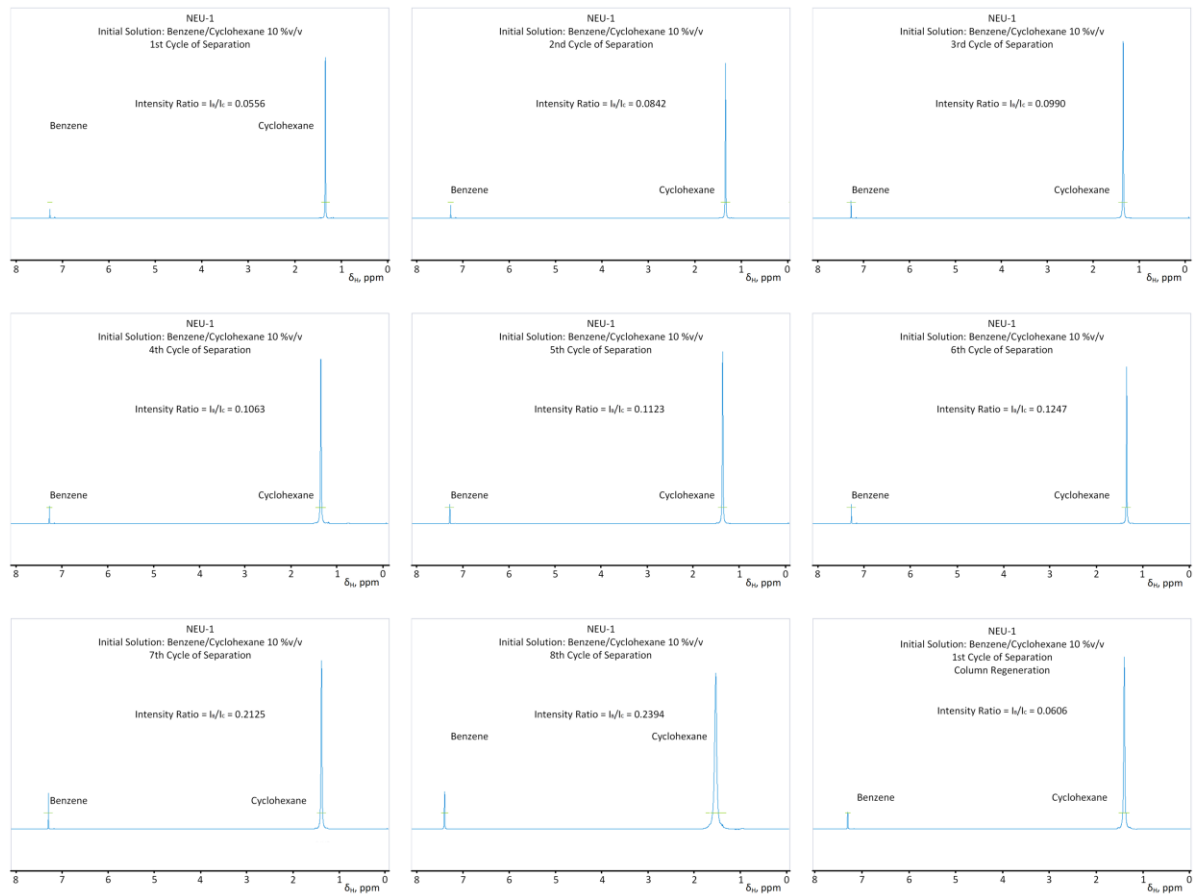


Fig. S49. ¹H NMR of benzene/cyclohexane eluent after 1st cs, 2nd cs, 3rd cs, 4th cs, 5th cs, 6th cs, 7th cs, 8th cs, and after 1st cs and 1st regeneration in NEU-1c (initial mixture 10 %v/v).

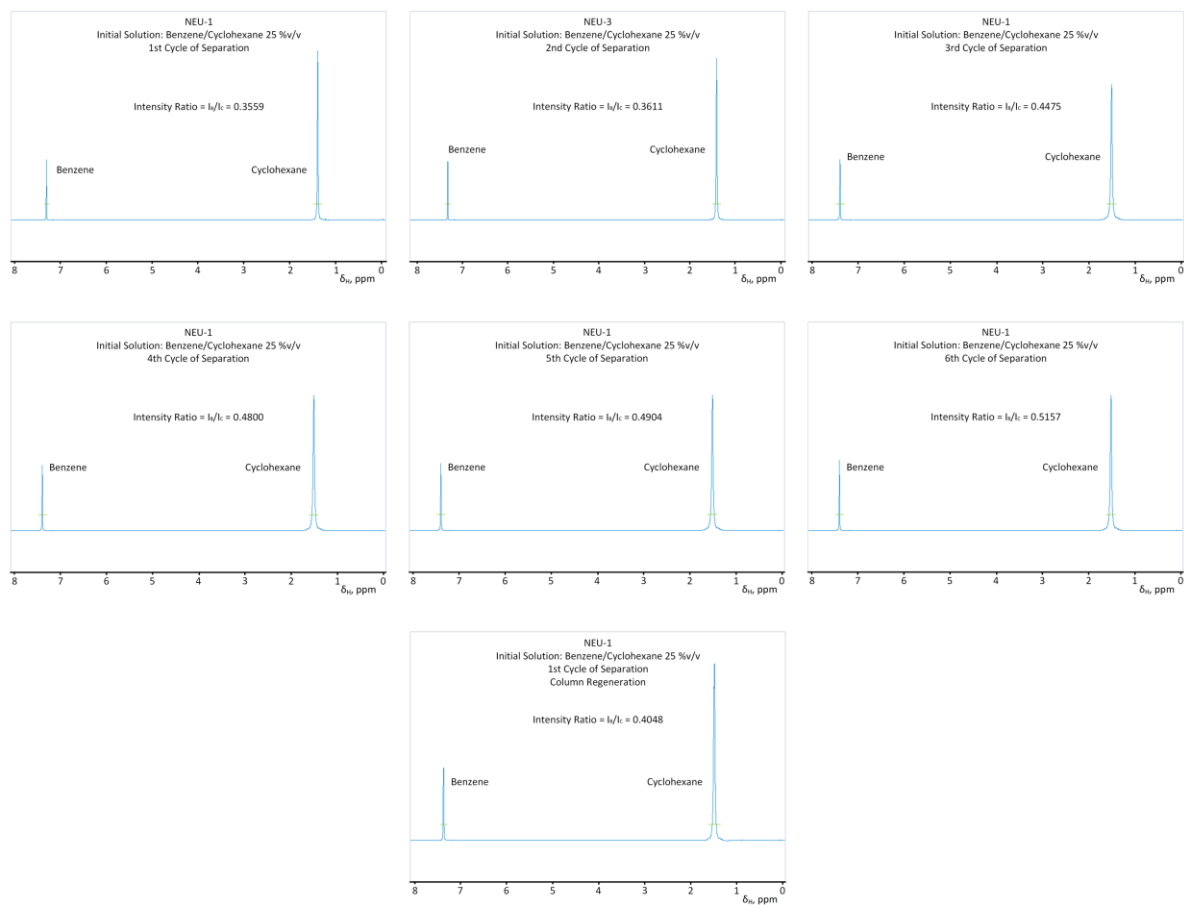


Fig. S50. ^1H NMR of benzene/cyclohexane eluent after 1st cs, 2nd cs, 3rd cs, 4th cs, 5th cs, 6th cs, and after 1st cs and 1st regeneration in NEU-1c (initial mixture 25 %v/v).

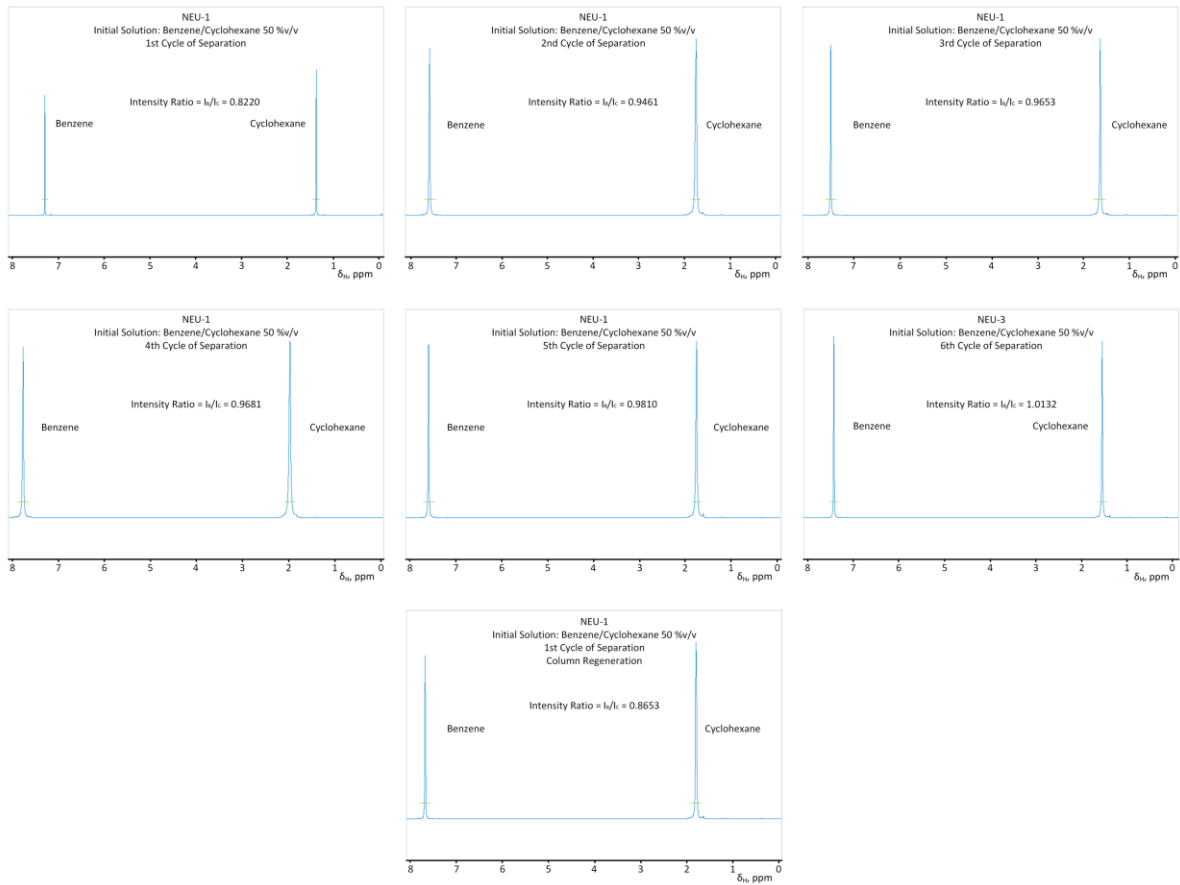


Fig. S51. ^1H NMR of benzene/cyclohexane eluent after 1st cs, 2nd cs, 3rd cs, 4th cs, 5th cs, 6th cs, and after 1st cs and 1st regeneration in NEU-1c (initial mixture 50 %v/v).

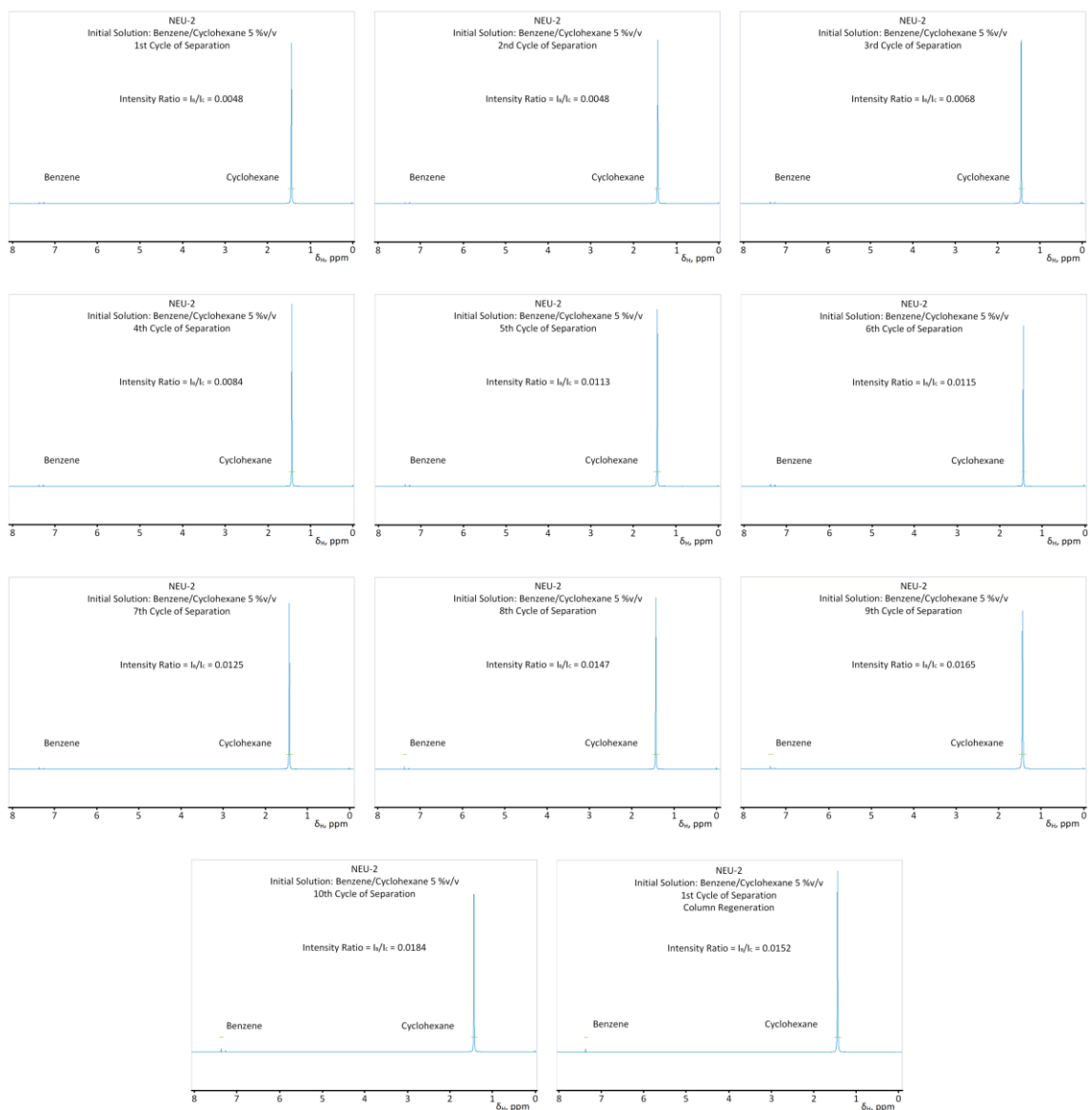


Fig. S52. ¹H NMR of benzene/cyclohexane eluent after 1st cs, 2nd cs, 3rd cs, 4th cs, 5th cs, 6th cs, 7th cs, 8th cs, 9th cs, 10th cs, and after 1st cs and 1st regeneration in NEU-2 (initial mixture 5 %v/v).

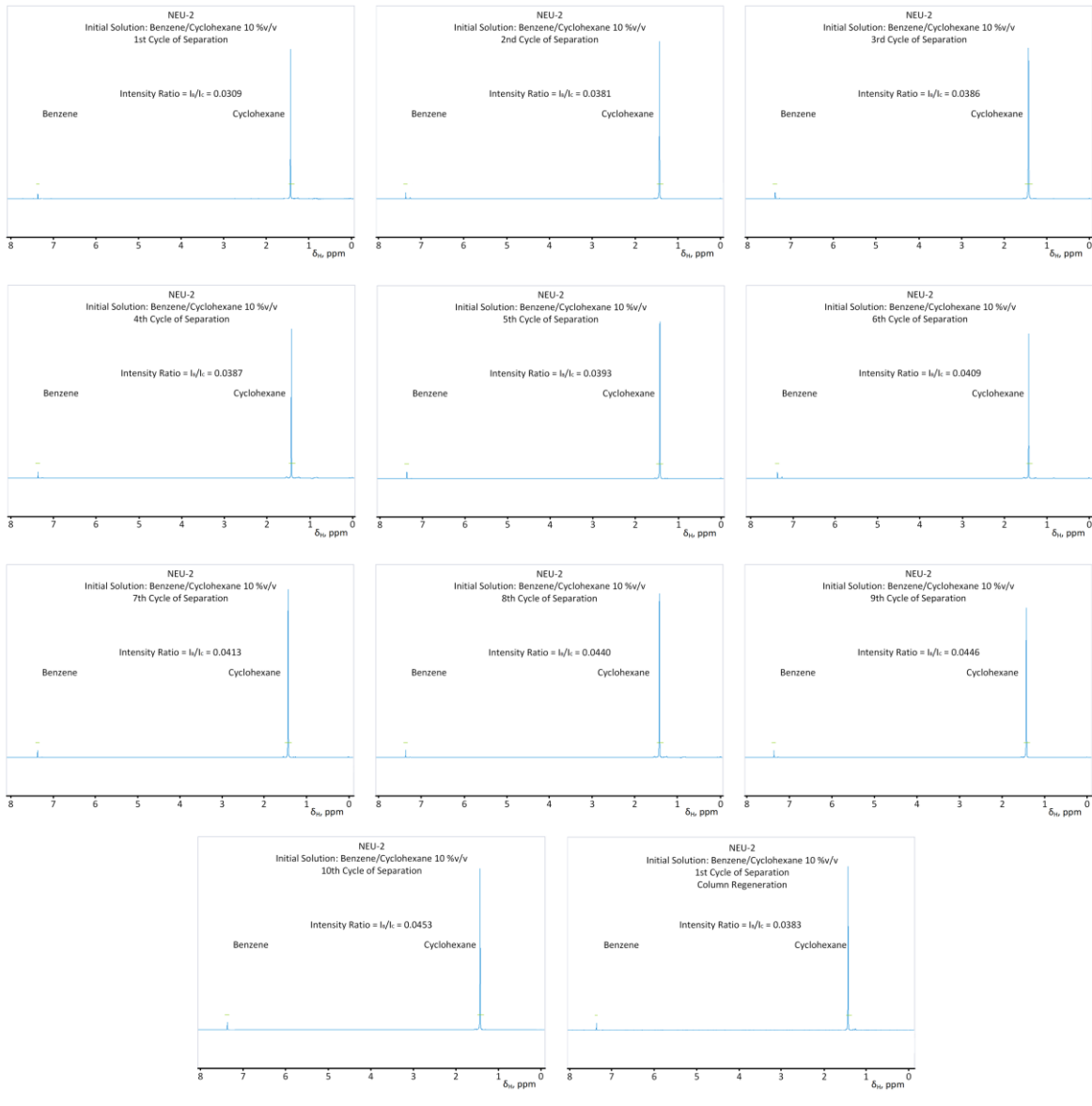


Fig. S53. ^1H NMR of benzene/cyclohexane eluent after 1st cs, 2nd cs, 3rd cs, 4th cs, 5th cs, 6th cs, 7th cs, 8th cs, 9th cs, 10th cs, and after 1st cs and 1st regeneration in NEU-2 (initial mixture 10 %v/v).

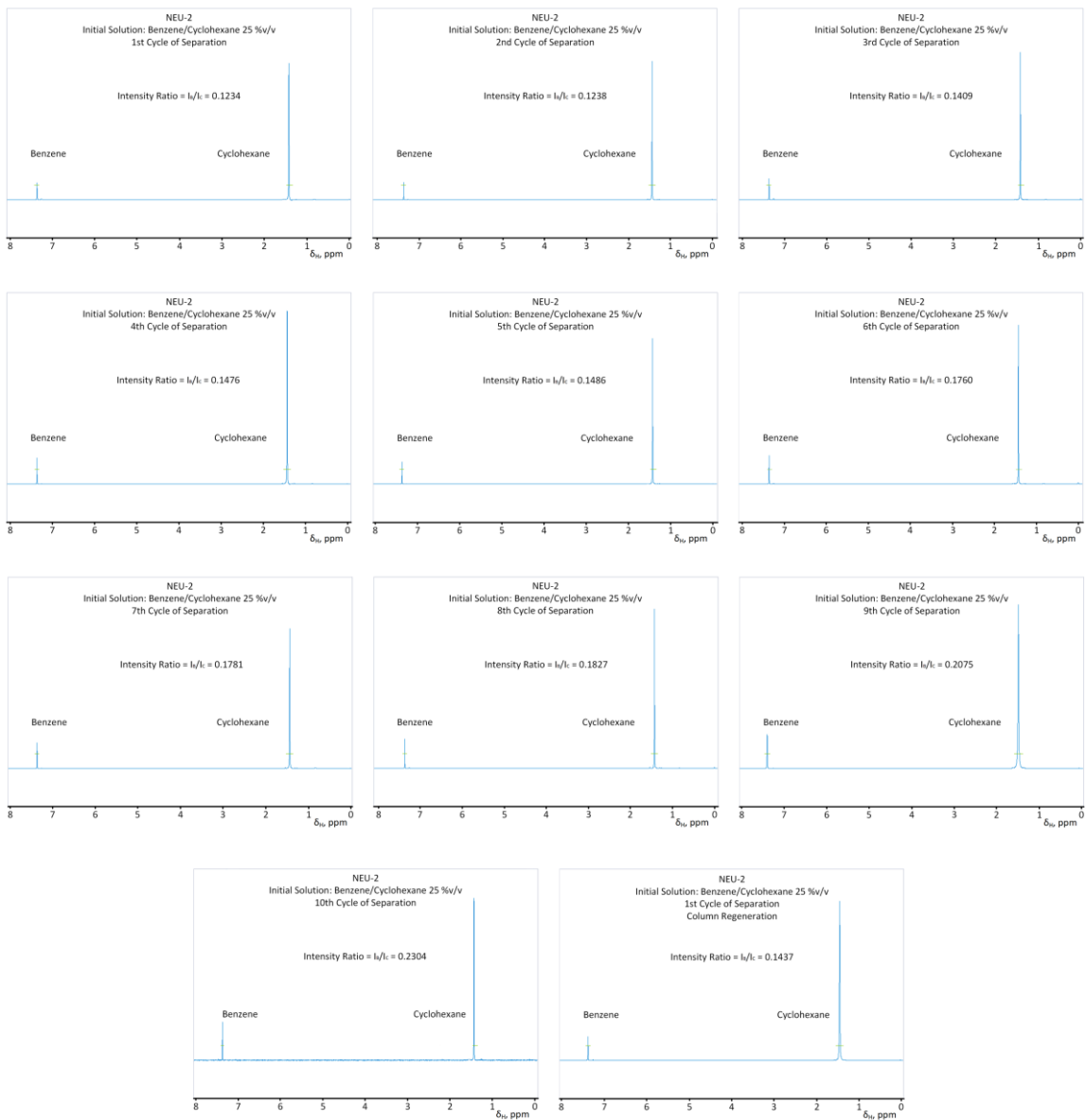


Fig. S54. ^1H NMR of benzene/cyclohexane eluent after 1st cs, 2nd cs, 3rd cs, 4th cs, 5th cs, 6th cs, 7th cs, 8th cs, 9th cs, 10th cs, and after 1st cs and 1st regeneration in NEU-2 (initial mixture 25 %v/v).

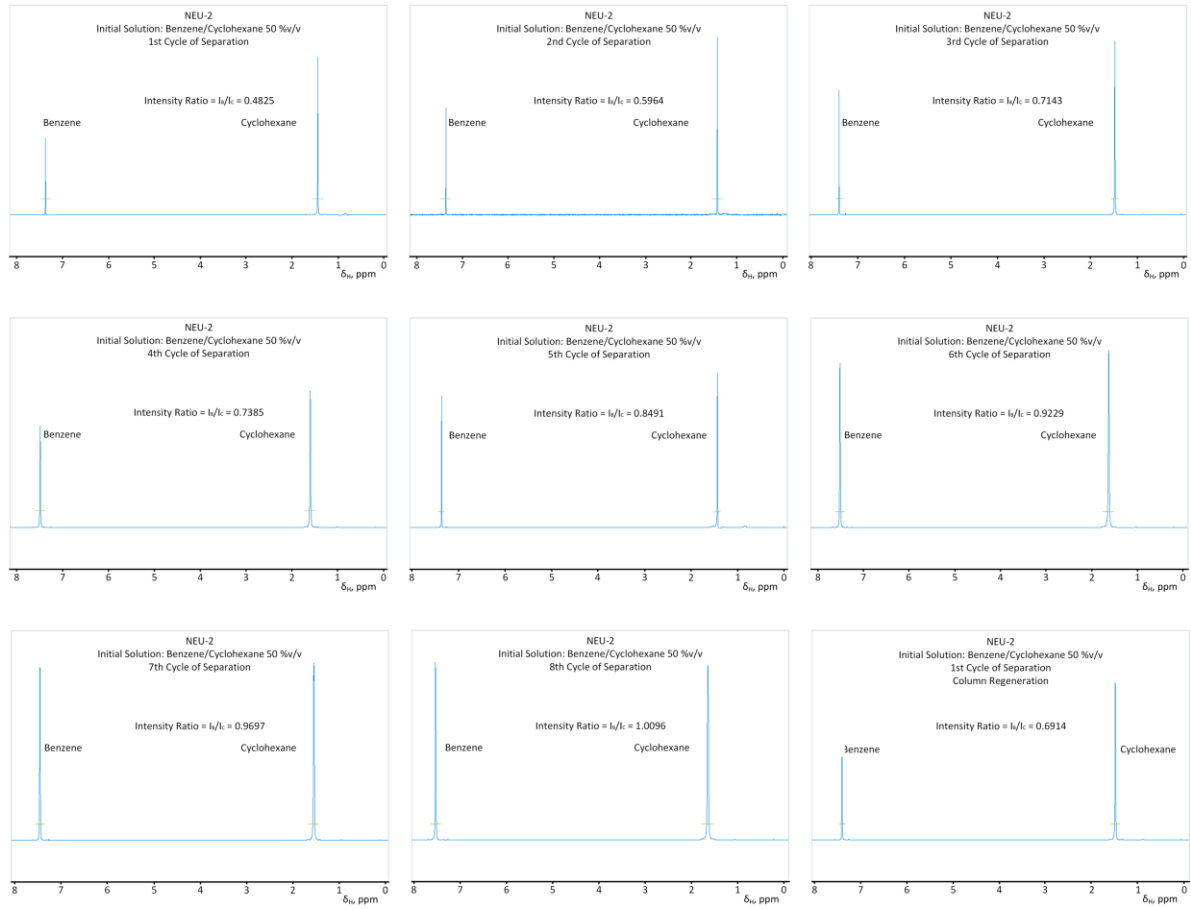


Fig. S55. ¹H NMR of benzene/cyclohexane eluent after 1st cs, 2nd cs, 3rd cs, 4th cs, 5th cs, 6th cs, 7th cs, 8th cs, and after 1st cs and 1st regeneration in NEU-2 (initial mixture 50 %v/v).

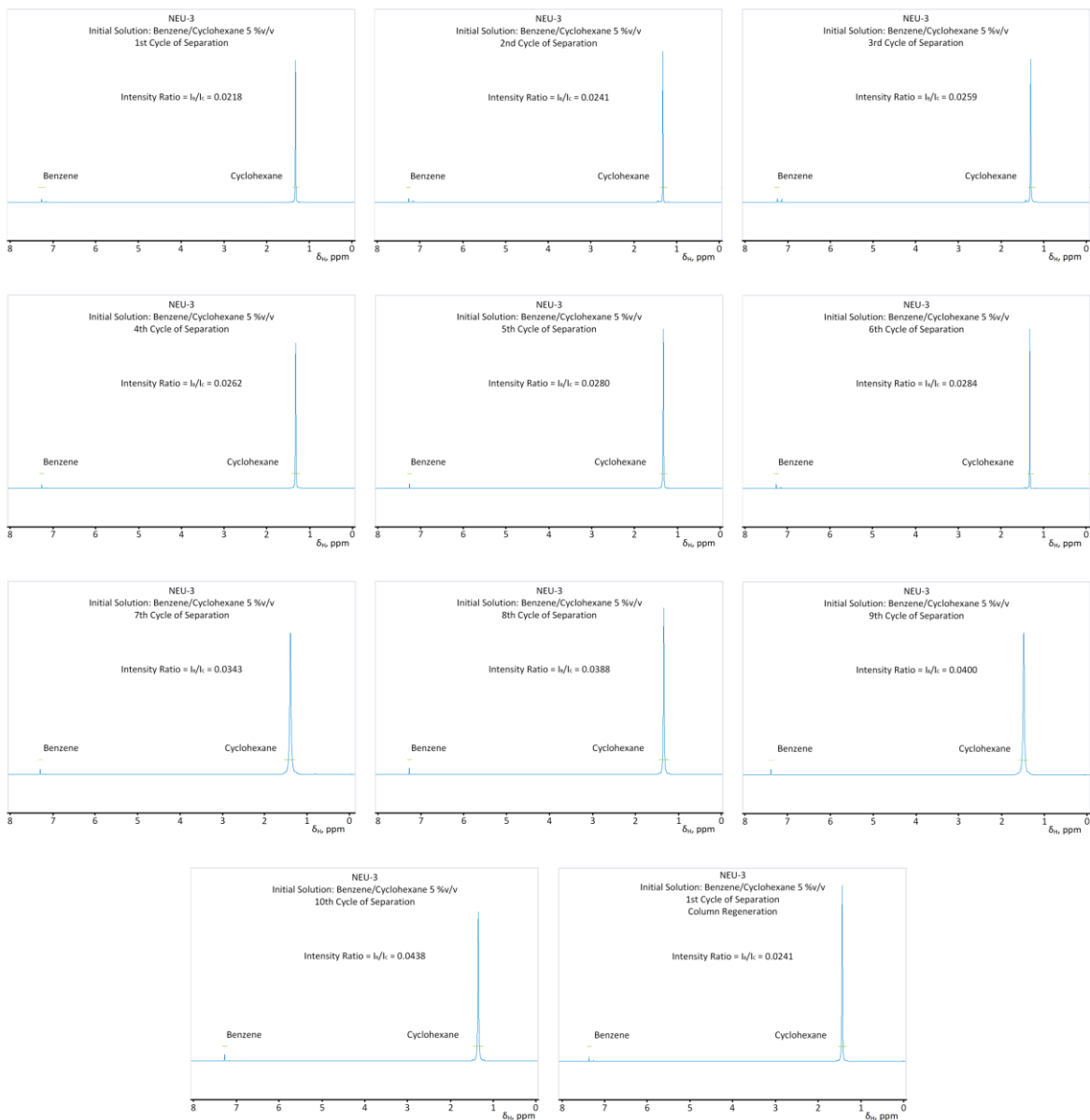


Fig. S56. ^1H NMR of benzene/cyclohexane eluent after 1st cs, 2nd cs, 3rd cs, 4th cs, 5th cs, 6th cs, 7th cs, 8th cs, 9th cs, 10th cs, and after 1st cs and 1st regeneration in NEU-3 (initial mixture 5 %v/v).

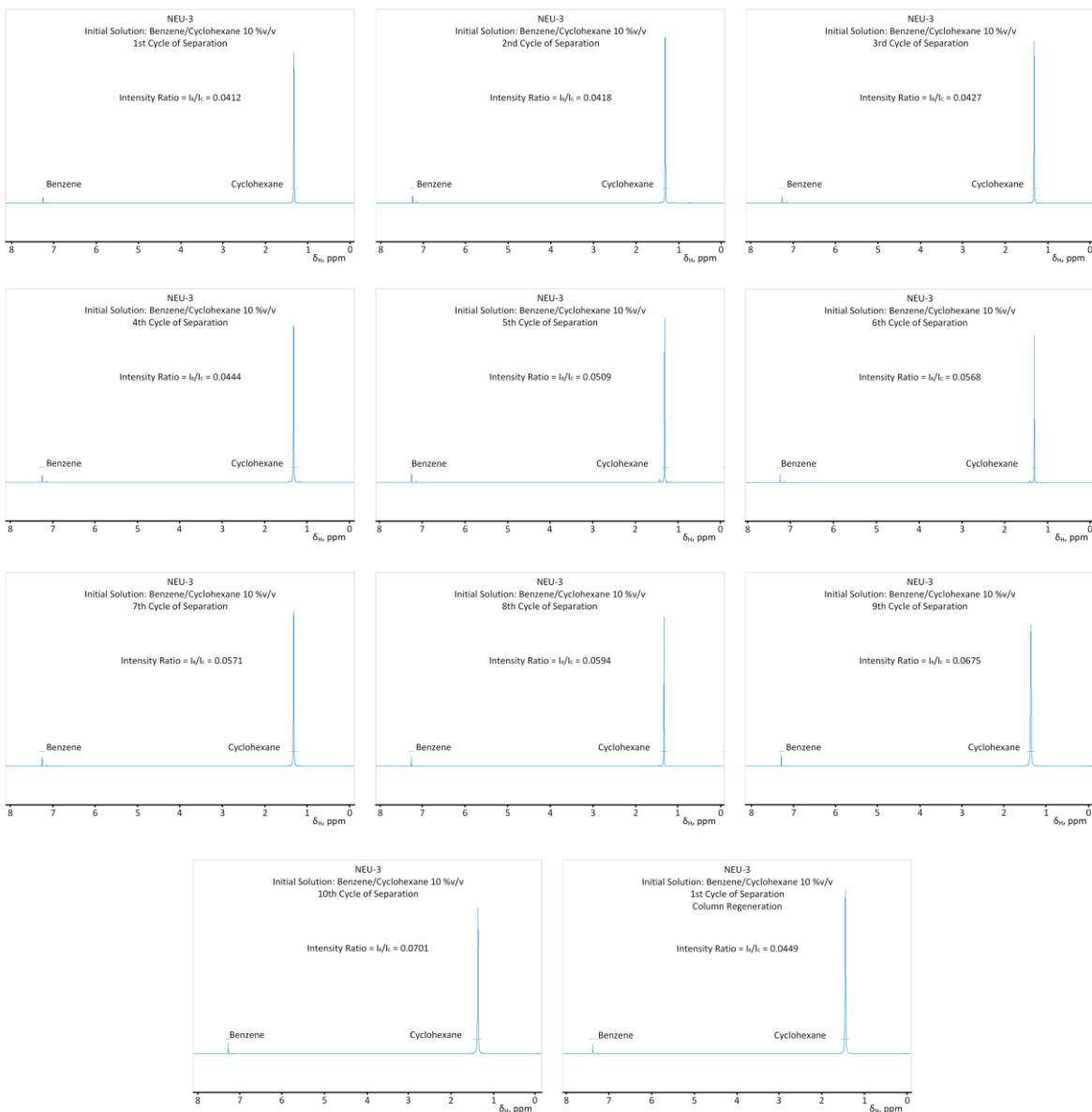


Fig. S57. ${}^1\text{H}$ NMR of benzene/cyclohexane eluent after 1st cs, 2nd cs, 3rd cs, 4th cs, 5th cs, 6th cs, 7th cs, 8th cs, 9th cs, 10th cs, and after 1st cs and 1st regeneration in NEU-3 (initial mixture 10 %v/v).

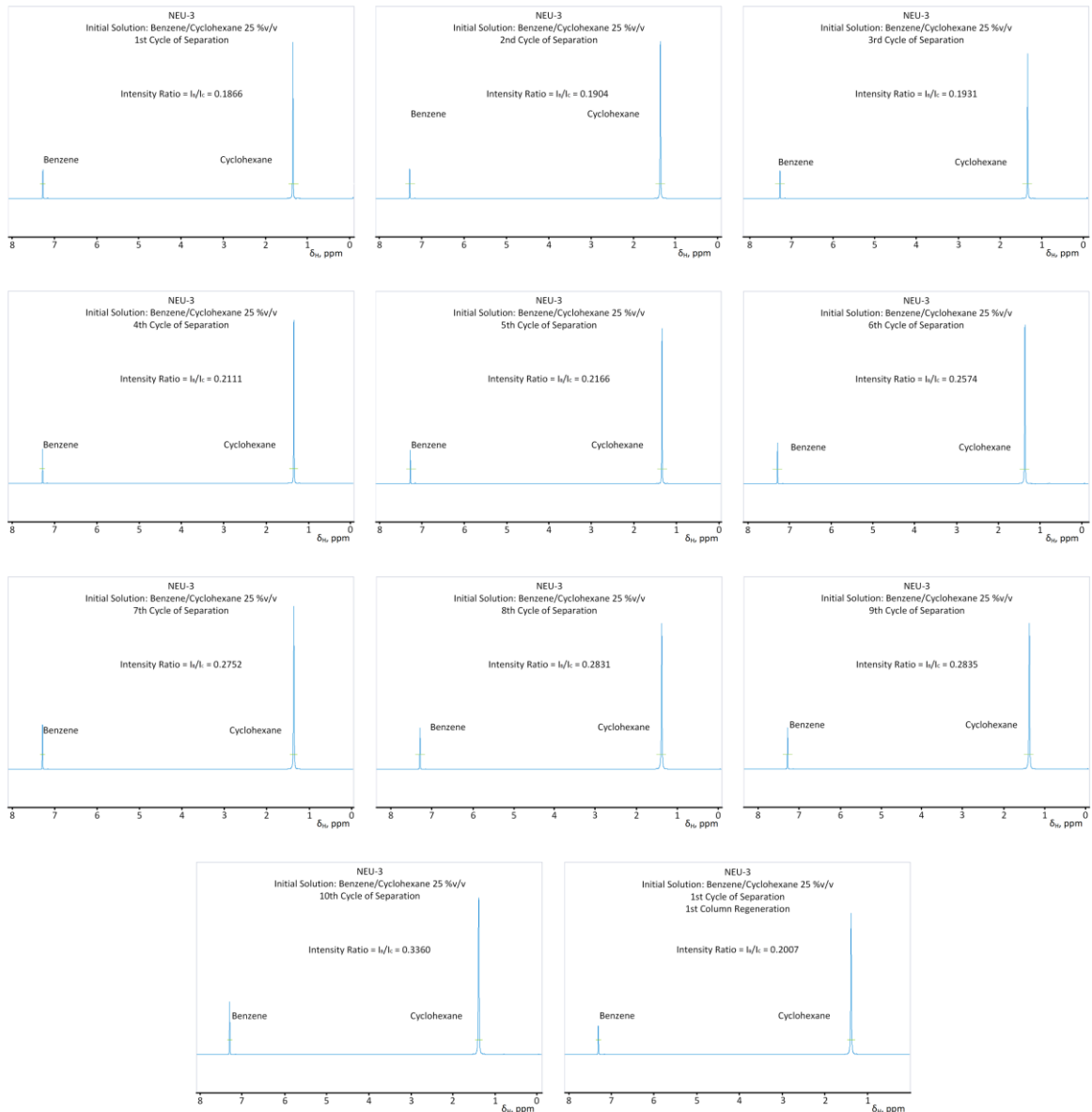


Fig. S58. ¹H NMR of benzene/cyclohexane eluent after 1st cs, 2nd cs, 3rd cs, 4th cs, 5th cs, 6th cs, 7th cs, 8th cs, 9th cs, 10th cs, and after 1st cs and 1st regeneration in NEU-3 (initial mixture 25 %v/v).

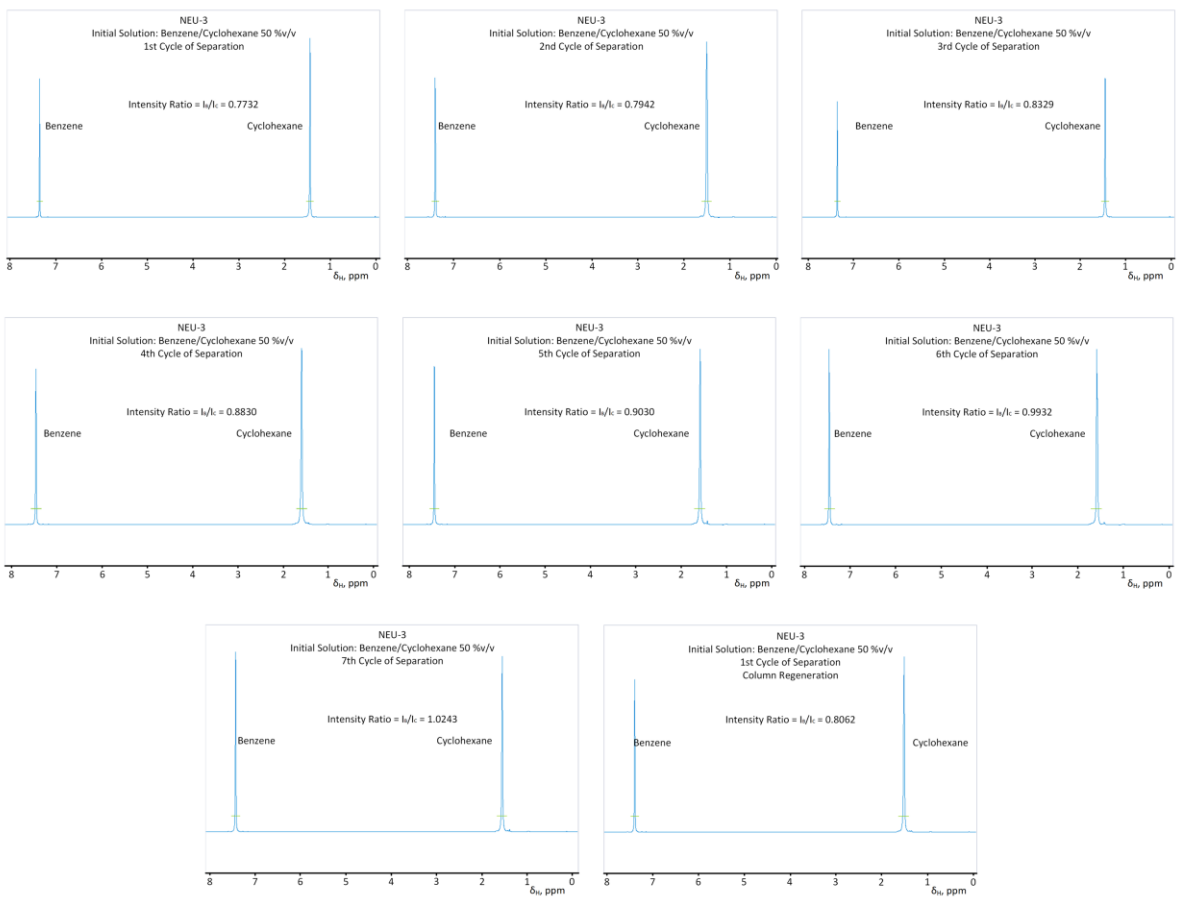


Fig. S59. ^1H NMR of benzene/cyclohexane eluent after 1st cs, 2nd cs, 3rd cs, 4th cs, 5th cs, 6th cs, 7th cs, and after 1st cs and 1st regeneration in NEU-3 (initial mixture 50 %v/v).

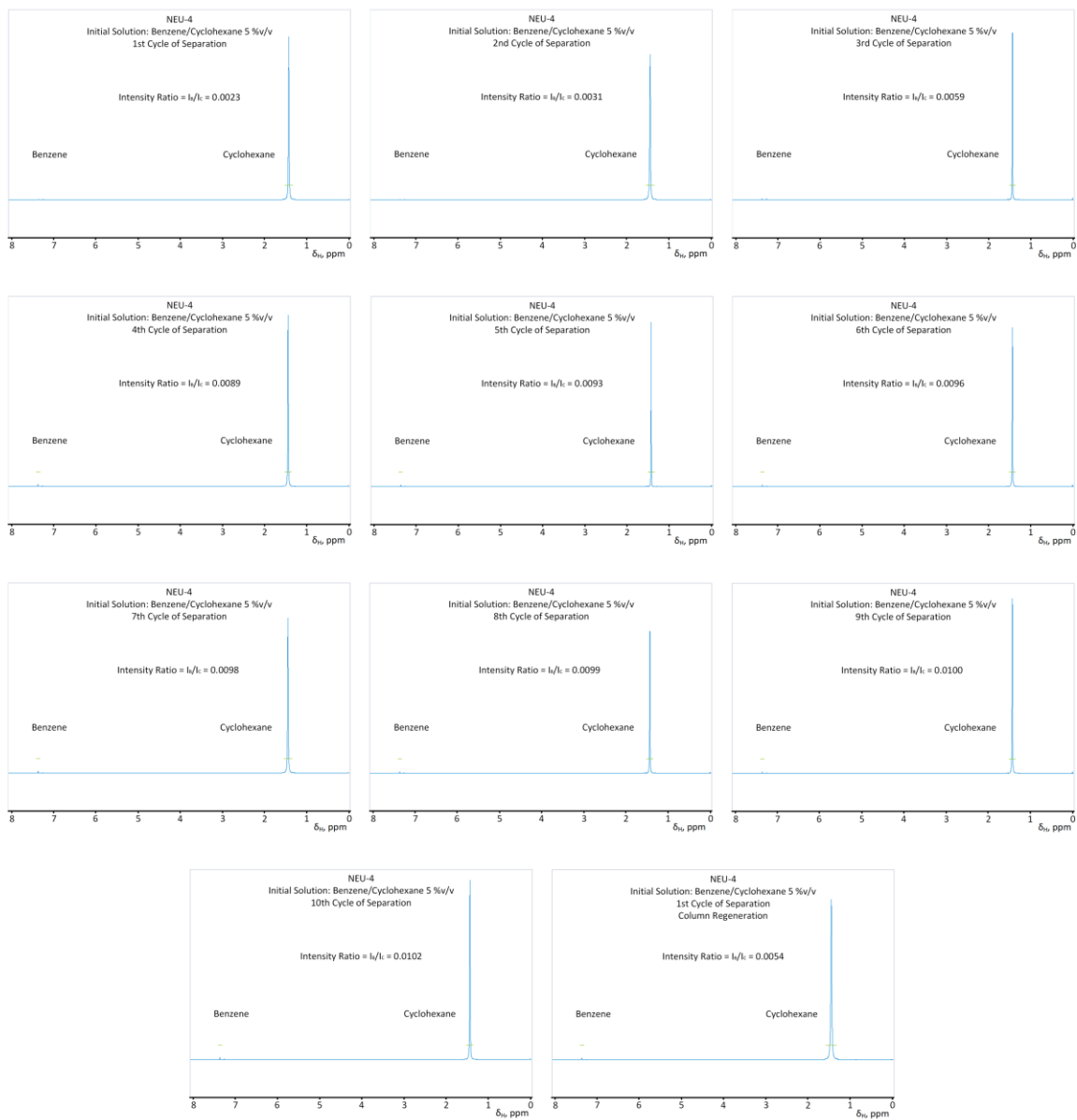


Fig. S60. ${}^1\text{H}$ NMR of benzene/cyclohexane eluent after 1st cs, 2nd cs, 3rd cs, 4th cs, 5th cs, 6th cs, 7th cs, 8th cs, 9th cs, 10th cs, and after 1st cs and 1st regeneration in NEU-4 (initial mixture 5 %v/v).

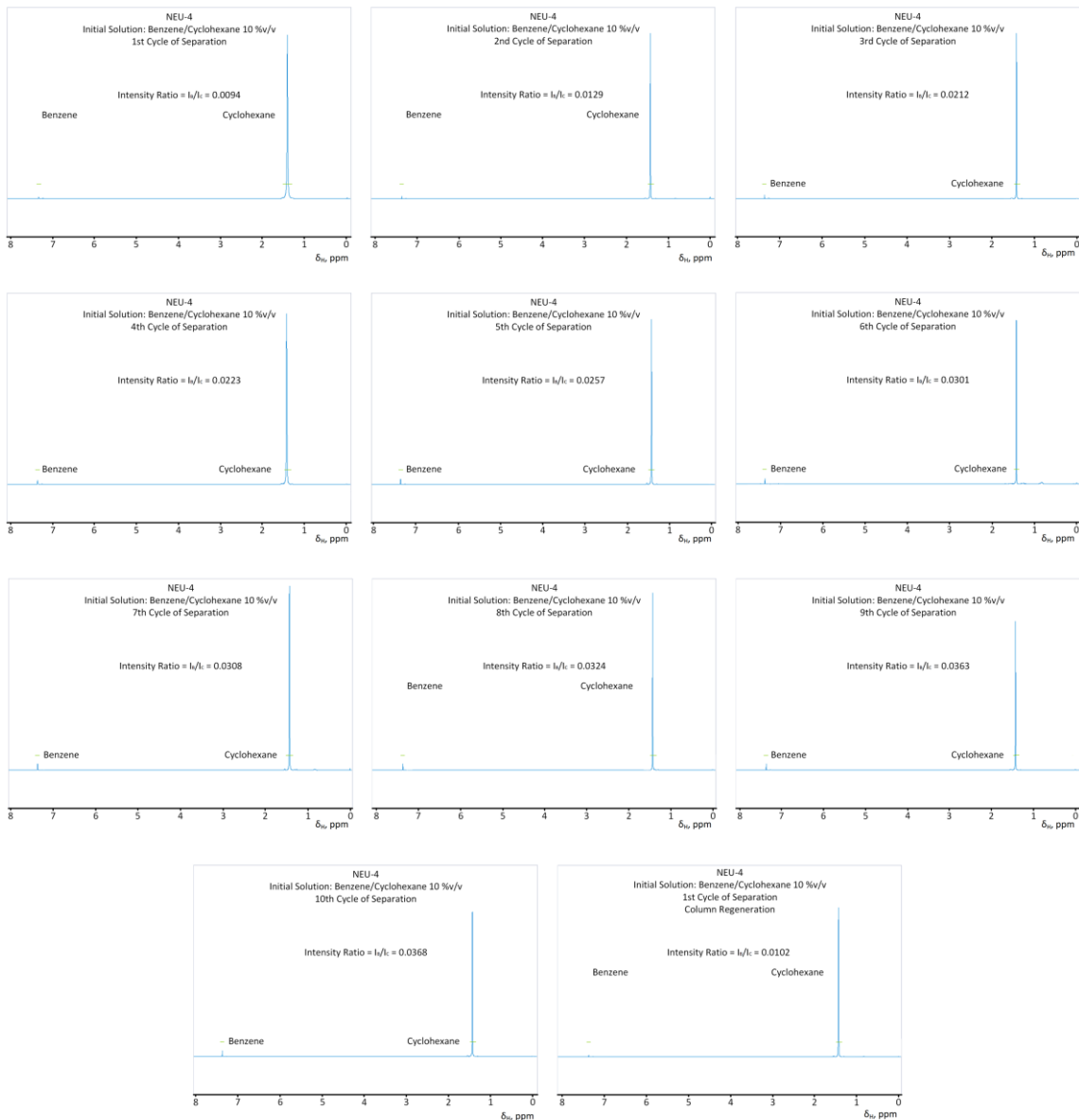


Fig. S61. ¹H NMR of benzene/cyclohexane eluent after 1st cs, 2nd cs, 3rd cs, 4th cs, 5th cs, 6th cs, 7th cs, 8th cs, 9th cs, 10th cs, and after 1st cs and 1st regeneration in NEU-4 (initial mixture 10 %v/v).

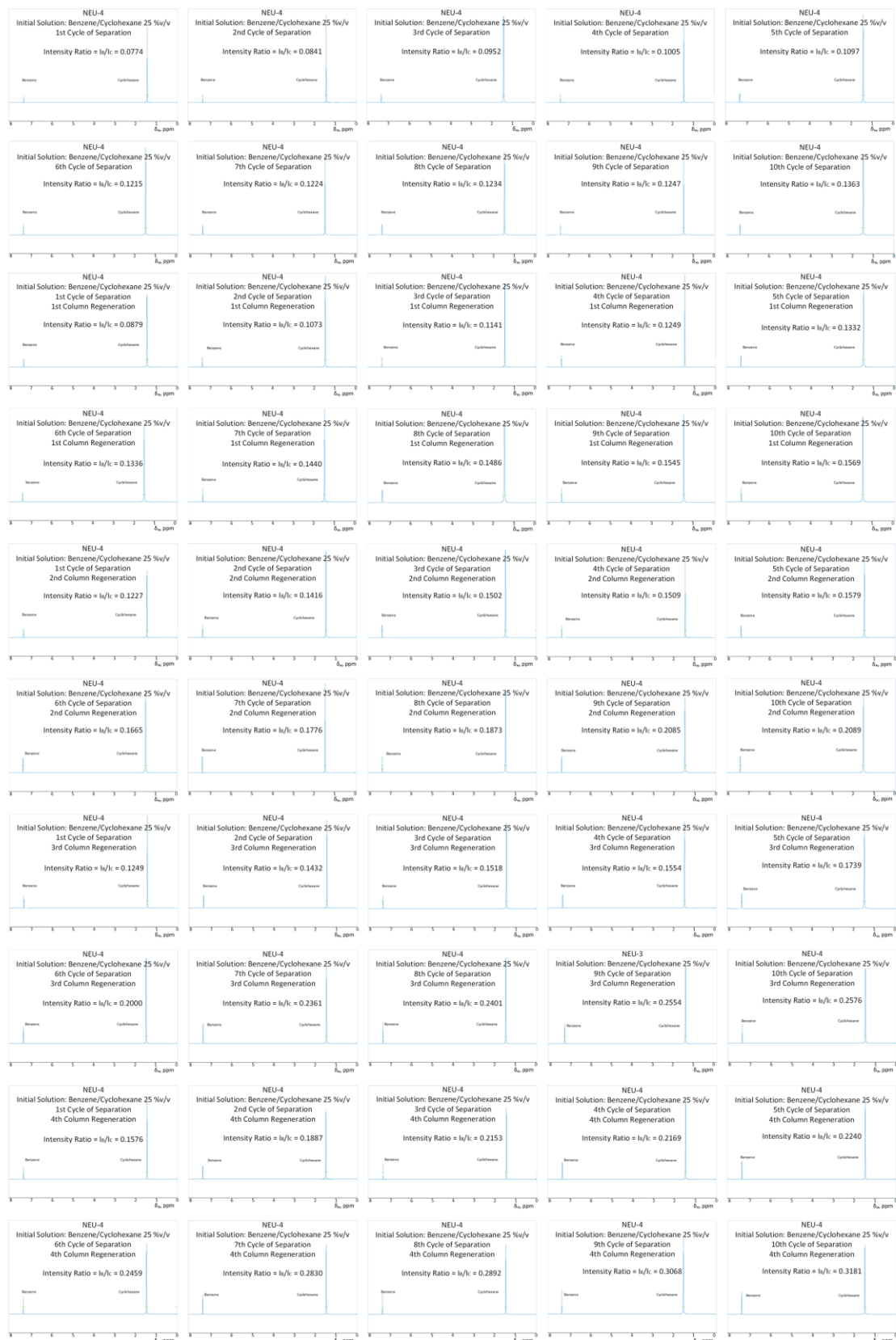


Fig. S62. ^1H NMR of benzene/cyclohexane eluent after 1th cs, 2nd cs, 3rd cs, 4th cs, 5th cs, 6th cs, 7th cs, 8th cs, 9th cs, 10th cs, after 1st cs and 1st regeneration, after 2nd cs and 1st regeneration, after

3rd cs and 1st regeneration, after 4th cs and 1st regeneration, after 5th cs and 1st regeneration, after 6th cs and 1st regeneration, after 7th cs and 1st regeneration, after 8th cs and 1st regeneration, after 9th cs and 1st regeneration, after 10th cs and 1st regeneration, after 1st cs and 2nd regeneration, after 2nd cs and 2nd regeneration, after 3rd cs and 2nd regeneration, after 4th cs and 2nd regeneration, after 5th cs and 2nd regeneration, after 6th cs and 2nd regeneration, after 7th cs and 2nd regeneration, after 8th cs and 2nd regeneration, after 9th cs and 2nd regeneration, after 10th cs and 2nd regeneration, after 1st cs and 3rd regeneration, after 2nd cs and 3rd regeneration, after 3rd cs and 3rd regeneration, after 4th cs and 3rd regeneration, after 5th cs and 3rd regeneration, after 6th cs and 3rd regeneration, after 7th cs and 3rd regeneration, after 8th cs and 3rd regeneration, after 9th cs and 3rd regeneration, after 10th cs and 3rd regeneration, after 1st cs and 4th regeneration, after 2nd cs and 4th regeneration, after 3rd cs and 4th regeneration, after 4th cs and 4th regeneration, after 5th cs and 4th regeneration, after 6th cs and 4th regeneration, after 7th cs and 4th regeneration, after 8th cs and 4th regeneration, after 9th cs and 4th regeneration, after 10th cs and 4th regeneration in NEU-4 (initial mixture 25 %v/v).

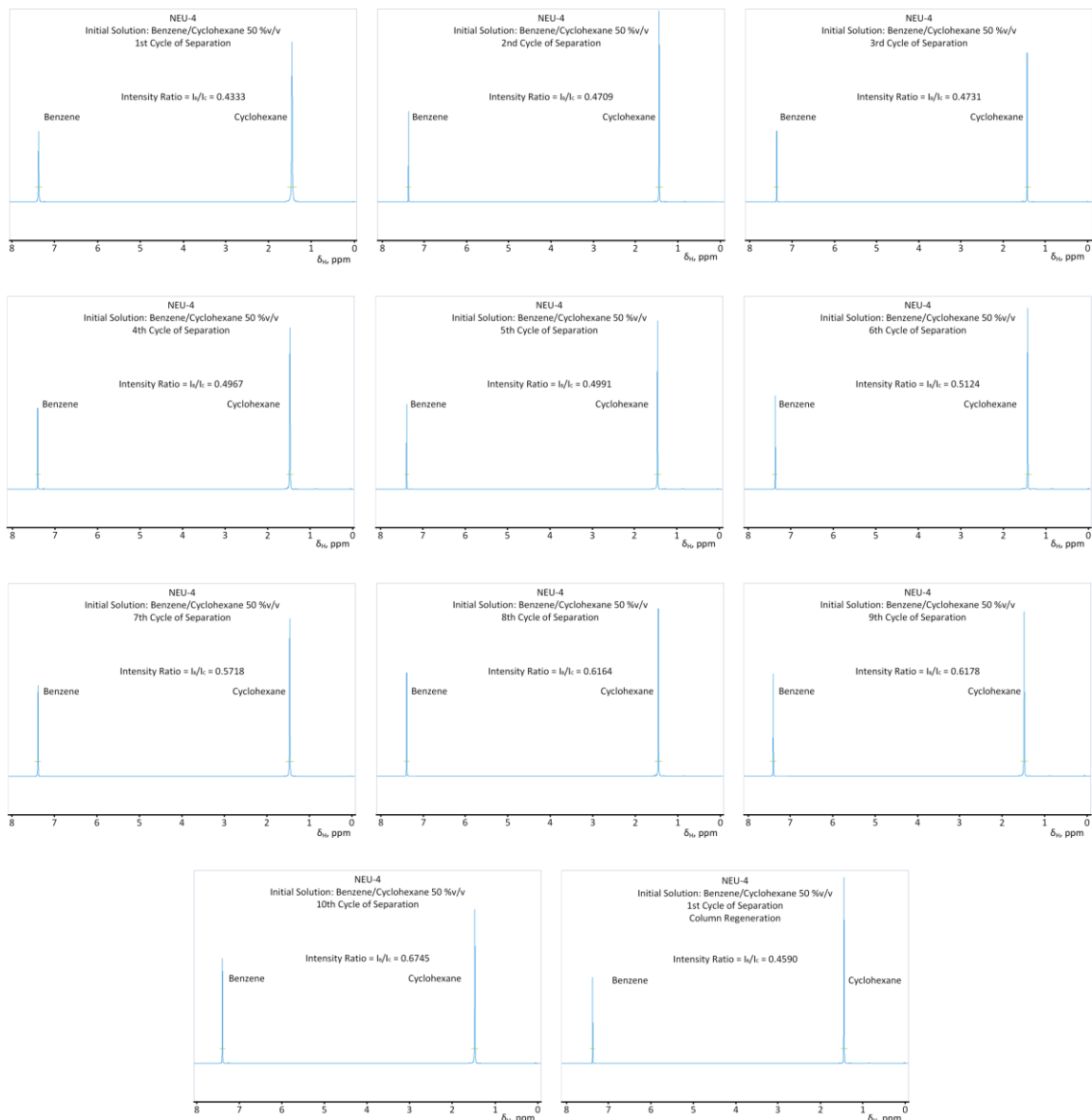


Fig. S63. ${}^1\text{H}$ NMR of benzene/cyclohexane eluent after 1st cs, 2nd cs, 3rd cs, 4th cs, 5th cs, 6th cs, 7th cs, 8th cs, 9th cs, 10th cs, and after 1st cs and 1st regeneration in NEU-4 (initial mixture 50 %v/v).

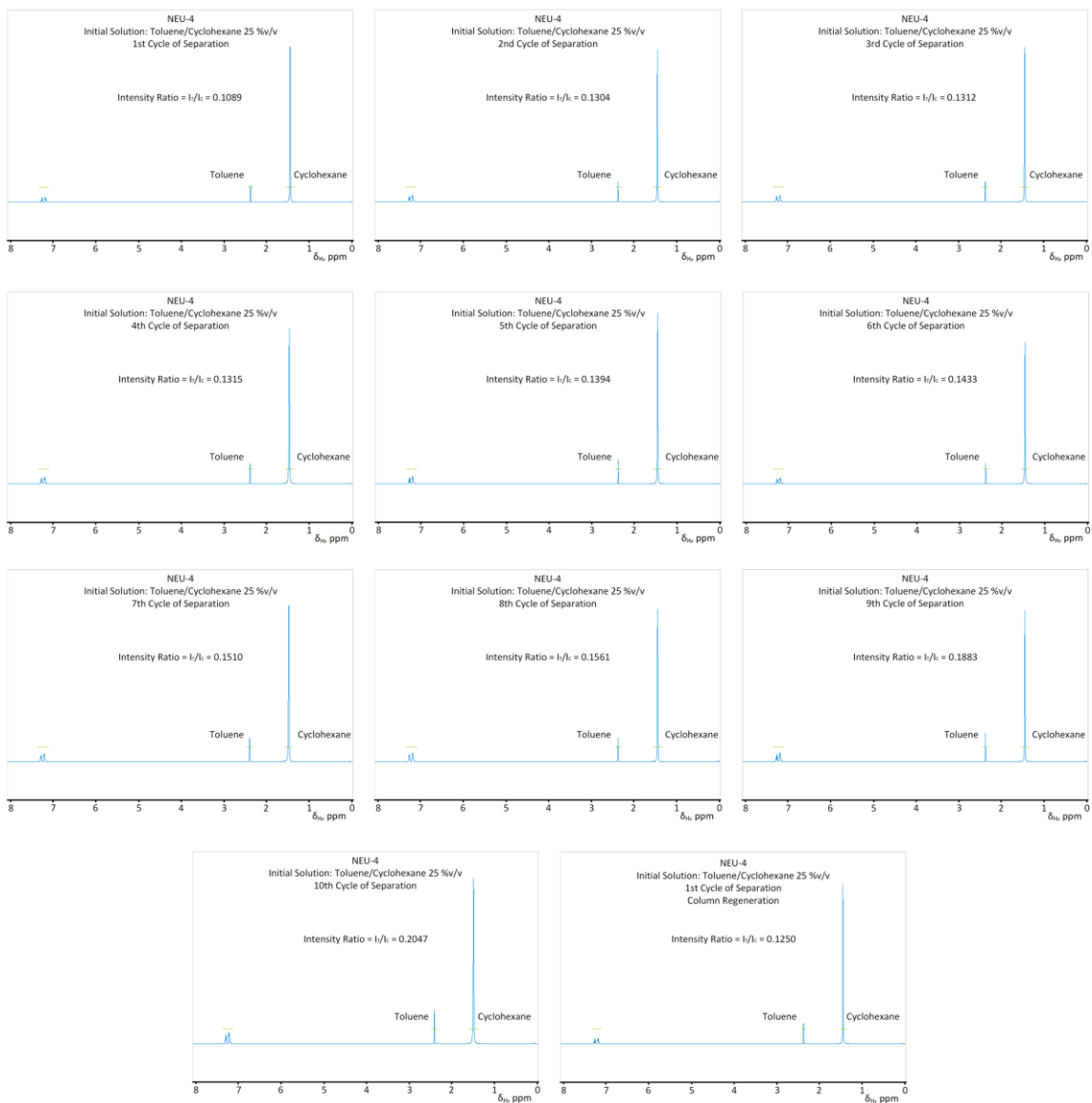


Fig. S64. ¹H NMR of toluene/cyclohexane eluent after 1st cs, 2nd cs, 3rd cs, 4th cs, 5th cs, 6th cs, 7th cs, 8th cs, 9th cs, 10th cs, and after 1st cs and 1st regeneration in NEU-4 (initial mixture 25 %v/v).

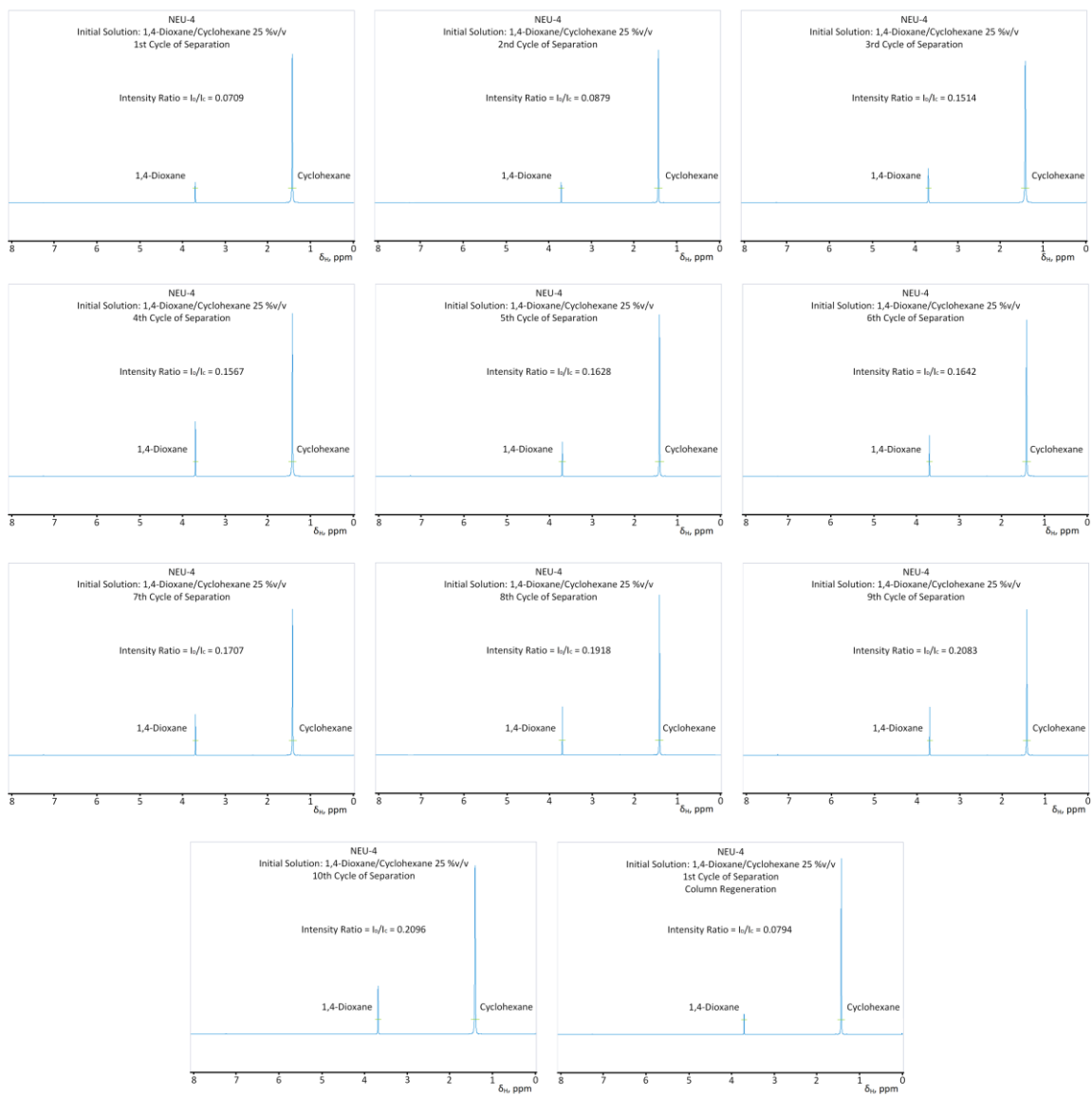


Fig. S65. ^1H NMR of 1,4-dioxane/cyclohexane eluent after 1st cs, 2nd cs, 3rd cs, 4th cs, 5th cs, 6th cs, 7th cs, 8th cs, 9th cs, 10th cs, and after 1st cs and 1st regeneration in NEU-4 (initial mixture 25 %v/v).

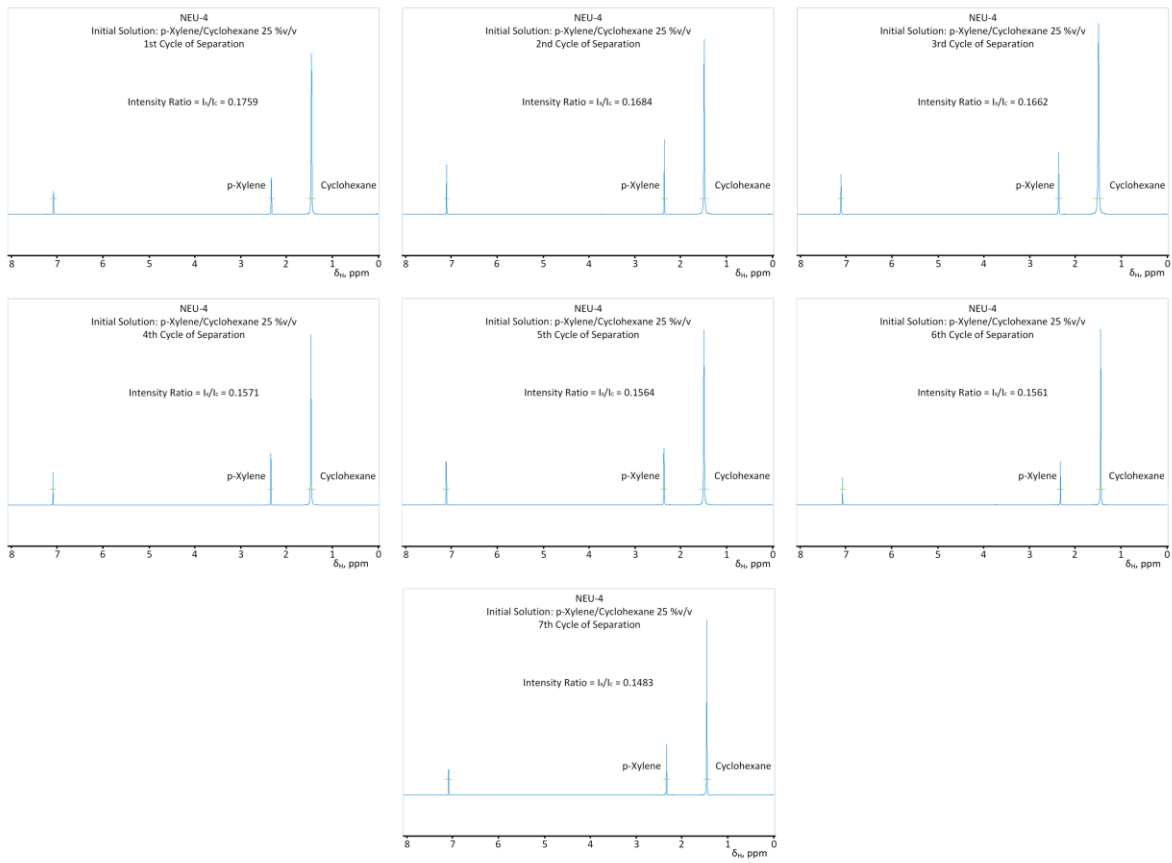


Fig. S66. ^1H NMR of p-xylene/cyclohexane eluent after 1st cs, 2nd cs, 3rd cs, 4th cs, 5th cs, 6th cs and 7th cs in NEU-4 (initial mixture 25 %v/v).

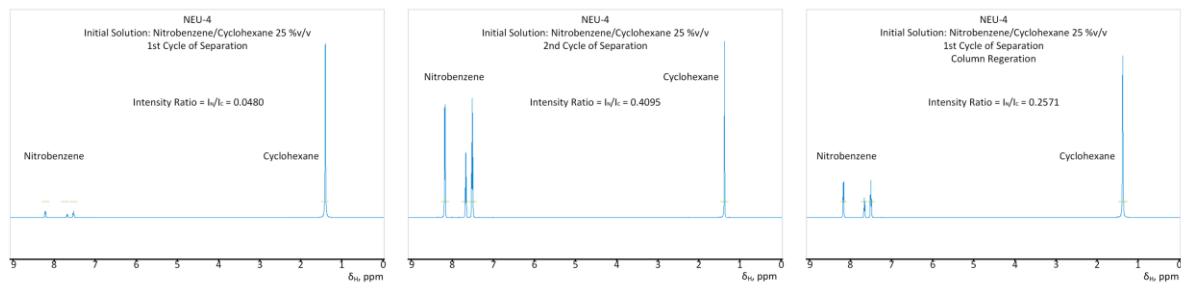


Fig. S67. ^1H NMR of nitrobenzene/cyclohexane eluent after 1st cs, 2nd cs, and after 1st cs and 1st regeneration in NEU-4 (initial mixture 25 %v/v).

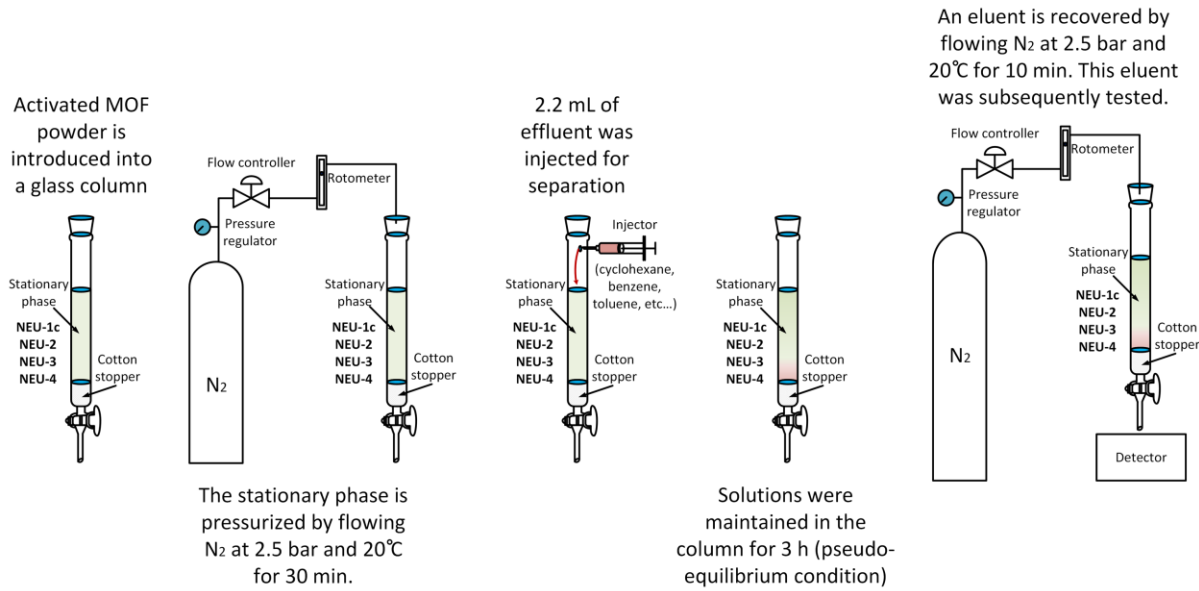


Fig. S68. Schematic procedure of the selective adsorptive separations.

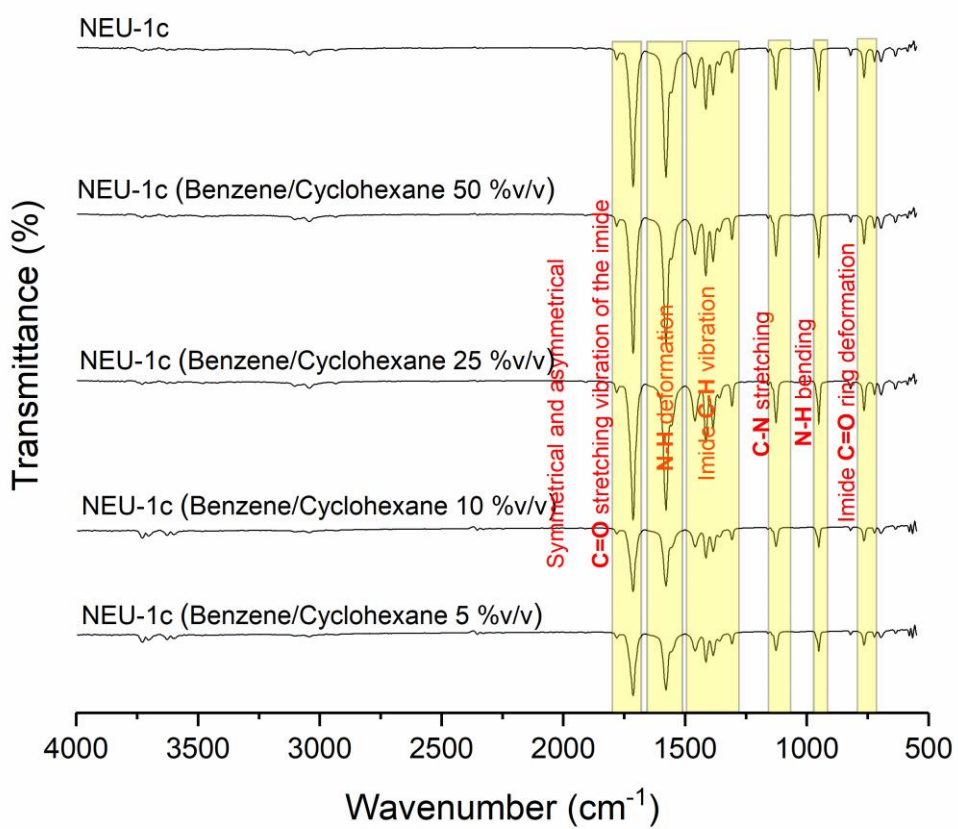


Fig. S69. FTIR spectra of NEU-1c before and after 10 cycles of benzene/cyclohexane (50 %v/v, 25 %v/v, 10 %v/v and 5 %v/v) separation and one regeneration. NEU-1c did not suffer structural alterations upon selective separations.

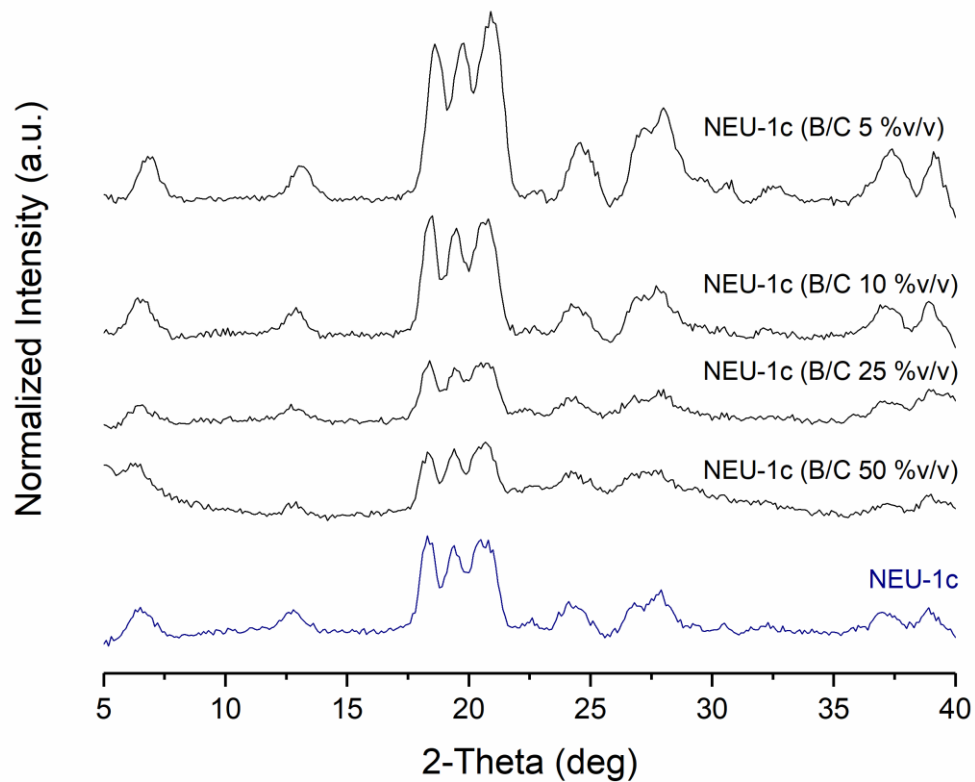


Fig. S70. XRD of NEU-1c before and after 10 cycles of benzene/cyclohexane (50 %v/v, 25 %v/v, 10 %v/v and 5 %v/v) separation and one regeneration. NEU-1c did not suffer structural alterations upon selective separations.

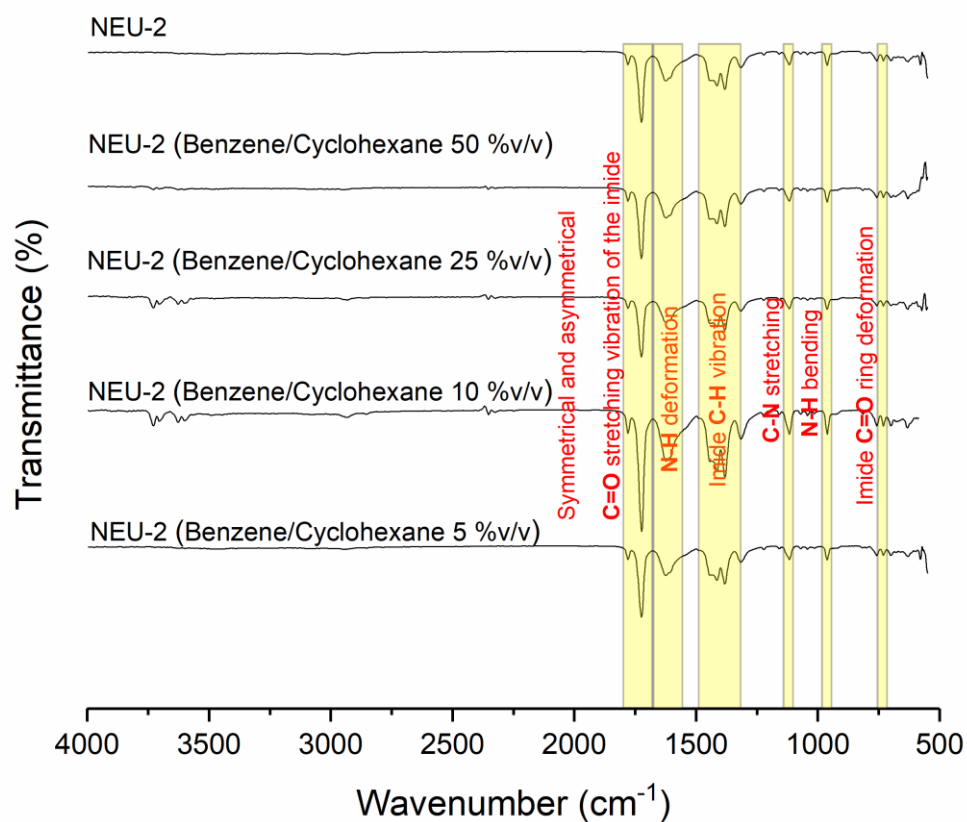


Fig. S71. FTIR spectra of NEU-2 before and after 10 cycles of benzene/cyclohexane (50 %v/v, 25 %v/v, 10 %v/v and 5 %v/v) separation and one regeneration. NEU-2 did not suffer structural alterations upon selective separations.

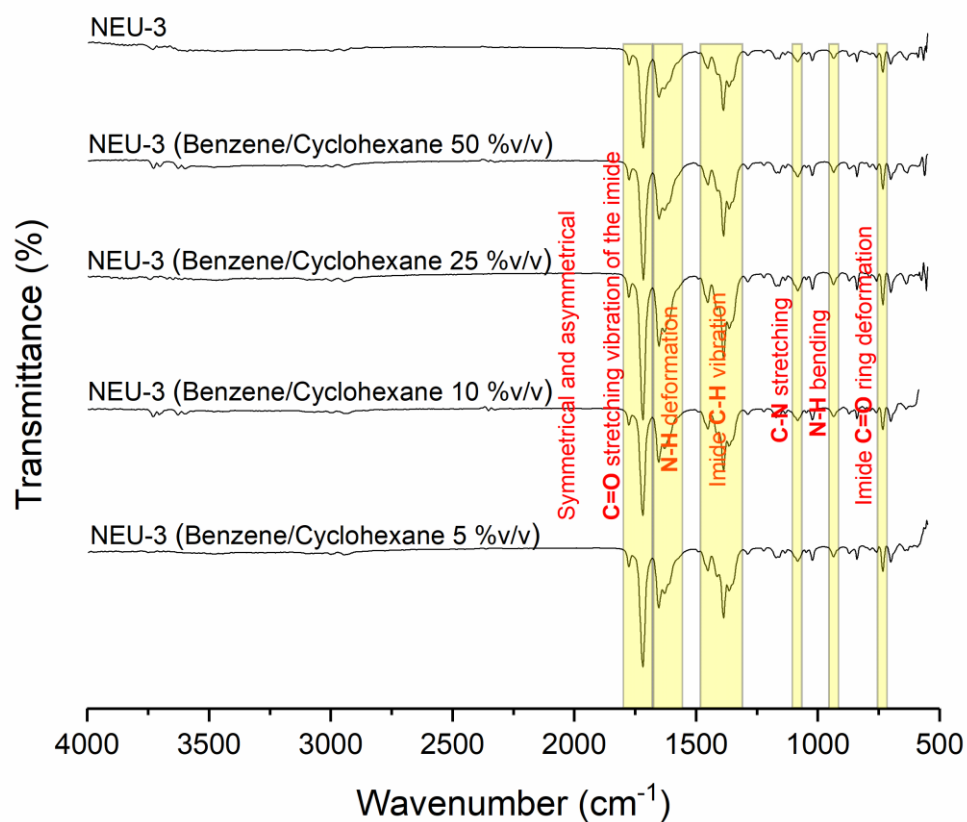


Fig. S72. FTIR spectra of NEU-3 before and after 10 cycles of benzene/cyclohexane (50 %v/v, 25 %v/v, 10 %v/v and 5 %v/v) separation and one regeneration. NEU-3 did not suffer structural alterations upon selective separations.

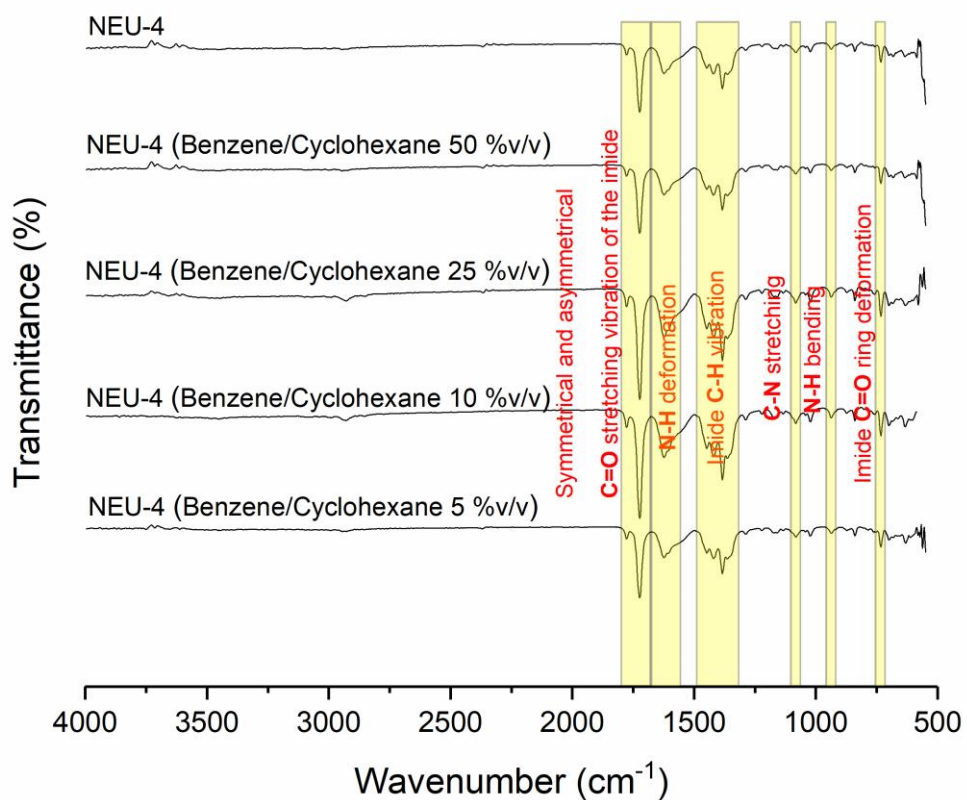


Fig. S73. FTIR spectra of NEU-4 before and after 10 cycles of benzene/cyclohexane (50 %v/v, 10 %v/v and 5 %v/v) separation and one regeneration (50 cycles of benzene/cyclohexane 25 %v/v separation and 4 regenerations). NEU-4 did not suffer structural alterations upon selective separations.

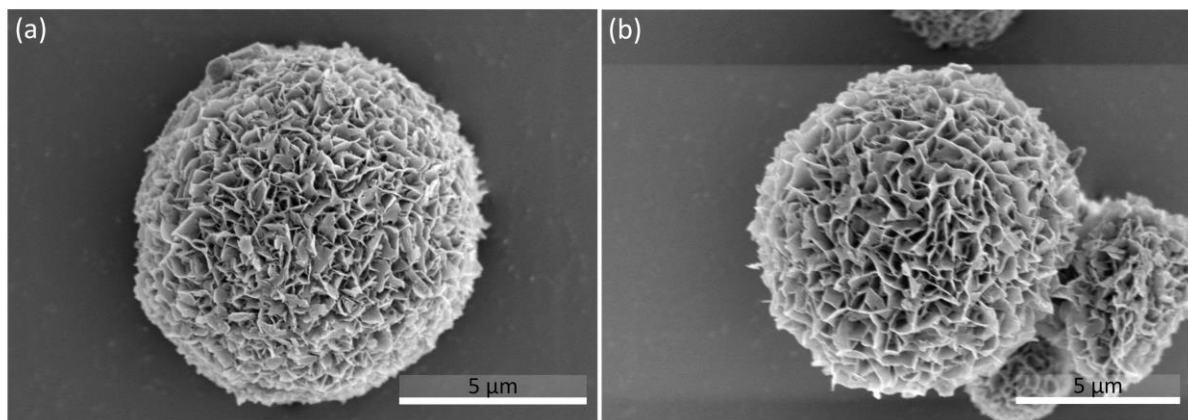


Fig. S74. SEM of NEU-1c (a) before and (b) after 10 cycles of benzene/cyclohexane 50 % v/v separation and one regeneration. The overall morphology of the frameworks was maintained.

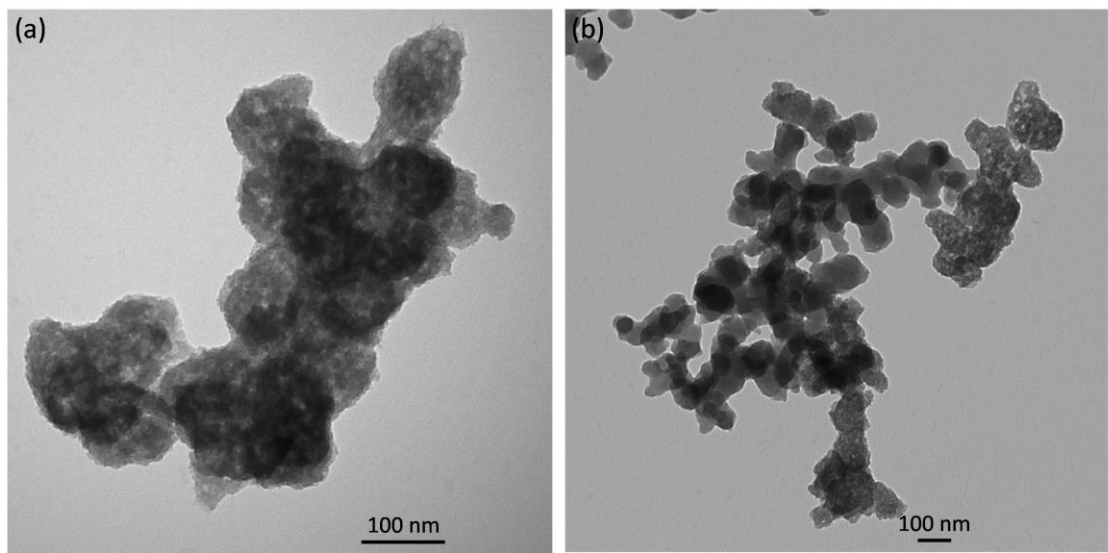


Fig. S75. TEM of NEU-1c (a) before and (b) after 10 cycles of benzene/cyclohexane 50 %v/v separation and one regeneration. The overall morphology of the frameworks was maintained.

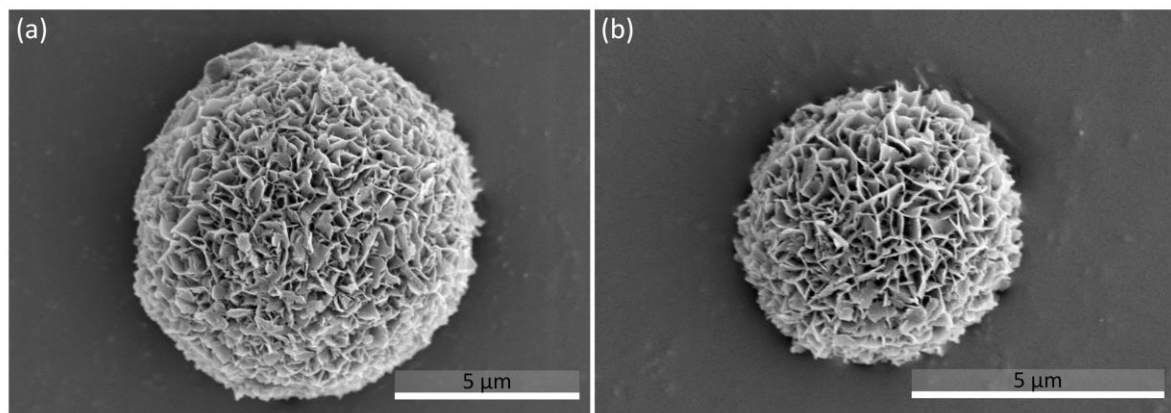


Fig. S76. SEM of NEU-1c (a) before and (b) after 10 cycles of benzene/cyclohexane 25 %v/v separation and one regeneration. The overall morphology of the frameworks was maintained.

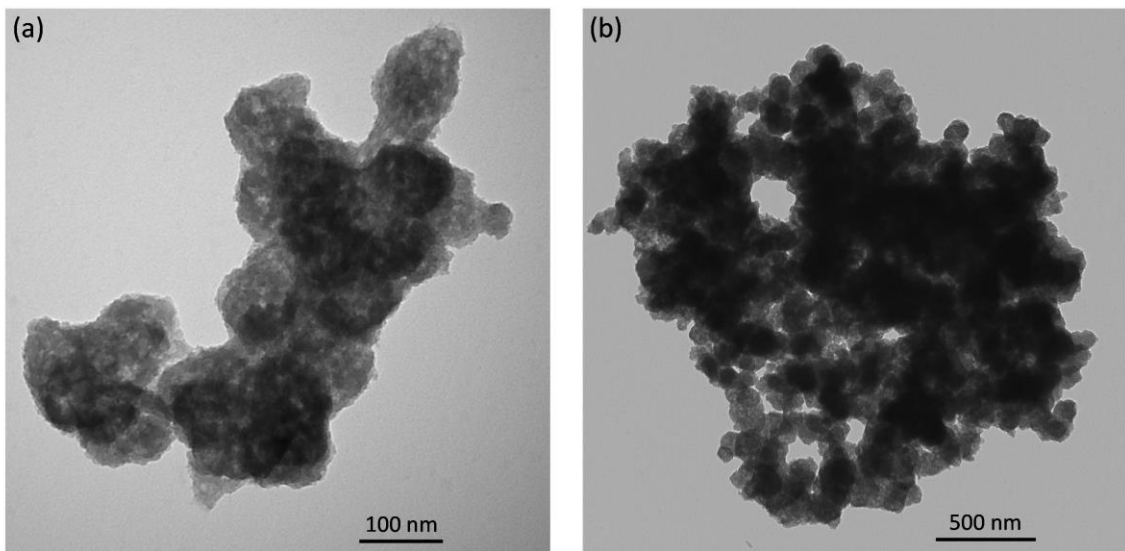


Fig. S77. TEM of NEU-1c (a) before and (b) after 10 cycles of benzene/cyclohexane 25 %v/v separation and one regeneration. The overall morphology of the frameworks was maintained.

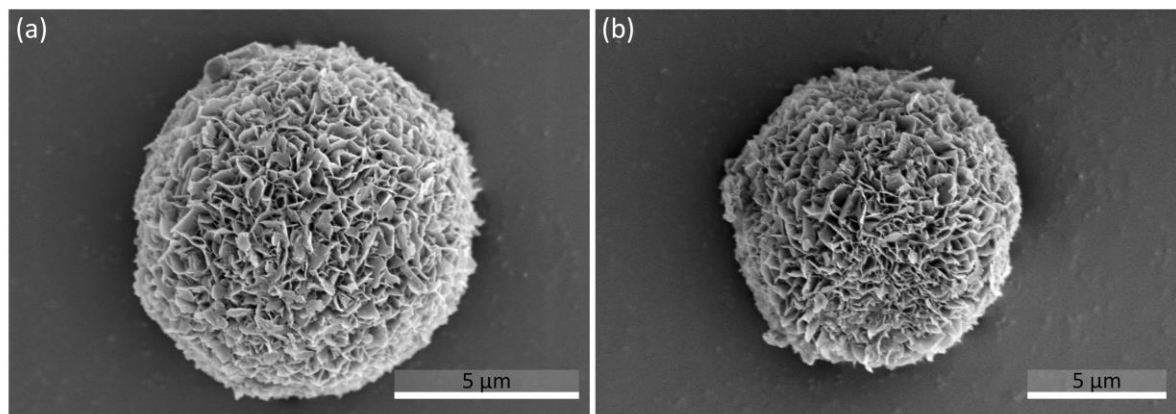


Fig. S78. SEM of NEU-1c (a) before and (b) after 10 cycles of benzene/cyclohexane 10 %v/v separation and one regeneration. The overall morphology of the frameworks was maintained.

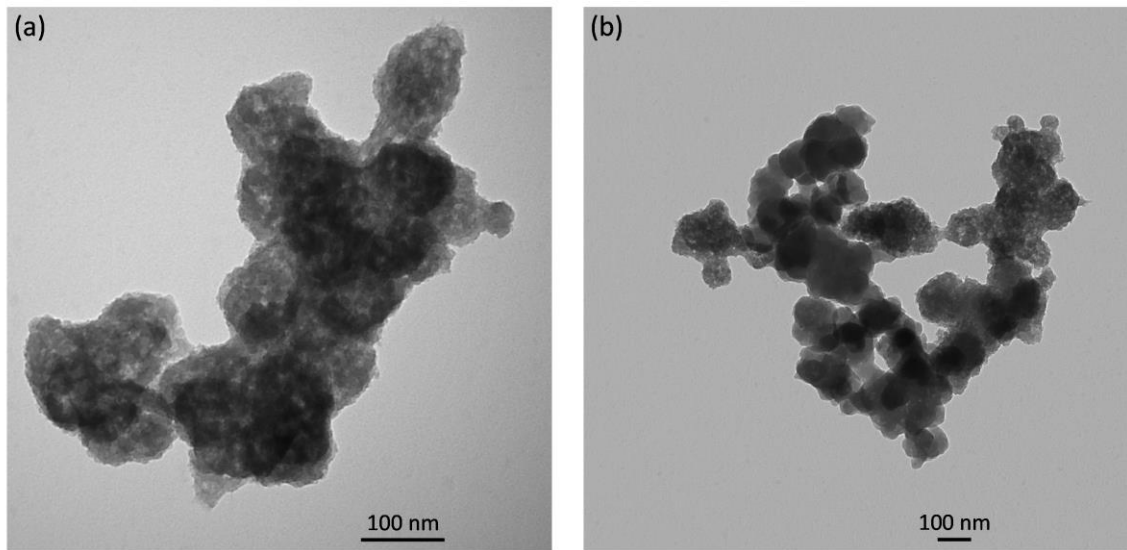


Fig. S79. TEM of NEU-1c (a) before and (b) after 10 cycles of benzene/cyclohexane 10 %v/v separation and one regeneration. The overall morphology of the frameworks was maintained.

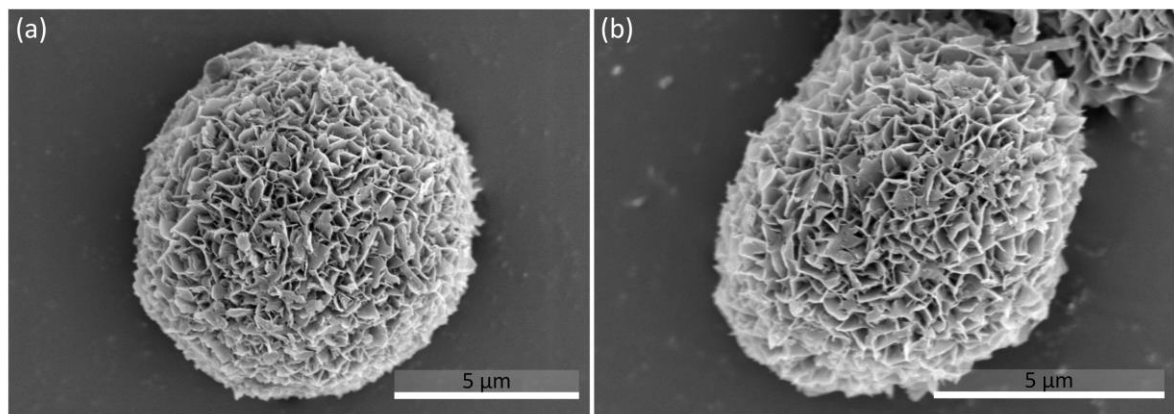


Fig. S80. SEM of NEU-1c (a) before and (b) after 10 cycles of benzene/cyclohexane 5 %v/v separation and one regeneration. The overall morphology of the frameworks was maintained.

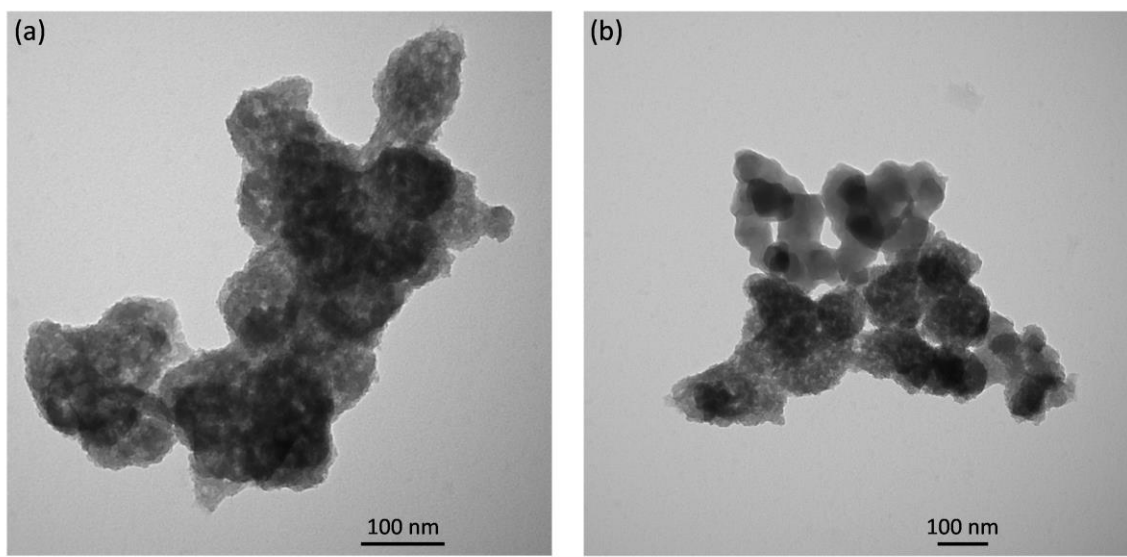


Fig. S81. TEM of NEU-1c (a) before and (b) after 10 cycles of benzene/cyclohexane 5 %v/v separation and one regeneration. The overall morphology of the frameworks was maintained.

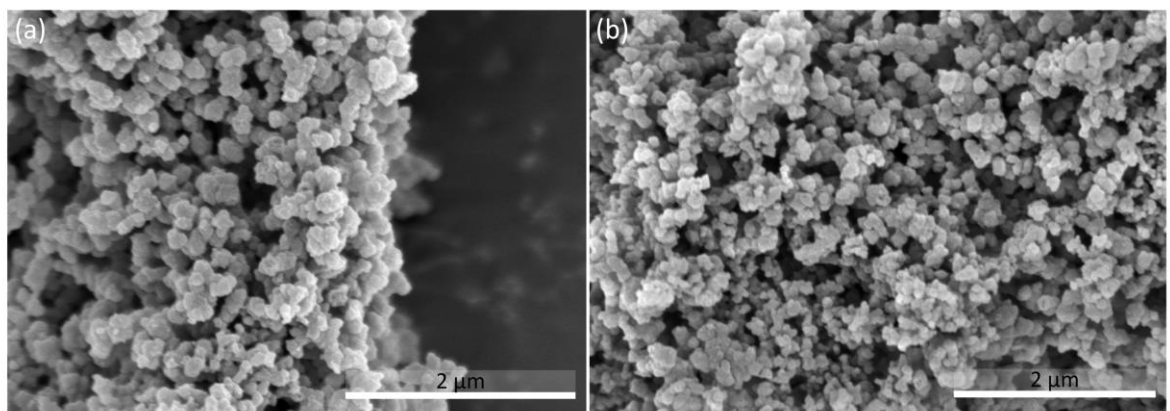


Fig. S82. SEM of NEU-2 (a) before and (b) after 10 cycles of benzene/cyclohexane 50 %v/v separation and one regeneration. The overall morphology of the frameworks was maintained.

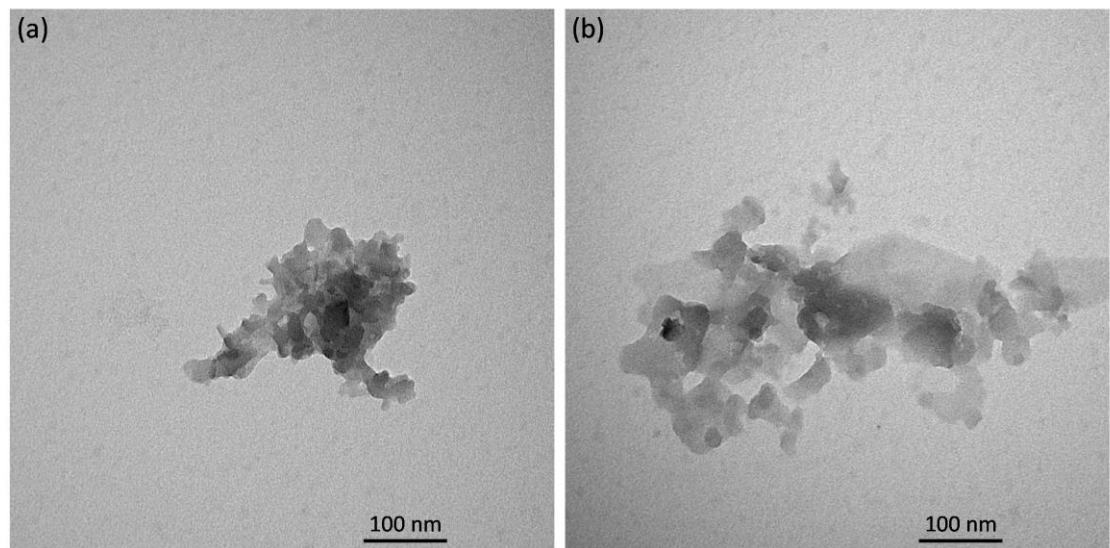


Fig. S83. TEM of NEU-2 (a) before and (b) after 10 cycles of benzene/cyclohexane 50 %v/v separation and one regeneration. The overall morphology of the frameworks was maintained.

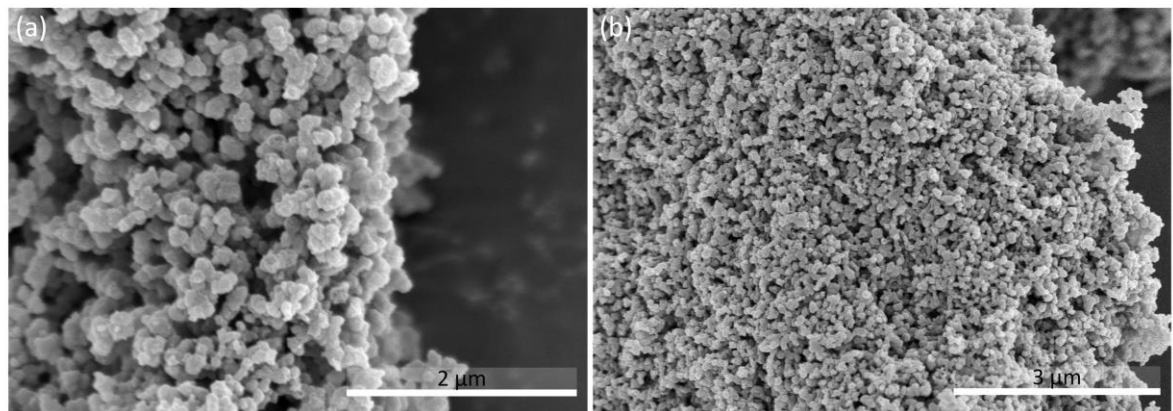


Fig. S84. SEM of NEU-2 (a) before and (b) after 10 cycles of benzene/cyclohexane 25 %v/v separation and one regeneration. The overall morphology of the frameworks was maintained.

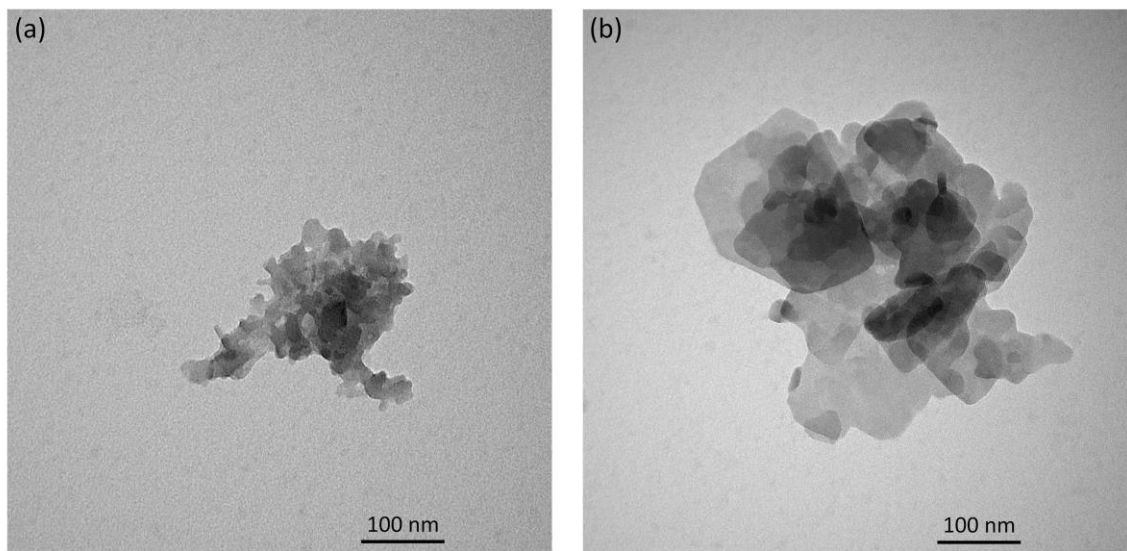


Fig. S85. TEM of NEU-2 (a) before and (b) after 10 cycles of benzene/cyclohexane 25 %v/v separation and one regeneration. The overall morphology of the frameworks was maintained.

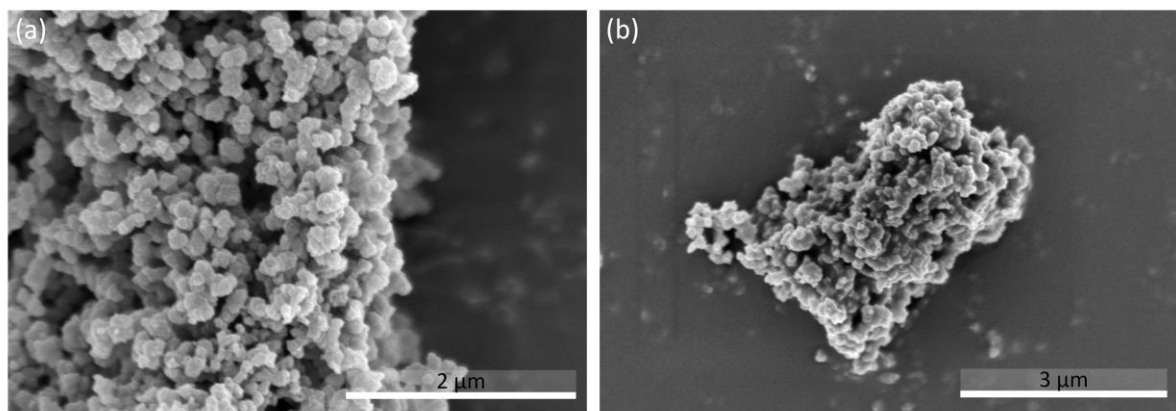


Fig. S86. SEM of NEU-2 (a) before and (b) after 10 cycles of benzene/cyclohexane 10 %v/v separation and one regeneration. The overall morphology of the frameworks was maintained.

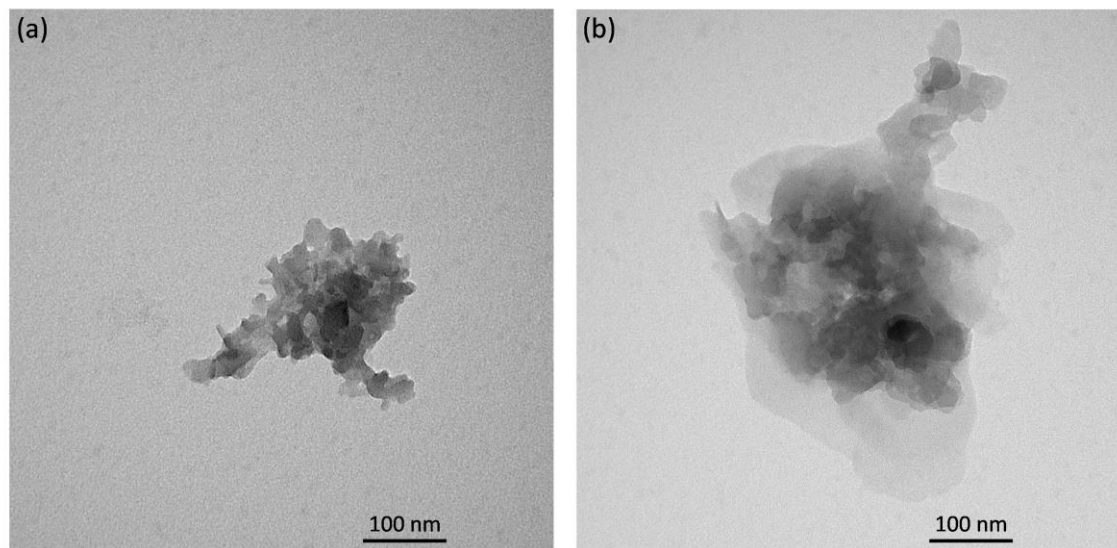


Fig. S87. TEM of NEU-2 (a) before and (b) after 10 cycles of benzene/cyclohexane 10 %v/v separation and one regeneration. The overall morphology of the frameworks was maintained.

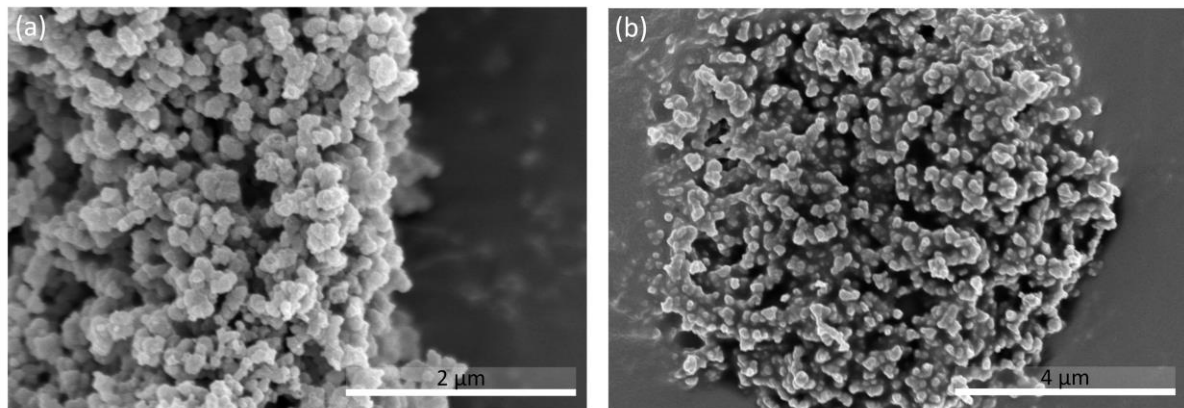


Fig. S88. SEM of NEU-2 (a) before and (b) after 10 cycles of benzene/cyclohexane 5 %v/v separation and one regeneration. The overall morphology of the frameworks was maintained.

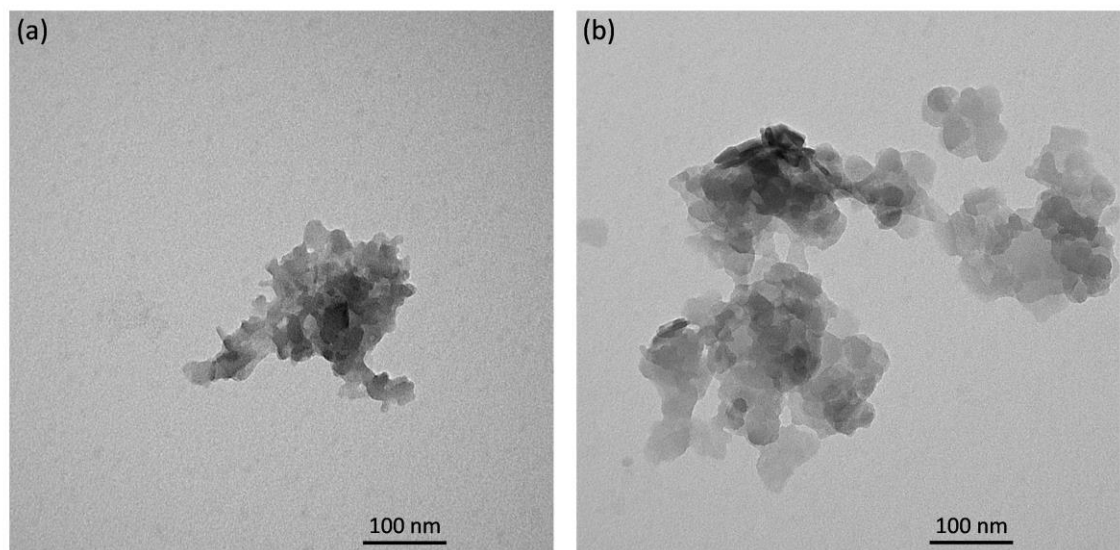


Fig. S89. TEM of NEU-2 (a) before and (b) after 10 cycles of benzene/cyclohexane 5 %v/v separation and one regeneration. The overall morphology of the frameworks was maintained.

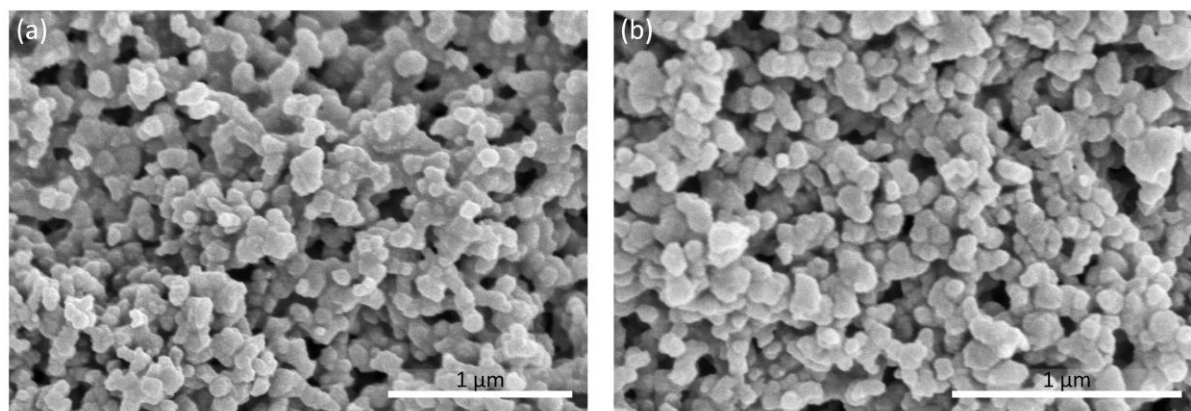


Fig. S90. SEM of NEU-3 (a) before and (b) after 10 cycles of benzene/cyclohexane 50 %v/v separation and one regeneration. The overall morphology of the frameworks was maintained.

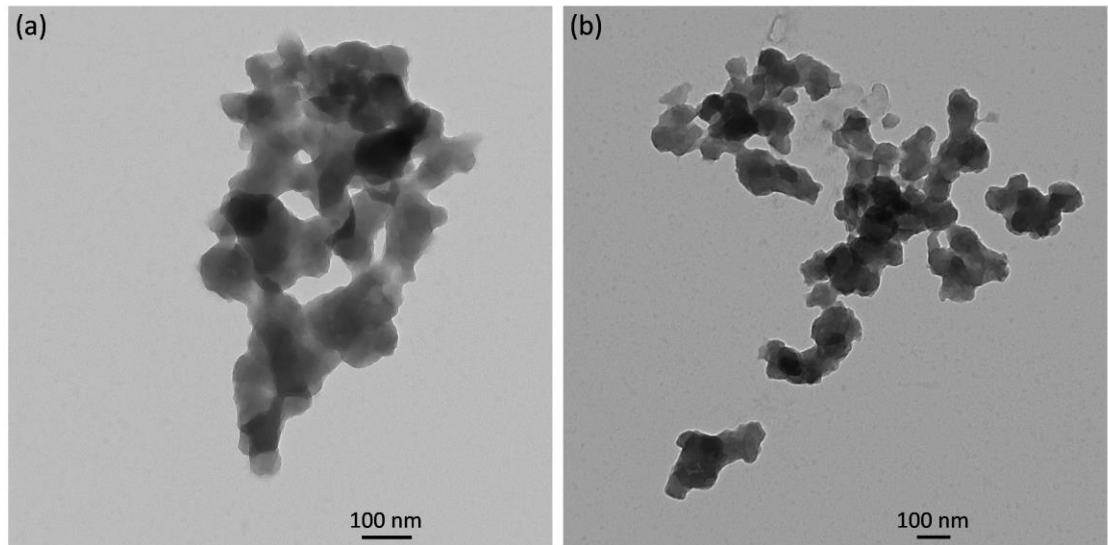


Fig. S91. TEM of NEU-3 (a) before and (b) after 10 cycles of benzene/cyclohexane 50 %v/v separation and one regeneration. The overall morphology of the frameworks was maintained.

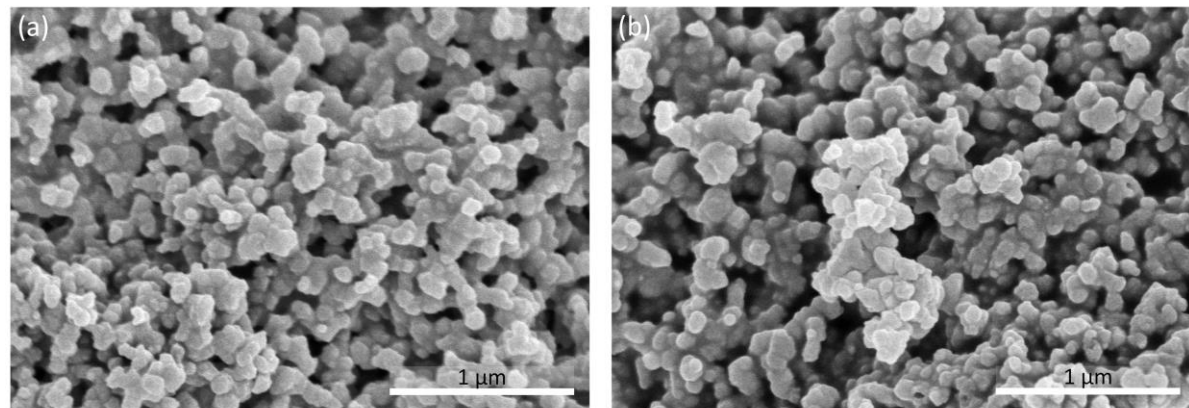


Fig. S92. SEM of NEU-3 (a) before and (b) after 10 cycles of benzene/cyclohexane 25 %v/v separation and one regeneration. The overall morphology of the frameworks was maintained.

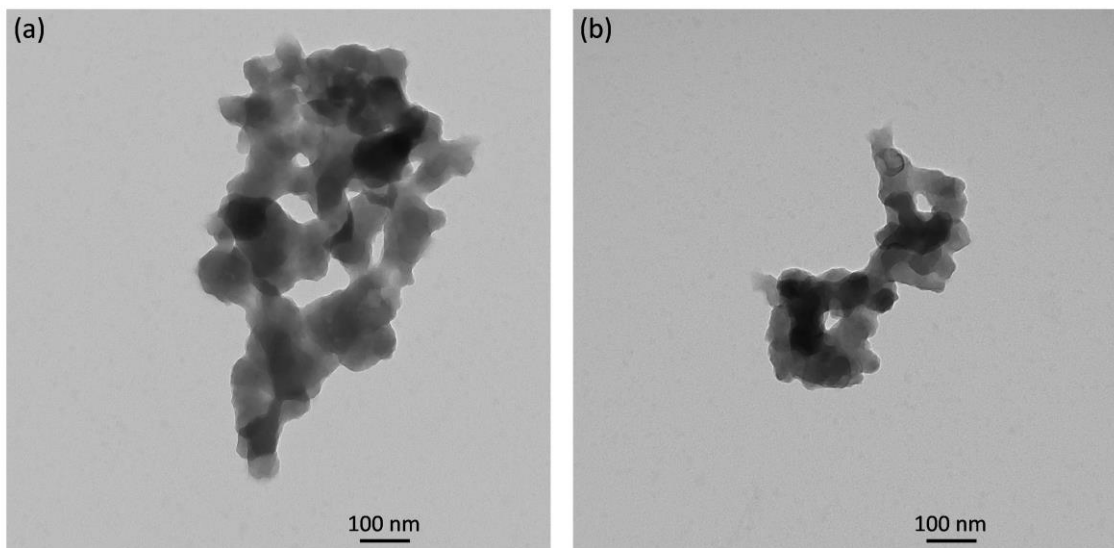


Fig. S93. TEM of NEU-3 (a) before and (b) after 10 cycles of benzene/cyclohexane 25 %v/v separation and one regeneration. The overall morphology of the frameworks was maintained.

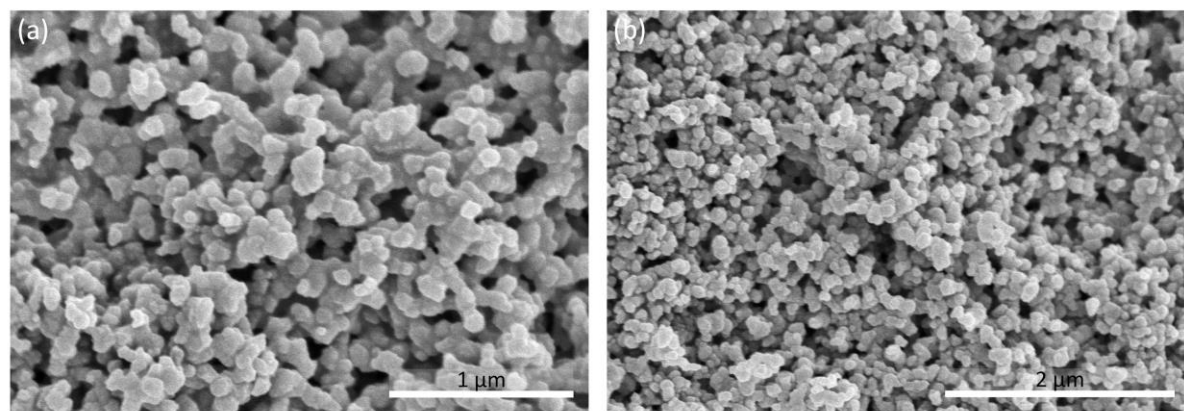


Fig. S94. SEM of NEU-3 (a) before and (b) after 10 cycles of benzene/cyclohexane 10 %v/v separation and one regeneration. The overall morphology of the frameworks was maintained.

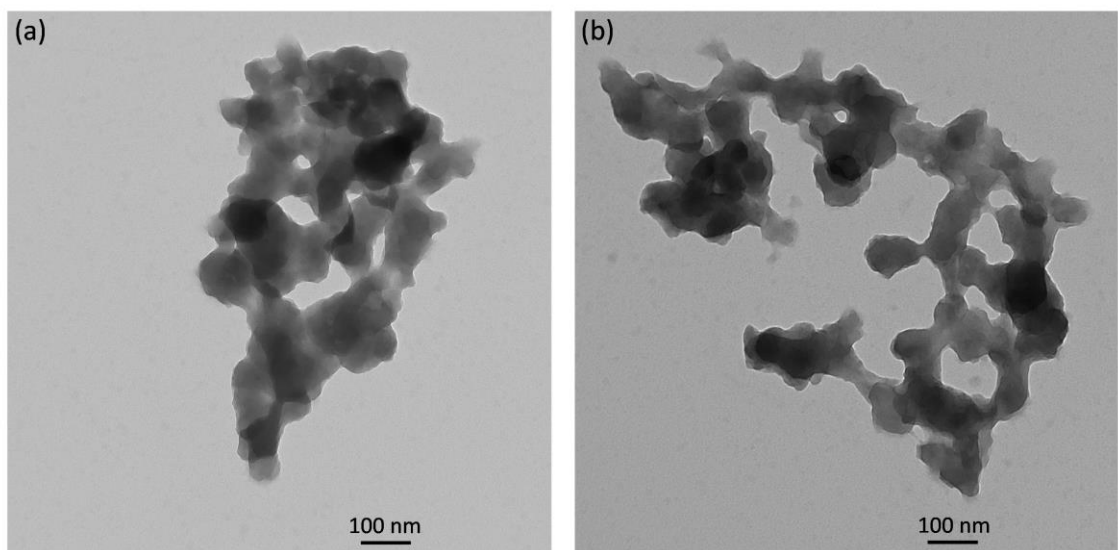


Fig. S95. TEM of NEU-3 (a) before and (b) after 10 cycles of benzene/cyclohexane 10 %v/v separation and one regeneration. The overall morphology of the frameworks was maintained.

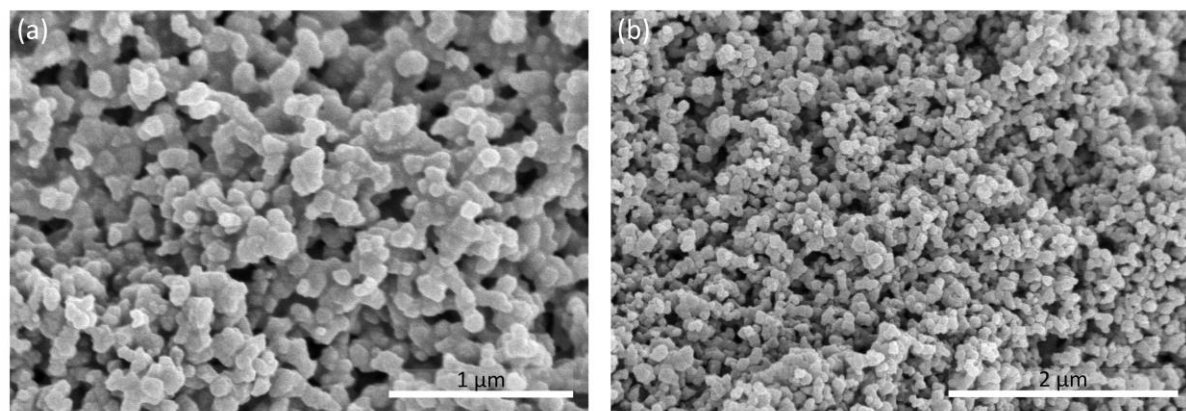


Fig. S96. SEM of NEU-3 (a) before and (b) after 10 cycles of benzene/cyclohexane 5 %v/v separation and one regeneration. The overall morphology of the frameworks was maintained.

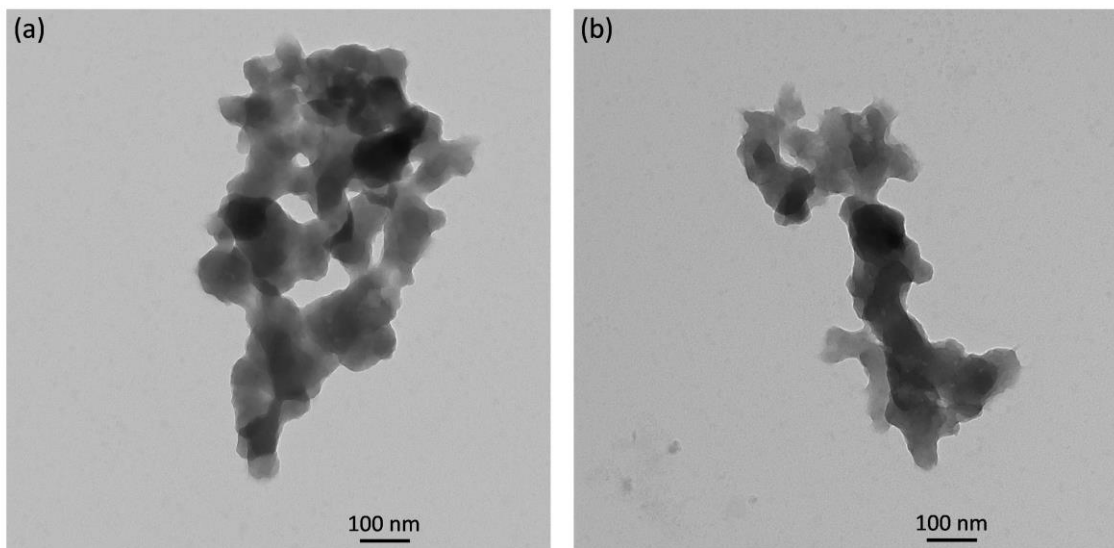


Fig. S97. TEM of NEU-3 (a) before and (b) after 10 cycles of benzene/cyclohexane 5 %v/v separation and one regeneration. The overall morphology of the frameworks was maintained.

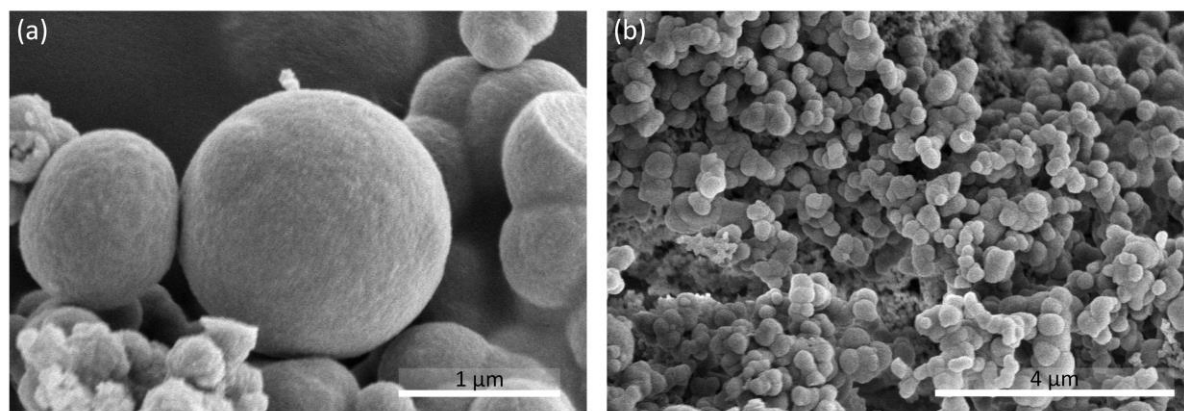


Fig. S98. SEM of NEU-4 (a) before and (b) after 10 cycles of benzene/cyclohexane 50 %v/v separation and one regeneration. The overall morphology of the frameworks was maintained.

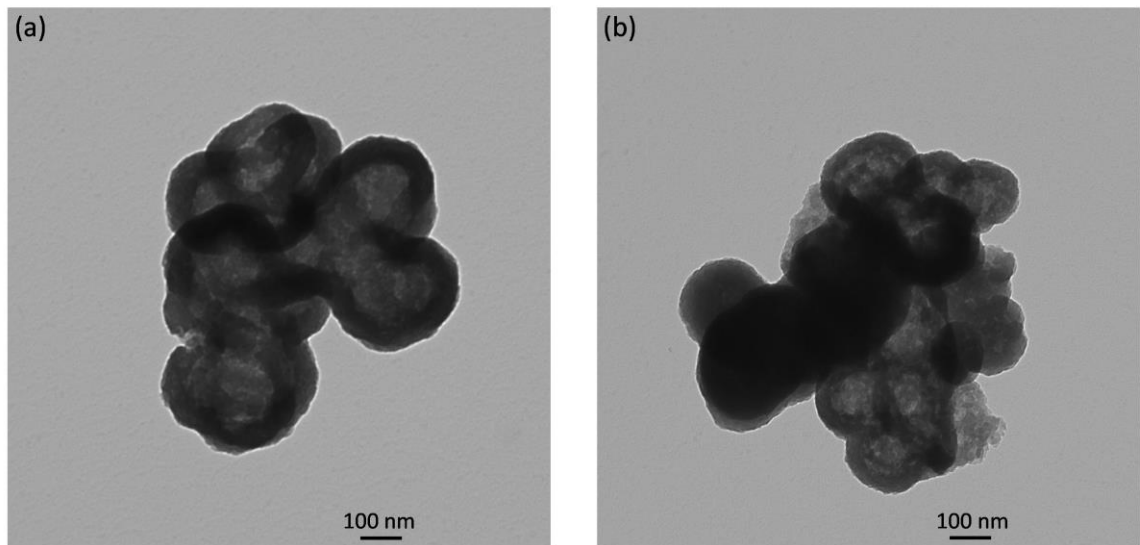


Fig. S99. TEM of NEU-4 (a) before and (b) after 10 cycles of benzene/cyclohexane 50 %v/v separation and one regeneration. The overall morphology of the frameworks was maintained.

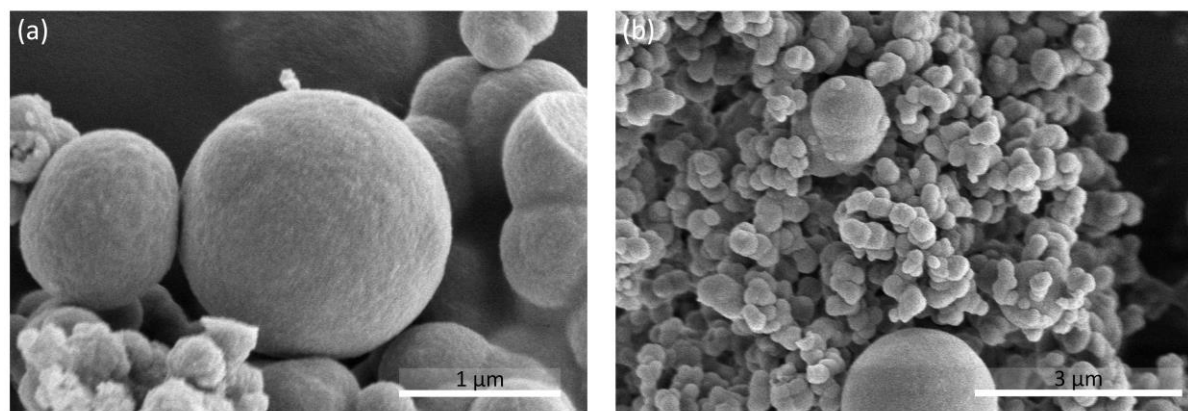


Fig. S100. SEM of NEU-4 (a) before and (b) after 50 cycles of benzene/cyclohexane 25 %v/v separation and four regenerations. The overall morphology of the frameworks was maintained.

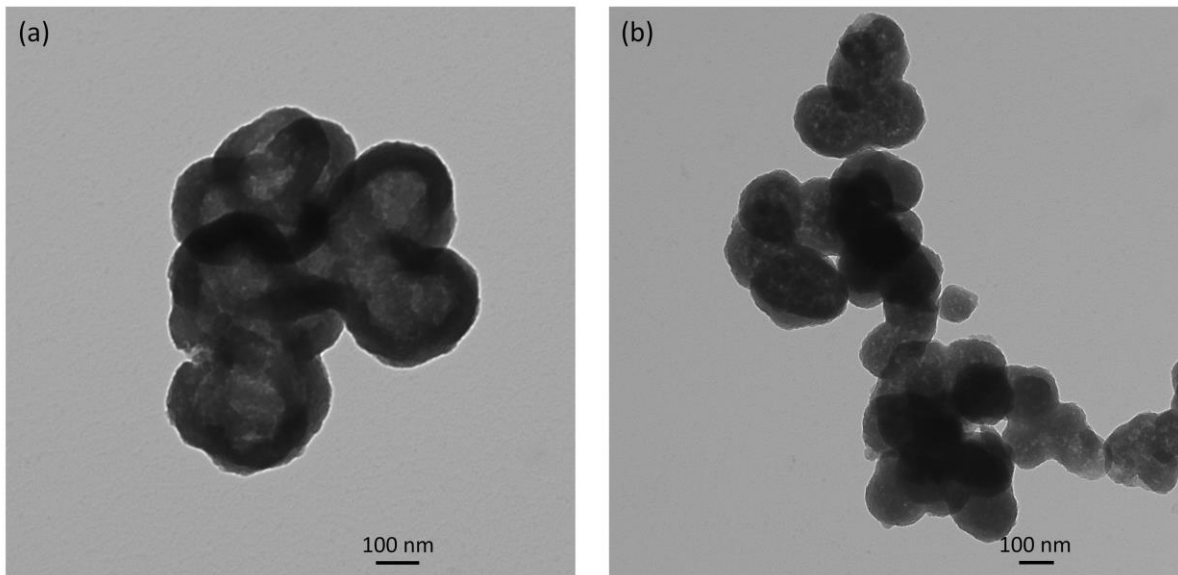


Fig. S101. TEM of NEU-4 (a) before and (b) after 50 cycles of benzene/cyclohexane 25 %v/v separation and four regenerations. The overall morphology of the frameworks was maintained.

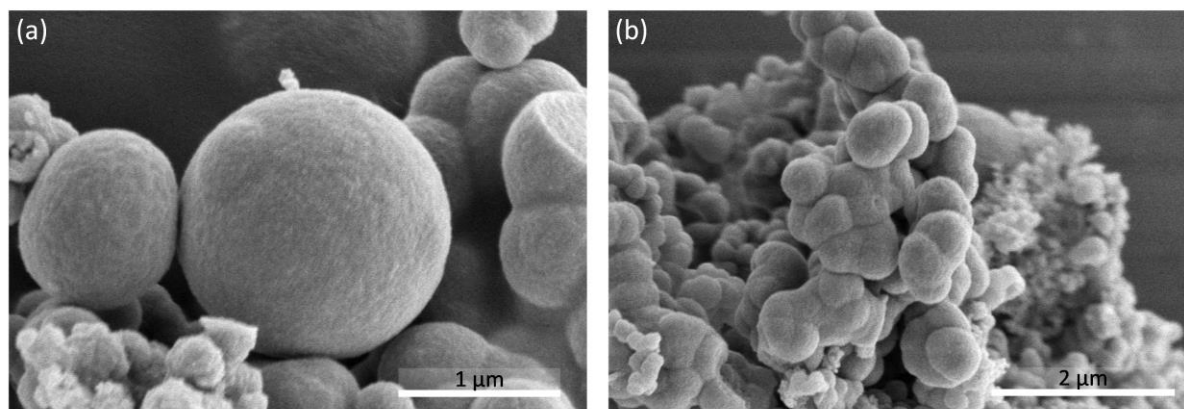


Fig. S102. SEM of NEU-4 (a) before and (b) after 10 cycles of benzene/cyclohexane 10 %v/v separation and one regeneration. The overall morphology of the frameworks was maintained.

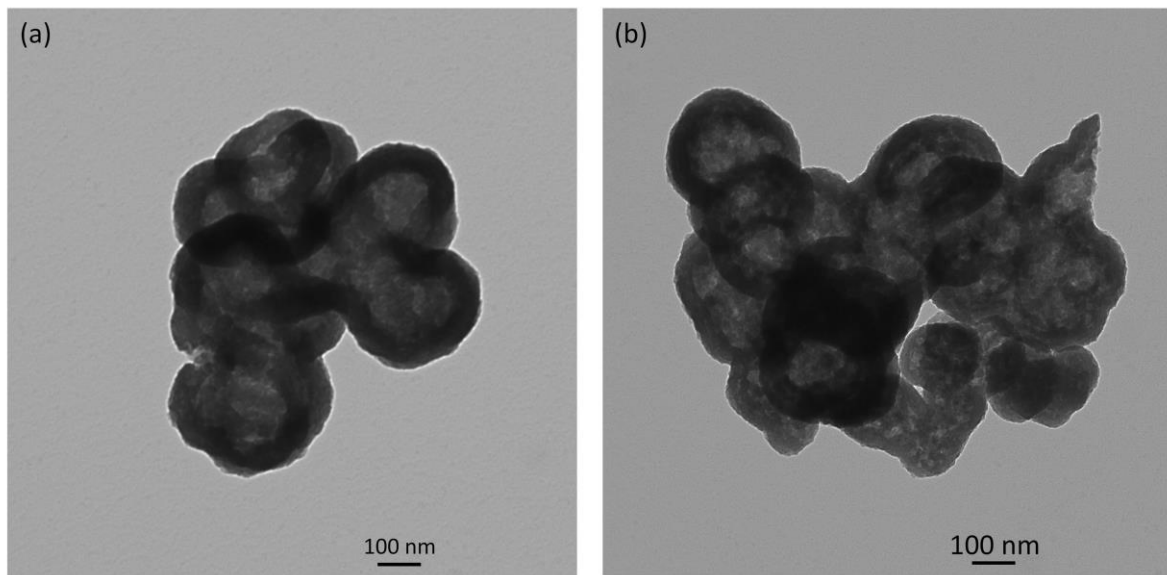


Fig. S103. TEM of NEU-4 (a) before and (b) after 10 cycles of benzene/cyclohexane 10 %v/v separation and one regeneration. The overall morphology of the frameworks was maintained.

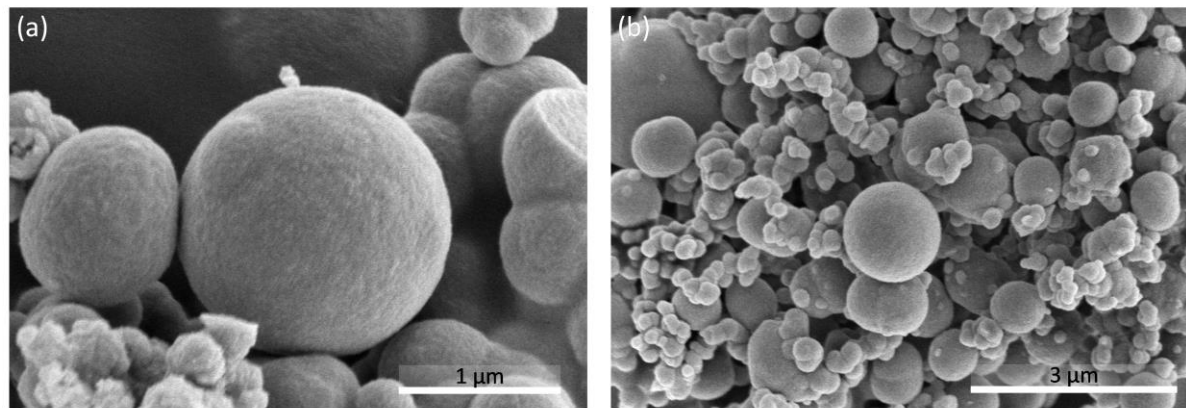


Fig. S104. SEM of NEU-4 (a) before and (b) after 10 cycles of benzene/cyclohexane 5 %v/v separation and one regeneration. The overall morphology of the frameworks was maintained.

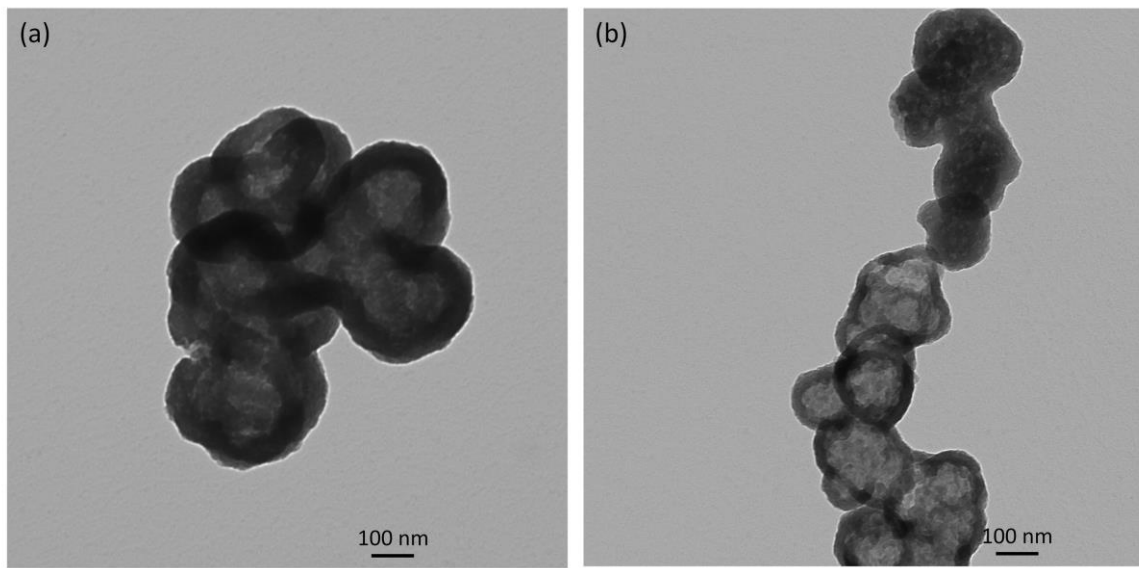


Fig. S105. TEM of NEU-4 (a) before and (b) after 10 cycles of benzene/cyclohexane 5 %v/v separation and one regeneration. The overall morphology of the frameworks was maintained.

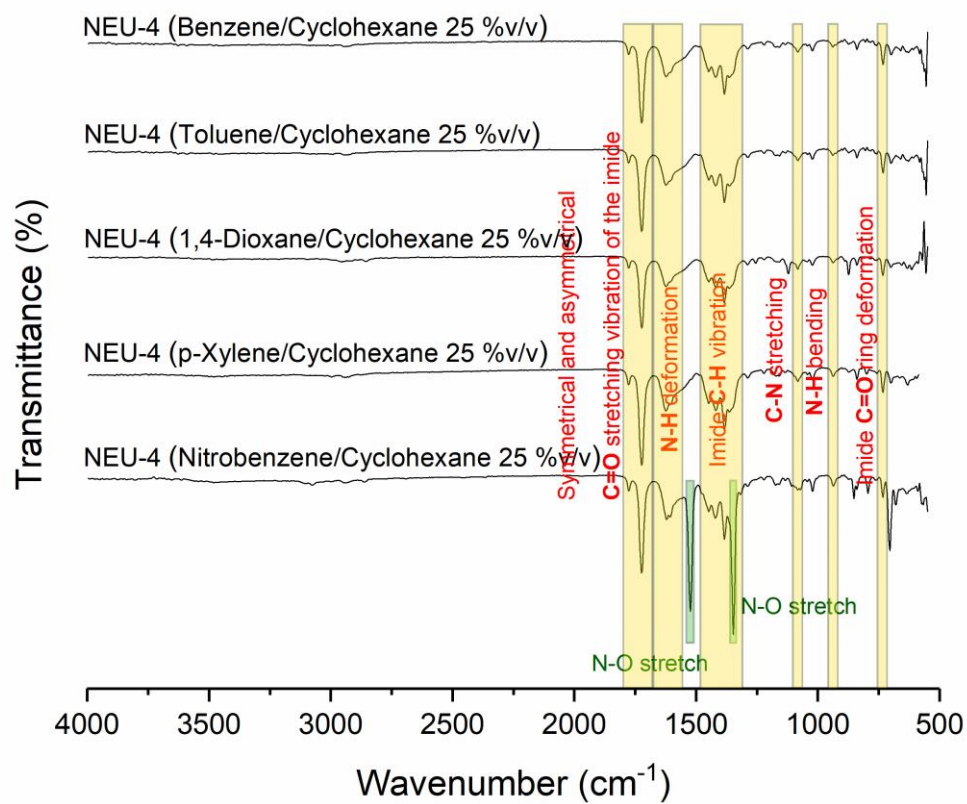


Fig. S106. FTIR spectra of NEU-4 after separation of aliphatic-aromatic hydrocarbons (25 %v/v). NEU-4 did not suffer structural alterations upon selective separations.

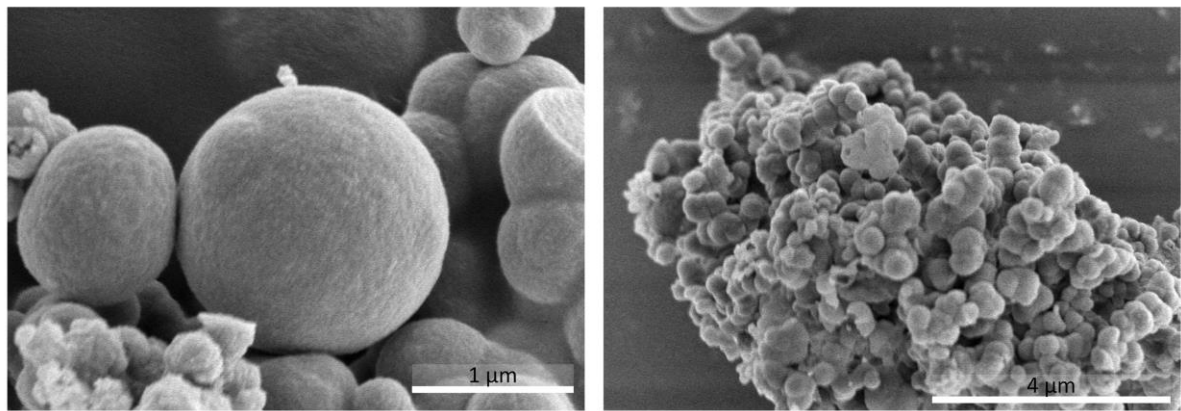


Fig. S107. SEM of NEU-4 (a) before and (b) after separation of toluene/cyclohexane (25 % v/v).

The overall morphology of NEU-4 was maintained.

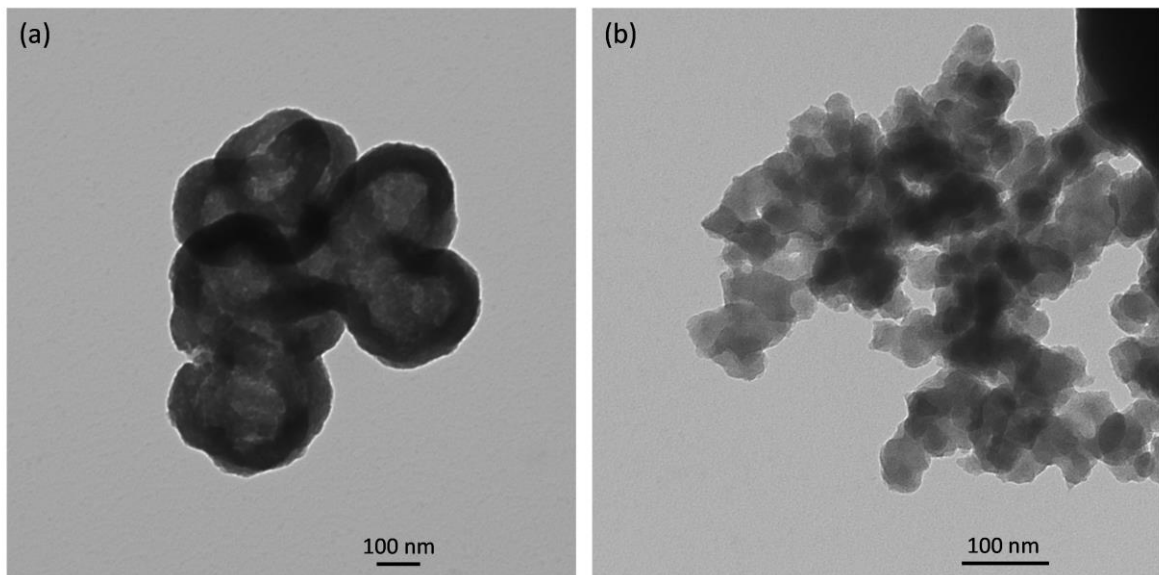


Fig. S108. TEM of NEU-4 (a) before and (b) after separation of toluene/cyclohexane (25 %v/v).

The overall morphology of NEU-4 was maintained.

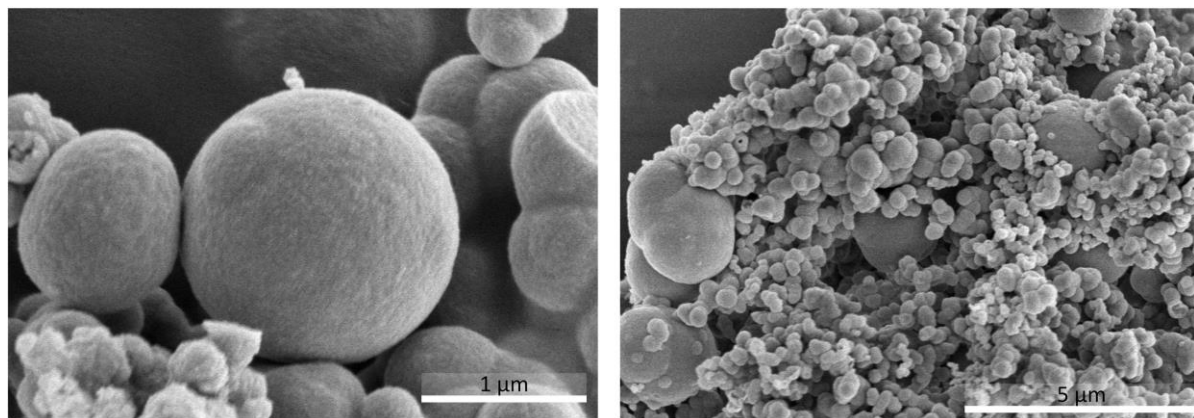


Fig. S109. SEM of NEU-4 (a) before and (b) after separation of 1,4-dioxane/cyclohexane (25 %v/v). The overall morphology of NEU-4 was maintained.

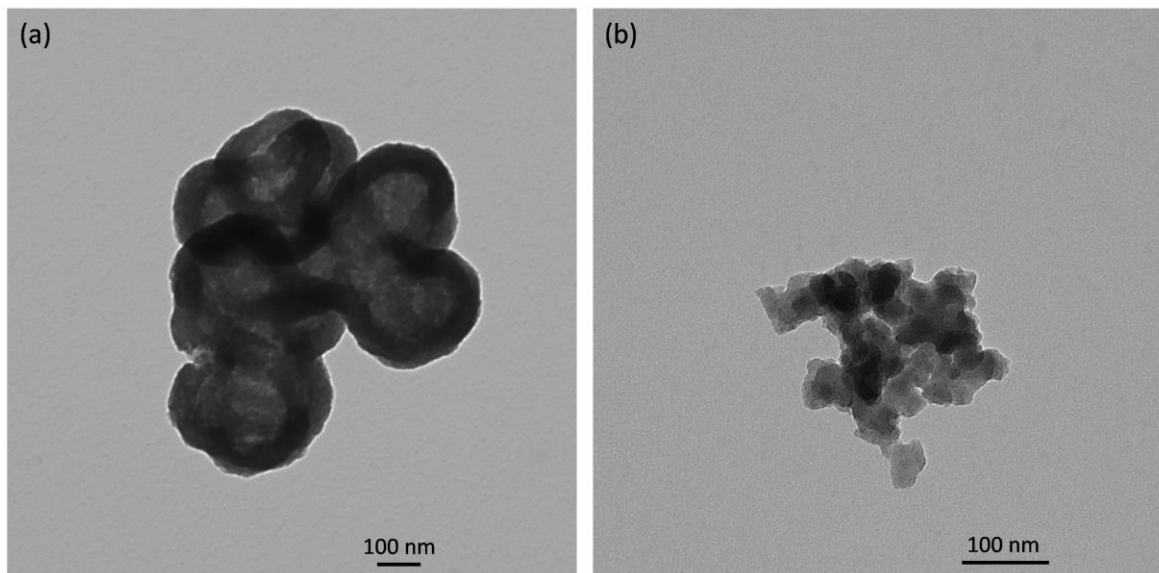


Fig. S110. TEM of NEU-4 (a) before and (b) after separation of 1,4-dioxane/cyclohexane (25 %v/v). The overall morphology of NEU-4 was maintained.

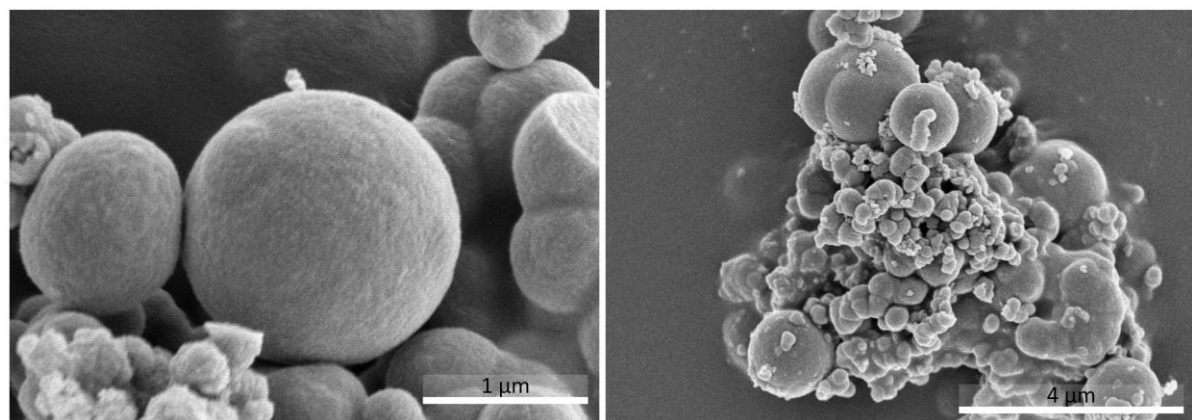


Fig. S111. SEM of NEU-4 (a) before and (b) after separation of p-xylene/cyclohexane (25 %v/v). The overall morphology of NEU-4 was maintained.

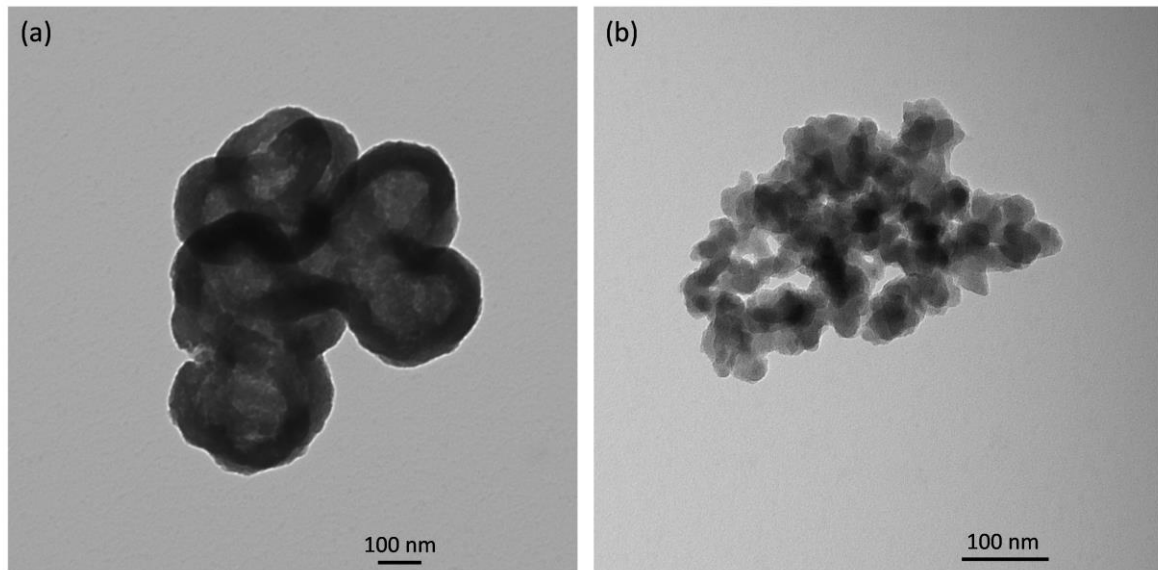


Fig. S112. TEM of NEU-4 (a) before and (b) after separation of p-xylene/cyclohexane (25 %v/v). The overall morphology of NEU-4 was maintained.

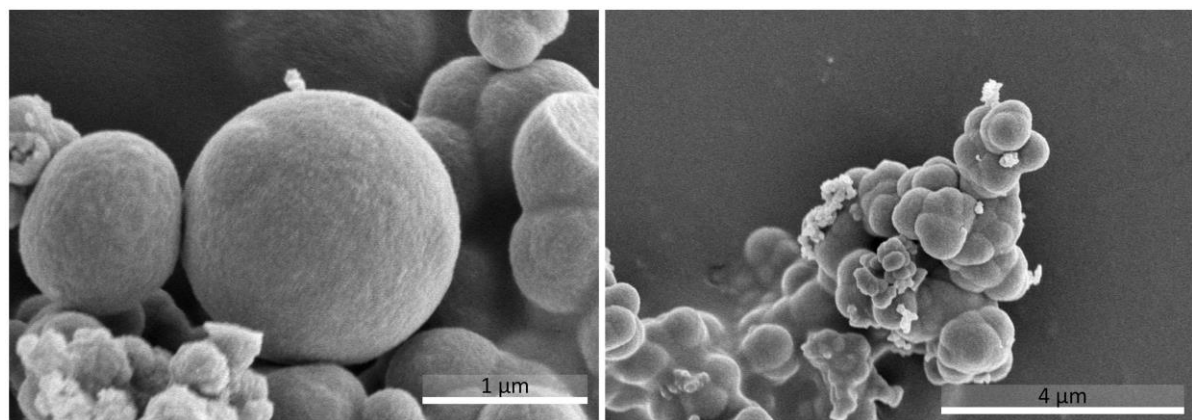


Fig. S113. SEM of NEU-4 (a) before and (b) after separation of nitrobenzene/cyclohexane (25 %v/v). The overall morphology of NEU-4 was maintained.

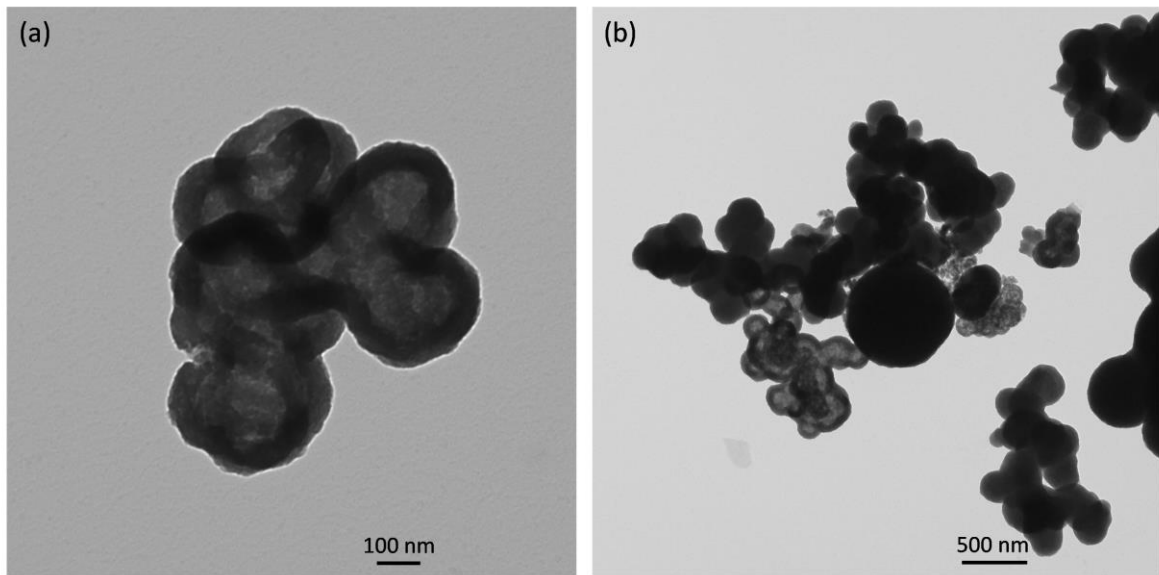


Fig. S114. TEM of NEU-4 (a) before and (b) after separation of nitrobenzene/cyclohexane (25 %v/v). The overall morphology of NEU-4 was maintained.

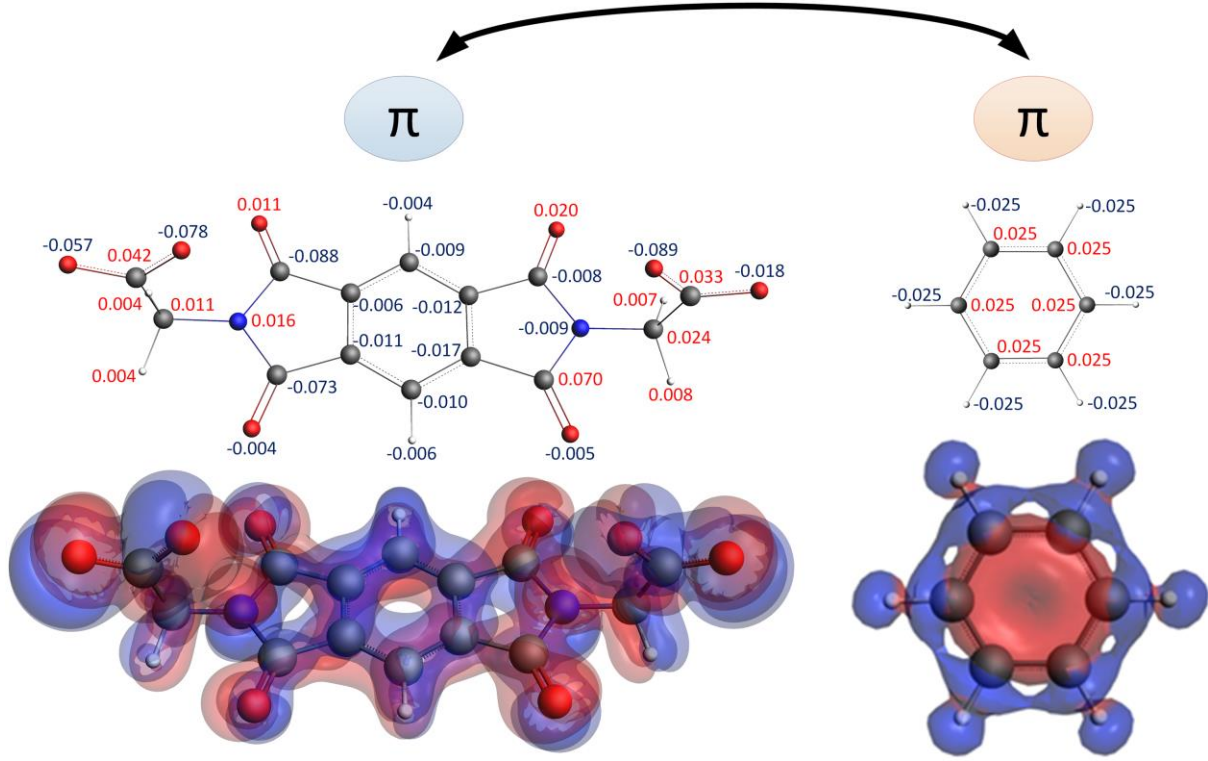


Fig. S115. Condensed Fukui functions determined for Bader charges and isosurface of dual descriptor of BPDI²⁻ and benzene. It is worth noting that both NEU-1c and NEU-2 are made up of BPDI²⁻.

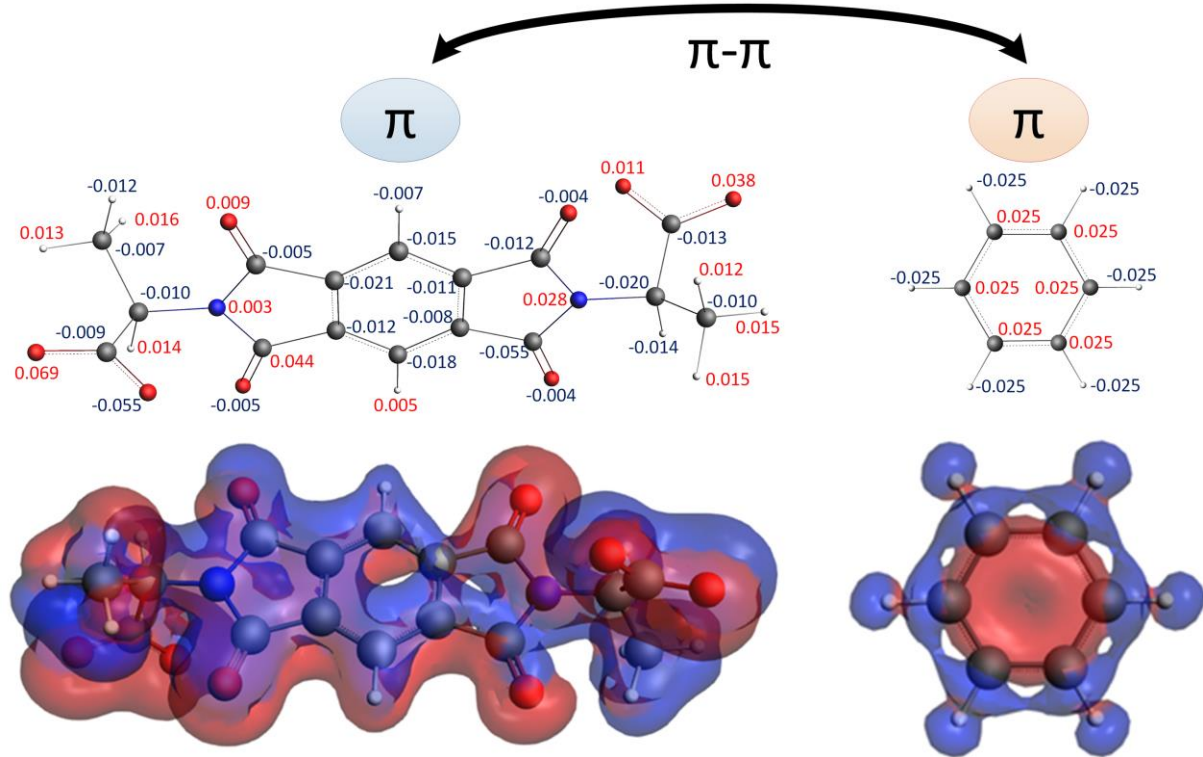


Fig. S116. Condensed Fukui functions determined for Bader charges and isosurface of dual descriptor of PMDA²⁻ and benzene. It is worth noting that both NEU-3 and NEU-4 are made up of PMDA²⁻.

2. Supplementary Tables

Table S1. Summaries of the EXAFS fitting results of the NEU-3.

Scattering	R (Å)	N	σ^2 (Å ²)
Zn-N ₁	1.95630 ± 0.02028	2	0.01666
Zn-O ₁	1.96290 ± 0.02893	4	0.00893
Zn-C ₁	2.32730 ± 0.04528	1	0.01635
Zn-C ₂	3.27840 ± 0.02504	4	0.02239
Zn-N ₁ -C ₂	3.49680 ± 0.05517	8	0.02563
Zn-C ₃	3.62250 ± 0.05757	2	0.00200
Zn-O ₁ -C ₃	3.63070 ± 0.06385	4	0.02944
Zn-O ₁ -C ₃ -O ₁	3.63890 ± 0.07012	2	0.00349
Zn-C ₁ -C ₅	3.84700 ± 0.06814	2	0.00305
Zn-O ₁ -O ₂	3.92510 ± 0.00461	4	0.00200
Zn-O ₁	3.92590 ± 0.10611	4	0.02283
Zn-C ₆	4.34180 ± 0.26663	4	0.02445
Zn-N ₁ -C ₆	4.37890 ± 0.30245	8	0.01394
Zn-O ₅	4.38950 ± 0.03644	4	0.02390
Zn-N ₁ -C ₆ -N ₁	4.41590 ± 0.20205	4	0.01149
Zn-O ₁ -O ₅	4.56420 ± 0.30988	8	0.00895
Zn-C ₇	4.75500 ± 0.31434	4	0.02442
Zn-O ₁ -C ₇	4.76490 ± 0.21591	4	0.00993
Zn-N ₁ -C ₉	4.76650 ± 0.09097	4	0.01591
Zn-N ₁ -C ₉ -N ₁	4.76650 ± 0.19865	2	0.01668

Fits were done at the Zn K-edge in R-space, k^{1,2,3} weighting. 1.0 < R < 4.8 Å and Δk = 3.000 – 11.938 Å⁻¹ were used for fitting. The fitting result of the E₀ and S₀² are -3.18382462 ± 0.31019616 eV and 1.02914124 ± 0.02891619, respectively. The goodness of the fit is reflected by $\chi^2_v = 472.89$ and R-factor = 0.0111470.

Table S2. Summaries of the EXAFS fitting results of the NEU-4.

Scattering	R (Å)	N	σ^2 (Å ²)
Fe-O ₁	1.96330 ± 0.01953	4	0.02416
Fe-N ₁	2.02100 ± 0.01404	2	0.00590
Fe-C ₁	2.50470 ± 0.02080	1	0.00614
Fe-O ₁ -O ₂	3.35160 ± 0.01127	8	0.01570
Fe-O ₁ -N ₁	3.40100 ± 0.00863	16	0.00753
Fe-C ₂	3.40760 ± 0.09377	4	0.00708
Fe-N ₁ -C ₂	3.59220 ± 0.05092	8	0.02210
Fe-C ₃	3.70440 ± 0.01769	1	0.01108
Fe-O ₃ -C ₃	3.70820 ± 0.07602	2	0.00484
Fe-O ₃ -C ₃ -O ₃	3.71200 ± 0.08780	1	0.00578
Fe-O ₁	3.92670 ± 0.35328	4	0.00512
Fe-O ₁ -O ₂	3.92670 ± 0.09137	4	0.00290
Fe-O ₁	3.92670 ± 0.01520	4	0.01305
Fe-C ₄	4.02570 ± 0.38941	1	0.01706
Fe-C ₁ -C ₄	4.02570 ± 0.01609	2	0.01082
Fe-C ₁ -C ₄ -C ₁	4.02580 ± 0.06858	1	0.00807
Fe-N ₁	4.04210 ± 0.00040	2	0.01556
Fe-O ₄	4.39020 ± 0.00846	2	0.00346

Fits were done at the Fe K-edge in R-space, $k^{1,2,3}$ weighting. $1.0 < R < 4.0 \text{ \AA}$ and $\Delta k = 3.000 - 11.877 \text{ \AA}^{-1}$ were used for fitting. The fitting result of the E_0 and S_0^2 are $-7.10198747 \pm 0.27683104 \text{ eV}$ and $1.59626043 \pm 0.04358904$, respectively. The goodness of the fit is reflected by $\chi_v^2 = 170.23$ and R-factor = 0.0188484.

Table S3. BET surface area and total pore volume before and after separation.

Sample	Conditions	BET m ² g ⁻¹	Total pore volume cm ³ g ⁻¹
NEU-1c	Pristine	171.3	0.698
	After 1 cycle of benzene/cyclohexane 5 % v/v separation	109.8	0.518
	After 1 cycle of benzene/cyclohexane 10 % v/v separation	107.6	0.502
	After 1 cycle of benzene/cyclohexane 25 % v/v separation	86.5	0.432
	After 1 cycle of benzene/cyclohexane 50 % v/v separation	79.2	0.421
NEU-2	Pristine	220.9	0.554
	After 1 cycle of benzene/cyclohexane 5 % v/v separation	136.6	0.403
	After 1 cycle of benzene/cyclohexane 10 % v/v separation	112.7	0.324
	After 1 cycle of benzene/cyclohexane 25 % v/v separation	112.1	0.305
	After 1 cycle of benzene/cyclohexane 50 % v/v separation	108.6	0.281
NEU-3	Pristine	94.2	0.598
	After 1 cycle of benzene/cyclohexane 5 % v/v separation	67.9	0.391
	After 1 cycle of benzene/cyclohexane 10 % v/v separation	59.6	0.329
	After 1 cycle of benzene/cyclohexane 25 % v/v separation	54.1	0.254
	After 1 cycle of benzene/cyclohexane 50 % v/v separation	52.7	0.252
NEU-4	Pristine	293.8	0.649
	After 1 cycle of benzene/cyclohexane 5 % v/v separation	31.6	0.010
	After 1 cycle of benzene/cyclohexane 10 % v/v separation	30.4	0.010
	After 1 cycle of benzene/cyclohexane 25 % v/v separation	25.7	0.009
	After 1 cycle of benzene/cyclohexane 50 % v/v separation	25.2	0.009
	After 1 cycle of 1,4-dioxane/cyclohexane 25 % v/v separation	21.5	0.008
	After 1 cycle of toluene/cyclohexane 25 % v/v separation	20.0	0.006
	After 1 cycle of p-xylene/cyclohexane 25 % v/v separation	11.4	0.004
	After 1 cycle of nitrobenzene/cyclohexane 25 % v/v separation	1.6	0.001

Table S4. Condensed and local Fukui functions of BPDI²⁻ gotten by using Hirshfeld, Mulliken, Voronoi and Bader charges.

Condensed Fukui minus functions:

	Hirshfeld	Mulliken	Voronoi	Bader
C(1)	0.016	0.009	0.017	0.018
C(2)	0.016	0.010	0.014	0.020
C(3)	0.023	0.026	0.016	0.025
C(4)	0.018	0.013	0.017	0.022
C(5)	0.019	0.012	0.016	0.022
C(6)	0.022	0.027	0.016	0.021
C(7)	0.025	0.031	0.012	-0.004
O(8)	0.092	0.092	0.105	-0.012
C(9)	0.025	0.030	0.014	-0.022
O(10)	0.092	0.093	0.106	0.000
N(11)	0.025	0.009	0.025	-0.008
C(12)	0.015	-0.005	0.002	-0.019
C(13)	0.011	0.012	-0.000	-0.012
O(14)	0.055	0.057	0.062	-0.000
O(15)	0.022	0.019	0.026	0.113
C(16)	0.022	0.023	0.010	0.113
O(17)	0.081	0.082	0.094	0.006
N(18)	0.022	0.009	0.023	0.002
C(19)	0.023	0.024	0.013	0.104
C(20)	0.021	0.007	0.009	0.006
C(21)	0.026	0.022	0.011	0.111
O(22)	0.059	0.054	0.067	0.101
O(23)	0.090	0.091	0.099	0.052
O(24)	0.080	0.082	0.089	0.004
H(25)	0.017	0.027	0.025	0.022
H(26)	0.017	0.027	0.023	0.024
H(27)	0.015	0.024	0.019	0.023
H(28)	0.016	0.027	0.021	0.027
H(29)	0.017	0.031	0.021	0.031
H(30)	0.020	0.034	0.027	0.035

Local Fukui minus softness:

	Hirshfeld	Mulliken	Voronoi	Bader
C(1)	0.724	0.409	0.772	0.819
C(2)	0.724	0.454	0.636	0.928
C(3)	1.041	1.181	0.727	1.122

C(4)	0.815	0.590	0.772	0.979
C(5)	0.860	0.545	0.727	0.980
C(6)	0.996	1.226	0.727	0.973
C(7)	1.132	1.408	0.545	-0.195
O(8)	4.166	4.178	4.768	-0.531
C(9)	1.132	1.362	0.636	-1.008
O(10)	4.166	4.223	4.814	0.043
N(11)	1.132	0.409	1.135	-0.348
C(12)	0.679	-0.227	0.091	-0.864
C(13)	0.498	0.545	-0.000	-0.553
O(14)	2.490	2.589	2.816	-0.022
O(15)	0.996	0.863	1.181	5.131
C(16)	0.996	1.045	0.454	5.128
O(17)	3.667	3.724	4.269	2.959
N(18)	0.996	0.409	1.045	0.886
C(19)	1.041	1.090	0.590	4.717
C(20)	0.951	0.318	0.409	2.983
C(21)	1.177	0.999	0.500	5.056
O(22)	2.671	2.452	3.043	4.579
O(23)	4.075	4.133	4.496	2.350
O(24)	3.622	3.724	4.042	1.903
H(25)	0.770	1.226	1.135	0.999
H(26)	0.770	1.226	1.045	1.105
H(27)	0.679	1.090	0.863	1.050
H(28)	0.724	1.226	0.954	1.215
H(29)	0.770	1.408	0.954	1.403
H(30)	0.906	1.544	1.226	1.581

Condensed Fukui plus functions:

	Hirshfeld	Mulliken	Voronoi	Bader
C(1)	0.007	0.002	0.005	0.007
C(2)	0.007	0.002	0.006	0.014
C(3)	0.013	0.017	0.011	0.016
C(4)	0.007	0.002	0.006	0.010
C(5)	0.006	0.002	0.005	0.005
C(6)	0.014	0.016	0.011	0.011
C(7)	0.007	0.003	0.005	-0.012
O(8)	0.027	0.031	0.029	0.008
C(9)	0.007	0.002	0.004	0.048
O(10)	0.026	0.029	0.028	-0.005
N(11)	0.003	-0.011	-0.001	-0.017
C(12)	0.024	0.003	0.008	0.005
C(13)	0.049	0.060	0.022	0.021
O(14)	0.147	0.141	0.162	-0.018

O(15)	0.130	0.131	0.146	0.024
C(16)	0.006	0.003	0.002	0.025
O(17)	0.027	0.030	0.030	0.017
N(18)	0.004	-0.011	0.000	0.018
C(19)	0.007	0.003	0.004	0.031
C(20)	0.024	0.002	0.006	0.017
C(21)	0.049	0.059	0.021	0.153
O(22)	0.129	0.130	0.142	0.023
O(23)	0.144	0.139	0.162	-0.005
O(24)	0.027	0.030	0.030	0.000
H(25)	0.010	0.020	0.015	0.018
H(26)	0.010	0.020	0.015	0.018
H(27)	0.022	0.037	0.032	0.030
H(28)	0.023	0.037	0.033	0.035
H(29)	0.022	0.036	0.031	0.035
H(30)	0.023	0.037	0.033	0.039

Local Fukui plus softness:

	Hirshfeld	Mulliken	Voronoi	Bader
C(1)	0.317	0.091	0.226	0.337
C(2)	0.317	0.091	0.271	0.644
C(3)	0.589	0.770	0.498	0.743
C(4)	0.317	0.091	0.271	0.461
C(5)	0.272	0.091	0.226	0.247
C(6)	0.635	0.724	0.498	0.515
C(7)	0.317	0.136	0.226	-0.548
O(8)	1.224	1.404	1.312	0.352
C(9)	0.317	0.091	0.181	2.197
O(10)	1.178	1.313	1.267	-2.262
N(11)	0.136	-0.498	-0.045	-0.787
C(12)	1.088	0.136	0.362	0.217
C(13)	2.221	2.717	0.995	0.955
O(14)	6.662	6.384	7.328	-0.806
O(15)	5.892	5.931	6.604	1.087
C(16)	0.272	0.136	0.090	1.139
O(17)	1.224	1.358	1.357	7.757
N(18)	0.181	-0.498	0.000	8.077
C(19)	0.317	0.136	0.181	1.394
C(20)	1.088	0.091	0.271	7.766
C(21)	2.221	2.671	0.950	6.955
O(22)	5.847	5.886	6.423	1.031
O(23)	6.526	6.294	7.328	-0.224
O(24)	1.224	1.358	1.357	0.192
H(25)	0.453	0.906	0.678	0.836

H(26)	0.453	0.906	0.678	0.821
H(27)	0.997	1.675	1.447	1.360
H(28)	1.042	1.675	1.493	1.565
H(29)	0.997	1.630	1.402	1.572
H(30)	1.042	1.675	1.493	1.775

Table S5. Condensed and local Fukui functions of PMDA²⁻ gotten by using Hirshfeld, Mulliken, Voronoi and Bader charges.

Fukui minus functions:

	Hirshfeld	Mulliken	Voronoi	Bader
C(1)	0.021	0.020	0.015	0.023
C(2)	0.016	0.009	0.013	0.019
C(3)	0.016	0.009	0.015	0.014
C(4)	0.023	0.024	0.016	0.026
C(5)	0.019	0.012	0.017	0.017
C(6)	0.018	0.012	0.017	0.022
N(7)	0.022	0.011	0.023	-0.026
C(8)	0.021	0.037	0.012	0.012
H(9)	0.018	0.026	0.027	-0.011
N(10)	0.024	0.010	0.025	0.009
C(11)	0.024	0.037	0.015	-0.007
H(12)	0.016	0.023	0.025	0.001
C(13)	0.024	0.048	0.013	0.000
O(14)	0.091	0.086	0.104	-0.008
O(15)	0.081	0.080	0.093	0.001
C(16)	0.022	0.022	0.012	0.000
O(17)	0.080	0.073	0.089	0.003
O(18)	0.067	0.070	0.077	0.004
H(19)	0.019	0.032	0.021	0.032
H(20)	0.008	0.012	0.009	0.030
H(21)	0.012	0.021	0.016	0.023
H(22)	0.017	0.035	0.022	0.003
C(23)	0.015	-0.002	0.012	0.030
C(24)	0.025	0.039	0.010	0.026
O(25)	0.080	0.073	0.088	0.028
O(26)	0.056	0.046	0.064	0.007
C(27)	0.015	-0.017	-0.000	0.026
H(28)	0.017	0.034	0.026	0.020
C(29)	0.009	-0.022	0.004	0.012
C(30)	0.011	-0.013	-0.000	0.009
C(31)	0.008	0.017	0.001	0.010
O(32)	0.018	0.013	0.021	0.073
O(33)	0.047	0.047	0.053	0.099
H(34)	0.013	0.024	0.014	0.004
H(35)	0.016	0.031	0.020	0.002
H(36)	0.010	0.021	0.012	0.005

Local Fukui minus softness:

	Hirshfeld	Mulliken	Voronoi	Bader
C(1)	0.862	0.820	0.615	0.962
C(2)	0.657	0.369	0.533	0.768
C(3)	0.657	0.369	0.615	0.566
C(4)	0.944	0.984	0.656	1.063
C(5)	0.780	0.492	0.697	0.192
C(6)	0.739	0.492	0.697	0.901
N(7)	0.903	0.451	0.942	-1.076
C(8)	0.862	1.518	0.492	0.507
H(9)	0.739	1.066	1.106	-0.432
N(10)	0.985	0.410	1.024	0.371
C(11)	0.985	1.518	0.615	-0.304
H(12)	0.657	0.943	1.024	0.180
C(13)	0.985	1.969	0.533	0.004
O(14)	3.736	3.528	4.262	-0.328
O(15)	3.326	3.282	3.811	0.033
C(16)	0.903	0.902	0.492	0.003
O(17)	3.285	2.994	3.647	1.522
O(18)	2.751	2.871	3.155	1.725
H(19)	0.780	1.313	0.861	1.301
H(20)	0.328	0.492	0.369	1.223
H(21)	0.493	0.861	0.656	0.946
H(22)	0.698	1.436	0.902	0.141
C(23)	0.616	-0.082	0.492	1.239
C(24)	1.026	1.600	0.410	1.080
O(25)	3.285	2.994	3.606	1.150
O(26)	2.299	1.887	2.623	0.271
C(27)	0.616	-0.697	-0.000	1.048
H(28)	0.698	1.395	1.065	0.825
C(29)	0.370	-0.902	0.164	4.943
C(30)	0.452	-0.533	-0.000	3.874
C(31)	0.328	0.697	0.041	4.299
O(32)	0.739	0.533	0.861	2.991
O(33)	1.930	1.928	2.172	4.060
H(34)	0.534	0.984	0.574	2.119
H(35)	0.657	1.272	0.820	0.638
H(36)	0.411	0.861	0.492	2.214

Condensed Fukui plus functions:

	Hirshfeld	Mulliken	Voronoi	Bader
C(1)	0.012	0.015	0.009	0.008
C(2)	0.006	0.002	0.005	0.008

C(3)	0.007	0.001	0.005	0.006
C(4)	0.014	0.015	0.010	0.008
C(5)	0.007	0.001	0.006	0.005
C(6)	0.006	0.003	0.004	0.001
N(7)	0.002	-0.013	0.003	0.002
C(8)	0.004	0.003	0.002	-0.000
H(9)	0.011	0.019	0.017	-0.006
N(10)	0.002	-0.012	0.000	0.012
C(11)	0.008	0.006	0.003	0.037
H(12)	0.010	0.018	0.015	-0.006
C(13)	0.004	0.002	0.000	-0.005
O(14)	0.019	0.019	0.021	0.001
O(15)	0.027	0.027	0.031	-0.004
C(16)	0.008	0.006	0.004	-0.055
O(17)	0.019	0.020	0.022	-0.001
O(18)	0.027	0.026	0.030	0.000
H(19)	0.019	0.033	0.029	0.018
H(20)	0.012	0.021	0.013	0.018
H(21)	0.012	0.021	0.015	0.035
H(22)	0.015	0.021	0.019	0.018
C(23)	0.014	-0.009	-0.001	0.010
C(24)	0.043	0.069	0.018	0.013
O(25)	0.137	0.138	0.153	0.039
O(26)	0.130	0.131	0.144	0.045
C(27)	0.016	-0.020	0.001	0.016
H(28)	0.019	0.036	0.025	0.035
C(29)	0.014	-0.009	0.003	0.002
C(30)	0.016	-0.019	0.002	0.002
C(31)	0.043	0.070	0.020	0.001
O(32)	0.130	0.130	0.144	0.018
O(33)	0.136	0.138	0.154	0.168
H(34)	0.019	0.032	0.027	0.018
H(35)	0.015	0.020	0.020	0.018
H(36)	0.019	0.036	0.028	0.018

Local Fukui plus softness:

	Hirshfeld	Mulliken	Voronoi	Bader
C(1)	0.491	0.617	0.369	0.312
C(2)	0.246	0.082	0.205	0.315
C(3)	0.287	0.041	0.205	0.266
C(4)	0.573	0.617	0.410	0.343
C(5)	0.287	0.041	0.246	0.697
C(6)	0.246	0.123	0.164	0.041
N(7)	0.082	-0.535	0.123	0.095

C(8)	0.164	0.123	0.082	-0.015
H(9)	0.450	0.782	0.697	-0.230
N(10)	0.082	-0.494	0.000	0.494
C(11)	0.327	0.247	0.123	1.532
H(12)	0.409	0.741	0.615	-2.536
C(13)	0.164	0.082	0.000	-0.214
O(14)	0.778	0.782	0.861	0.025
O(15)	1.105	1.111	1.270	-0.163
C(16)	0.327	0.247	0.164	-2.274
O(17)	0.778	0.823	0.902	-0.270
O(18)	1.105	1.070	1.229	0.096
H(19)	0.778	1.358	1.188	0.755
H(20)	0.491	0.864	0.533	0.745
H(21)	0.491	0.864	0.615	1.418
H(22)	0.614	0.864	0.779	0.718
C(23)	0.573	-0.370	-0.041	0.397
C(24)	1.760	2.839	0.738	0.543
O(25)	5.608	5.678	6.270	1.612
O(26)	5.322	5.390	5.901	1.826
C(27)	0.655	-0.823	0.041	0.639
H(28)	0.778	1.481	1.024	1.436
C(29)	0.573	-0.370	0.123	0.930
C(30)	0.655	-0.782	0.082	0.894
C(31)	1.760	2.880	0.820	0.528
O(32)	5.322	5.349	5.901	0.745
O(33)	5.567	5.678	6.311	6.893
H(34)	0.778	1.317	1.106	7.659
H(35)	0.614	0.823	0.820	7.306
H(36)	0.778	1.481	1.147	7.460

Table S6. Condensed and local Fukui functions of cyclohexane gotten by using Hirshfeld, Mulliken, Voronoi and Bader charges.

Condensed Fukui minus functions:

	Hirshfeld	Mulliken	Voronoi	Bader
C(1)	0.046	-0.021	-0.000	-0.026
C(2)	0.046	-0.021	0.002	-0.026
C(3)	0.046	-0.021	-0.000	-0.026
C(4)	0.046	-0.021	0.002	-0.026
C(5)	0.046	-0.021	-0.000	-0.026
C(6)	0.046	-0.021	0.002	-0.026
H(7)	0.060	0.094	0.083	0.096
H(8)	0.060	0.094	0.083	0.096
H(9)	0.060	0.094	0.083	0.097
H(10)	0.060	0.094	0.083	0.097
H(11)	0.060	0.094	0.083	0.096
H(12)	0.060	0.094	0.083	0.096
H(13)	0.060	0.094	0.083	0.097
H(14)	0.060	0.094	0.083	0.097
H(15)	0.060	0.094	0.083	0.096
H(16)	0.060	0.094	0.083	0.096
H(17)	0.060	0.094	0.083	0.097
H(18)	0.060	0.094	0.083	0.097

Local Fukui minus softness:

	Hirshfeld	Mulliken	Voronoi	Bader
C(1)	0.187	-0.085	-0.000	-0.105
C(2)	0.187	-0.085	0.008	-0.104
C(3)	0.187	-0.085	-0.000	-0.105
C(4)	0.187	-0.085	0.008	-0.104
C(5)	0.187	-0.085	-0.000	-0.105
C(6)	0.187	-0.085	0.008	-0.104
H(7)	0.243	0.379	0.335	0.387
H(8)	0.243	0.379	0.335	0.387
H(9)	0.243	0.379	0.335	0.391
H(10)	0.243	0.379	0.335	0.391
H(11)	0.243	0.379	0.335	0.387
H(12)	0.243	0.379	0.335	0.387
H(13)	0.243	0.379	0.335	0.391
H(14)	0.243	0.379	0.335	0.391
H(15)	0.243	0.379	0.335	0.387

H(16)	0.243	0.379	0.335	0.387
H(17)	0.243	0.379	0.335	0.391
H(18)	0.243	0.379	0.335	0.391

Condensed Fukui plus functions:

	Hirshfeld	Mulliken	Voronoi	Bader
C(1)	0.047	-0.102	0.005	0.044
C(2)	0.047	-0.102	0.004	0.039
C(3)	0.047	-0.102	0.005	0.044
C(4)	0.047	-0.102	0.004	0.039
C(5)	0.047	-0.102	0.005	0.044
C(6)	0.047	-0.102	0.004	0.039
H(7)	0.060	0.134	0.081	0.064
H(8)	0.060	0.134	0.081	0.064
H(9)	0.060	0.134	0.081	0.061
H(10)	0.060	0.134	0.081	0.061
H(11)	0.060	0.134	0.081	0.064
H(12)	0.060	0.134	0.081	0.064
H(13)	0.060	0.134	0.081	0.061
H(14)	0.060	0.134	0.081	0.061
H(15)	0.060	0.134	0.081	0.064
H(16)	0.060	0.134	0.081	0.064
H(17)	0.060	0.134	0.081	0.061
H(18)	0.060	0.134	0.081	0.061

Local Fukui plus softness:

	Hirshfeld	Mulliken	Voronoi	Bader
C(1)	0.189	-0.412	0.020	0.178
C(2)	0.189	-0.412	0.016	0.157
C(3)	0.189	-0.412	0.020	0.178
C(4)	0.189	-0.412	0.016	0.157
C(5)	0.189	-0.412	0.020	0.178
C(6)	0.189	-0.412	0.016	0.157
H(7)	0.242	0.543	0.328	0.258
H(8)	0.242	0.543	0.328	0.258
H(9)	0.242	0.543	0.328	0.248
H(10)	0.242	0.543	0.328	0.248
H(11)	0.242	0.543	0.328	0.258
H(12)	0.242	0.543	0.328	0.258
H(13)	0.242	0.543	0.328	0.248
H(14)	0.242	0.543	0.328	0.248
H(15)	0.242	0.543	0.328	0.258
H(16)	0.242	0.543	0.328	0.258
H(17)	0.242	0.543	0.328	0.248

H(18) 0.242 0.543 0.328 0.248

Table S7. Condensed and local Fukui functions of benzene gotten by using Hirshfeld, Mulliken, Voronoi and Bader charges.

Condensed Fukui minus functions:

	Hirshfeld	Mulliken	Voronoi	Bader
C(1)	0.113	0.070	0.091	0.065
C(2)	0.113	0.070	0.091	0.065
C(3)	0.113	0.070	0.091	0.065
C(4)	0.113	0.070	0.091	0.065
C(5)	0.113	0.070	0.091	0.065
C(6)	0.113	0.070	0.091	0.065
H(7)	0.054	0.097	0.076	0.102
H(8)	0.054	0.097	0.076	0.102
H(9)	0.054	0.097	0.076	0.102
H(10)	0.054	0.097	0.076	0.102
H(11)	0.054	0.097	0.076	0.102
H(12)	0.054	0.097	0.076	0.102

Local Fukui minus softness:

	Hirshfeld	Mulliken	Voronoi	Bader
C(1)	0.583	0.361	0.469	0.334
C(2)	0.583	0.361	0.469	0.334
C(3)	0.583	0.361	0.469	0.334
C(4)	0.583	0.361	0.469	0.334
C(5)	0.583	0.361	0.469	0.334
C(6)	0.583	0.361	0.469	0.334
H(7)	0.279	0.500	0.392	0.527
H(8)	0.279	0.500	0.392	0.527
H(9)	0.279	0.500	0.392	0.527
H(10)	0.279	0.500	0.392	0.527
H(11)	0.279	0.500	0.392	0.527
H(12)	0.279	0.500	0.392	0.527

Condensed Fukui plus functions:

	Hirshfeld	Mulliken	Voronoi	Bader
C(1)	0.108	0.063	0.081	0.090
C(2)	0.108	0.063	0.081	0.090
C(3)	0.108	0.063	0.081	0.090
C(4)	0.108	0.063	0.081	0.090
C(5)	0.108	0.063	0.081	0.090
C(6)	0.108	0.063	0.081	0.090

H(7)	0.058	0.103	0.086	0.077
H(8)	0.058	0.103	0.086	0.077
H(9)	0.058	0.103	0.086	0.077
H(10)	0.058	0.103	0.086	0.077
H(11)	0.058	0.103	0.086	0.077
H(12)	0.058	0.103	0.086	0.077

Local Fukui plus softness:

	Hirshfeld	Mulliken	Voronoi	Bader
C(1)	0.561	0.327	0.418	0.463
C(2)	0.561	0.327	0.418	0.463
C(3)	0.561	0.327	0.418	0.463
C(4)	0.561	0.327	0.418	0.463
C(5)	0.561	0.327	0.418	0.463
C(6)	0.561	0.327	0.418	0.463
H(7)	0.301	0.535	0.444	0.399
H(8)	0.301	0.535	0.444	0.399
H(9)	0.301	0.535	0.444	0.399
H(10)	0.301	0.535	0.444	0.399
H(11)	0.301	0.535	0.444	0.399
H(12)	0.301	0.535	0.444	0.399

Table S8. Condensed and local Fukui functions of 1,4-dioxane gotten by using Hirshfeld, Mulliken, Voronoi and Bader charges.

Condensed Fukui minus functions:

	Hirshfeld	Mulliken	Voronoi	Bader
C(1)	0.050	-0.028	0.001	-0.039
C(2)	0.050	-0.028	0.001	-0.039
O(3)	0.153	0.137	0.167	-0.039
C(4)	0.050	-0.028	0.001	-0.039
C(5)	0.050	-0.028	0.001	0.160
O(6)	0.153	0.137	0.167	0.160
H(7)	0.062	0.105	0.083	0.104
H(8)	0.062	0.105	0.083	0.104
H(9)	0.062	0.105	0.083	0.104
H(10)	0.062	0.105	0.083	0.104
H(11)	0.062	0.105	0.083	0.104
H(12)	0.062	0.105	0.083	0.104
H(13)	0.062	0.105	0.083	0.104
H(14)	0.062	0.105	0.083	0.104

Local Fukui minus softness:

	Hirshfeld	Mulliken	Voronoi	Bader
C(1)	0.290	-0.162	0.006	-0.228
C(2)	0.290	-0.162	0.006	-0.228
O(3)	0.894	0.801	0.971	-0.228
C(4)	0.290	-0.162	0.006	-0.228
C(5)	0.290	-0.162	0.006	0.934
O(6)	0.894	0.801	0.971	0.934
H(7)	0.360	0.609	0.483	0.609
H(8)	0.360	0.609	0.483	0.609
H(9)	0.360	0.609	0.483	0.609
H(10)	0.360	0.609	0.483	0.609
H(11)	0.360	0.609	0.483	0.609
H(12)	0.360	0.609	0.483	0.609
H(13)	0.360	0.609	0.483	0.609
H(14)	0.360	0.609	0.483	0.609

Condensed Fukui plus functions:

	Hirshfeld	Mulliken	Voronoi	Bader
C(1)	0.085	0.093	0.033	0.137
C(2)	0.085	0.093	0.033	0.137

O(3)	0.145	-0.018	0.158	0.137
C(4)	0.085	0.093	0.033	0.137
C(5)	0.085	0.093	0.033	-0.012
O(6)	0.145	-0.018	0.158	-0.012
H(7)	0.046	0.083	0.069	0.059
H(8)	0.046	0.083	0.069	0.059
H(9)	0.046	0.083	0.069	0.059
H(10)	0.046	0.083	0.069	0.059
H(11)	0.046	0.083	0.069	0.059
H(12)	0.046	0.083	0.069	0.059
H(13)	0.046	0.083	0.069	0.059
H(14)	0.046	0.083	0.069	0.059

Local Fukui plus softness:

	Hirshfeld	Mulliken	Voronoi	Bader
C(1)	0.497	0.542	0.192	0.801
C(2)	0.497	0.542	0.192	0.801
O(3)	0.842	-0.105	0.921	0.801
C(4)	0.497	0.542	0.192	0.801
C(5)	0.497	0.542	0.192	-0.072
O(6)	0.842	-0.105	0.921	-0.072
H(7)	0.269	0.484	0.402	0.346
H(8)	0.269	0.484	0.402	0.346
H(9)	0.269	0.484	0.402	0.346
H(10)	0.269	0.484	0.402	0.346
H(11)	0.269	0.484	0.402	0.346
H(12)	0.269	0.484	0.402	0.346
H(13)	0.269	0.484	0.402	0.346
H(14)	0.269	0.484	0.402	0.346

Table S9. Condensed and local Fukui functions of toluene gotten by using Hirshfeld, Mulliken, Voronoi and Bader charges.

Condensed Fukui minus functions:

	Hirshfeld	Mulliken	Voronoi	Bader
C(1)	0.119	0.056	0.128	0.026
C(2)	0.078	0.053	0.059	0.066
C(3)	0.074	0.048	0.048	0.048
C(4)	0.146	0.089	0.136	0.078
C(5)	0.075	0.049	0.049	0.052
C(6)	0.079	0.054	0.059	0.064
H(7)	0.044	0.085	0.062	-0.014
H(8)	0.046	0.086	0.066	0.085
H(9)	0.055	0.094	0.079	0.090
H(10)	0.046	0.086	0.064	0.094
H(11)	0.044	0.085	0.062	0.085
C(12)	0.046	-0.009	-0.009	0.083
H(13)	0.042	0.071	0.053	0.074
H(14)	0.042	0.071	0.055	0.081
H(15)	0.062	0.082	0.091	0.089

Local Fukui minus softness:

	Hirshfeld	Mulliken	Voronoi	Bader
C(1)	0.648	0.304	0.694	0.142
C(2)	0.425	0.288	0.320	0.356
C(3)	0.403	0.261	0.260	0.260
C(4)	0.795	0.483	0.737	0.423
C(5)	0.408	0.266	0.266	0.280
C(6)	0.430	0.293	0.320	0.348
H(7)	0.240	0.462	0.336	-0.078
H(8)	0.250	0.467	0.358	0.463
H(9)	0.299	0.511	0.428	0.486
H(10)	0.250	0.467	0.347	0.513
H(11)	0.240	0.462	0.336	0.461
C(12)	0.250	-0.049	-0.049	0.451
H(13)	0.229	0.386	0.287	0.403
H(14)	0.229	0.386	0.298	0.439
H(15)	0.337	0.445	0.493	0.486

Condensed Fukui plus functions:

	Hirshfeld	Mulliken	Voronoi	Bader

C(1)	0.084	0.006	0.077	0.057
C(2)	0.062	0.025	0.029	0.013
C(3)	0.129	0.095	0.112	0.109
C(4)	0.104	0.061	0.078	0.099
C(5)	0.070	0.023	0.035	0.020
C(6)	0.125	0.112	0.111	0.109
H(7)	0.044	0.088	0.065	0.019
H(8)	0.061	0.102	0.093	0.075
H(9)	0.055	0.098	0.081	0.092
H(10)	0.048	0.090	0.066	0.072
H(11)	0.058	0.097	0.089	0.080
C(12)	0.035	-0.019	0.000	0.083
H(13)	0.048	0.072	0.057	0.063
H(14)	0.033	0.063	0.045	0.042
H(15)	0.046	0.084	0.061	0.065

Local Fukui plus softness:

	Hirshfeld	Mulliken	Voronoi	Bader
C(1)	0.455	0.033	0.419	0.308
C(2)	0.336	0.136	0.158	0.072
C(3)	0.699	0.518	0.609	0.594
C(4)	0.564	0.332	0.424	0.539
C(5)	0.380	0.125	0.190	0.109
C(6)	0.678	0.610	0.604	0.594
H(7)	0.239	0.480	0.353	0.104
H(8)	0.331	0.556	0.506	0.406
H(9)	0.298	0.534	0.440	0.502
H(10)	0.260	0.490	0.359	0.389
H(11)	0.314	0.529	0.484	0.434
C(12)	0.190	-0.104	0.000	0.452
H(13)	0.260	0.392	0.310	0.342
H(14)	0.179	0.343	0.245	0.231
H(15)	0.249	0.458	0.332	0.356

Table S10. Condensed and local Fukui functions of p-xylene gotten by using Hirshfeld, Mulliken, Voronoi and Bader charges.

Condensed Fukui minus functions:

	Hirshfeld	Mulliken	Voronoi	Bader
C(1)	0.110	0.052	0.117	0.053
C(2)	0.073	0.048	0.057	0.060
C(3)	0.066	0.048	0.045	0.034
C(4)	0.110	0.052	0.117	0.053
C(5)	0.073	0.048	0.057	0.061
C(6)	0.066	0.048	0.045	0.037
H(7)	0.041	0.079	0.057	-0.014
H(8)	0.041	0.079	0.059	-0.012
C(9)	0.040	-0.008	-0.009	0.072
H(10)	0.041	0.079	0.057	0.080
H(11)	0.041	0.079	0.059	0.072
C(12)	0.040	-0.008	-0.010	0.077
H(13)	0.049	0.070	0.067	0.077
H(14)	0.033	0.061	0.042	0.061
H(15)	0.048	0.070	0.068	0.075
H(16)	0.033	0.061	0.042	0.061
H(17)	0.049	0.070	0.067	0.080
H(18)	0.048	0.070	0.067	0.074

Local Fukui minus softness:

	Hirshfeld	Mulliken	Voronoi	Bader
C(1)	0.632	0.300	0.671	0.306
C(2)	0.420	0.277	0.327	0.347
C(3)	0.379	0.277	0.258	0.195
C(4)	0.632	0.300	0.671	0.303
C(5)	0.420	0.277	0.327	0.350
C(6)	0.379	0.277	0.258	0.213
H(7)	0.236	0.456	0.327	-0.082
H(8)	0.236	0.456	0.338	-0.070
C(9)	0.230	-0.046	-0.052	0.415
H(10)	0.236	0.456	0.327	0.462
H(11)	0.236	0.456	0.338	0.412
C(12)	0.230	-0.046	-0.057	0.443
H(13)	0.282	0.404	0.384	0.443
H(14)	0.190	0.352	0.241	0.353
H(15)	0.276	0.404	0.390	0.429

H(16)	0.190	0.352	0.241	0.352
H(17)	0.282	0.404	0.384	0.460
H(18)	0.276	0.404	0.384	0.427

Condensed Fukui plus functions:

	Hirshfeld	Mulliken	Voronoi	Bader
C(1)	0.076	0.004	0.069	0.051
C(2)	0.119	0.108	0.105	0.119
C(3)	0.060	0.029	0.032	0.015
C(4)	0.076	0.004	0.069	0.050
C(5)	0.119	0.108	0.106	0.118
C(6)	0.060	0.029	0.032	0.010
H(7)	0.055	0.094	0.088	0.009
H(8)	0.042	0.084	0.057	0.004
C(9)	0.033	-0.017	-0.005	0.066
H(10)	0.055	0.094	0.088	0.074
H(11)	0.042	0.084	0.057	0.067
C(12)	0.033	-0.017	-0.004	0.076
H(13)	0.042	0.073	0.057	0.066
H(14)	0.030	0.053	0.040	0.042
H(15)	0.043	0.072	0.055	0.064
H(16)	0.030	0.053	0.040	0.042
H(17)	0.042	0.073	0.057	0.063
H(18)	0.043	0.072	0.056	0.064

Local Fukui plus softness:

	Hirshfeld	Mulliken	Voronoi	Bader
C(1)	0.438	0.023	0.398	0.291
C(2)	0.685	0.622	0.605	0.685
C(3)	0.346	0.167	0.184	0.085
C(4)	0.438	0.023	0.398	0.290
C(5)	0.685	0.622	0.611	0.680
C(6)	0.346	0.167	0.184	0.059
H(7)	0.317	0.541	0.507	0.055
H(8)	0.242	0.484	0.329	0.025
C(9)	0.190	-0.098	-0.029	0.378
H(10)	0.317	0.541	0.507	0.426
H(11)	0.242	0.484	0.329	0.384
C(12)	0.190	-0.098	-0.023	0.438
H(13)	0.242	0.420	0.329	0.382
H(14)	0.173	0.305	0.231	0.242
H(15)	0.248	0.415	0.317	0.366
H(16)	0.173	0.305	0.231	0.242
H(17)	0.242	0.420	0.329	0.363

H(18) 0.248 0.415 0.323 0.366

Table S11. Condensed and local Fukui functions of nitrobenzene gotten by using Hirshfeld, Mulliken, Voronoi and Bader charges.

Condensed Fukui minus functions:

	Hirshfeld	Mulliken	Voronoi	Bader
C(1)	0.050	-0.028	0.001	-0.039
C(2)	0.050	-0.028	0.001	-0.039
O(3)	0.153	0.137	0.167	-0.039
C(4)	0.050	-0.028	0.001	-0.039
C(5)	0.050	-0.028	0.001	0.160
O(6)	0.153	0.137	0.167	0.160
H(7)	0.062	0.105	0.083	0.104
H(8)	0.062	0.105	0.083	0.104
H(9)	0.062	0.105	0.083	0.104
H(10)	0.062	0.105	0.083	0.104
H(11)	0.062	0.105	0.083	0.104
H(12)	0.062	0.105	0.083	0.104
H(13)	0.062	0.105	0.083	0.104
H(14)	0.062	0.105	0.083	0.104

Local Fukui minus softness:

	Hirshfeld	Mulliken	Voronoi	Bader
C(1)	0.290	-0.162	0.006	-0.228
C(2)	0.290	-0.162	0.006	-0.228
O(3)	0.894	0.801	0.971	-0.228
C(4)	0.290	-0.162	0.006	-0.228
C(5)	0.290	-0.162	0.006	0.934
O(6)	0.894	0.801	0.971	0.934
H(7)	0.360	0.609	0.483	0.609
H(8)	0.360	0.609	0.483	0.609
H(9)	0.360	0.609	0.483	0.609
H(10)	0.360	0.609	0.483	0.609
H(11)	0.360	0.609	0.483	0.609
H(12)	0.360	0.609	0.483	0.609
H(13)	0.360	0.609	0.483	0.609
H(14)	0.360	0.609	0.483	0.609

Condensed Fukui plus functions:

	Hirshfeld	Mulliken	Voronoi	Bader
C(1)	0.085	0.093	0.033	0.137
C(2)	0.085	0.093	0.033	0.137

O(3)	0.145	-0.018	0.158	0.137
C(4)	0.085	0.093	0.033	0.137
C(5)	0.085	0.093	0.033	-0.012
O(6)	0.145	-0.018	0.158	-0.012
H(7)	0.046	0.083	0.069	0.059
H(8)	0.046	0.083	0.069	0.059
H(9)	0.046	0.083	0.069	0.059
H(10)	0.046	0.083	0.069	0.059
H(11)	0.046	0.083	0.069	0.059
H(12)	0.046	0.083	0.069	0.059
H(13)	0.046	0.083	0.069	0.059
H(14)	0.046	0.083	0.069	0.059

Local Fukui plus softness:

	Hirshfeld	Mulliken	Voronoi	Bader
C(1)	0.497	0.542	0.192	0.801
C(2)	0.497	0.542	0.192	0.801
O(3)	0.842	-0.105	0.921	0.801
C(4)	0.497	0.542	0.192	0.801
C(5)	0.497	0.542	0.192	-0.072
O(6)	0.842	-0.105	0.921	-0.072
H(7)	0.269	0.484	0.402	0.346
H(8)	0.269	0.484	0.402	0.346
H(9)	0.269	0.484	0.402	0.346
H(10)	0.269	0.484	0.402	0.346
H(11)	0.269	0.484	0.402	0.346
H(12)	0.269	0.484	0.402	0.346
H(13)	0.269	0.484	0.402	0.346
H(14)	0.269	0.484	0.402	0.346

Table S12. Benzene/cyclohexane separation performance of different materials.

Mechanism of separation	Material	Conditions	Selectivity	Ref.
Selective adsorption	NEU-1c	298 K, 1 atm, 1.18 mol benzene/mol cyclohexane liquid phase	2.7	This work
	NEU-2	298 K, 1 atm, 1.18 mol benzene/mol cyclohexane liquid phase	3.5	
	NEU-3	298 K, 1 atm, 1.18 mol benzene/mol cyclohexane liquid phase	2.9	
	NEU-4	298 K, 1 atm, 1.18 mol benzene/mol cyclohexane liquid phase	3.7	
	NEU-1c	298 K, 1 atm, 0.13 mol benzene/mol cyclohexane liquid phase	5.7	
	NEU-2	298 K, 1 atm, 0.13 mol benzene/mol cyclohexane liquid phase	10.8	
	NEU-3	298 K, 1 atm, 0.13 mol benzene/mol cyclohexane liquid phase	10.1	
	NEU-4	298 K, 1 atm, 0.13 mol benzene/mol cyclohexane liquid phase	12.1	
	FAU-type zeolite membrane	373 K, 1 atm, 1 mol benzene/mol cyclohexane gas phase	~19	1
	[Zn(μ_4 -TCNQ-TCNQ)bpy]	298 K, 1 atm, 0.1 mol benzene/mol cyclohexane gas phase	~19	2
Pervaporation processes	Ni ₃ (OH)(Ina) ₃ (BDC) _{1.5}	298 K, 1 atm, 1 mol benzene/mol cyclohexane gas phase	~17	3
	Nonporous adaptive crystals of a hybrid[3]arene	373 K, 1 atm, 1 mol benzene/mol cyclohexane gas phase	~37	4
	PS/PAA	293 K, 1.05 mol benzene/mol cyclohexane	9.6	5
	PEMA-EGDM	313 K, 0.12 mol benzene/mol cyclohexane	6.7	6
Azeotropic distillation	PMMA-EGDM	313 K, 0.12 mol benzene/mol cyclohexane	3.9	6
	PVA (asymmetric)	323 K, 0.35 mol benzene/mol cyclohexane	10	7
	[EMIM][TCB]		~15	
	[EMIM][BF ₄]	Vapor-liquid equilibrium for benzene + cyclohexane containing IL at 1 atm	~23	8
Liquid-liquid extraction {cyclohexane + benzene + IL}	[BMIM][BF ₄]		~20	
	[BMPY][BF ₄]		~20	
	[BMIM][PF ₆]	298 K, 1 atm	~40	
	[PMIM][PF ₆]	298 K, 1 atm	~23	9
Liquid-liquid extraction {cyclohexane + benzene + DMSO + IL}	[HMIM][PF ₆]	298 K, 1 atm	~17	
	[MIM][DBP]	298 K, 1 atm	2.3	10
	[MMIM][DMP]	298 K, 1 atm	3.6	11
	[MMIM][DMP]	313 K, 1 atm	4.4	11
	[BMIM][BF ₄]	298 K, 1 atm	80.4	12
	[BMIM][PF ₆]	298 K, 1 atm	49.4	13

References

- [1] B.-H. Jeong, Y. Hasegawa, K.-I. Sotowa, K. Kusakabe and S. Morooka, *J. Membr. Sci.*, 2003, **213**, 115-124.
- [2] S. Shimomura, S. Horike, R. Matsuda and S. Kitagawa, *J. Am. Chem. Soc.*, 2007, **129**, 10990-10991.
- [3] G. Ren, S. Liu, F. Ma, F. Wei, Q. Tang, Y. Yang, D. Liang, S. Li and Y. Chen, *J. Mater. Chem.*, 2011, **21**, 15909-15913.
- [4] J. Zhou, G. Yu, Q. Li, M. Wang and F. Huang, *J. Am. Chem. Soc.*, 2020, **142**, 2228-2232.
- [5] F. Sun and E. Ruckenstein, *J. Membr. Sci.*, 1995, **99**, 273-284.
- [6] K. Inui, H. Okumura, T. Miyata and T. Uragami, *J. Membr. Sci.*, 1997, **132**, 193-202.
- [7] A. Yamasaki, T. Shinbo and K. Mizoguchi, *J. Appl. Polym. Sci.*, 1997, **64**, 1061-1065.
- [8] W. Li, B. Xu, Z. Lei and C. Dai, *Chem. Eng. Process.*, 2018, **126**, 81-89.
- [9] T. Zhou, Z. Wang, L. Chen, Y. Ye, Z. Qi, H. Freund and K. Sundmacher, *J. Chem. Thermodyn.*, 2012, **48**, 145-149.
- [10] R. Wang, C. Li, H. Meng, J. Wang and Z. Wang, *J. Chem. Eng. Data*, 2008, **53**, 2170-2174.
- [11] R. Wang, J. Wang, H. Meng, C. Li and Z. Wang, *J. Chem. Eng. Data*, 2008, **53**, 1159-1162.
- [12] T. Zhou, Z. Wang, Y. Ye, L. Chen, J. Xu and Z. Qi, *Ind. Eng. Chem. Res.*, 2012, **51**, 5559-5564.
- [13] T. Zhou, Z. Wang, L. Chen, Y. Ye, Z. Qi, H. Freund and K. Sundmacher, *J. Chem. Thermodyn.*, 2012, **48**, 145-149.